U.S. Department of Energy, Office of Fossil Energy

DOE Award: DE-FE0031834
October 1, 2019 – September 30, 2023

Development and Testing of an Integrated Acid Mine Drainage (AMD) Treatment and Rare Earth/Critical Mineral Plant

Final Scientific/Technical Report

Principal Investigator:
Paul Ziemkiewicz, PhD
Director, West Virginia Water Research Institute
West Virginia University
pziemkie@mail.wvu.edu
304-293-6958

Submitted by:
Paul Ziemkiewicz, PhD
Director, West Virginia Water Research Institute

Submission Date:
December 29, 2023

West Virginia University Research Corporation
DUNS Number: 191510239
886 Chestnut Ridge Road, PO Box 6845
Morgantown, WV 26506-6845

WVU Team Members
Virginia Polytechnic Institute State University
West Virginia Department of Environmental Protection
Rockwell Automation
Solmax

Acknowledgment: "This material is based upon work supported by the Department of Energy National Energy Technology Laboratory under Award Number DE-FE0031834."

Contents

Executive Summary

The overall objective of this project was to design, construct, and test a pilot-scale continuous process for efficiently treating acid mine drainage (AMD) while producing rare earth element/critical mineral (REE/CM) concentrates. The process technology evaluated in this project included two distinct operations:

1. an upstream pre-concentration unit that treats raw AMD to environmentally compliant discharge standards while capturing an REE/CM preconcentrate, and
2. a downstream REE purification process that further enriches the pre-concentrate while producing mixed or partially separated rare earth oxides (REOs).

The project team members successfully completed all of the proposed goals of the project and advanced the technology readiness levels (TRL) of the constituent operations to TRL 7 for the upstream concentration unit (full-scale system demonstration) and TRL 6 for the downstream purification process (pilot-scale demonstration).

In November of 2020, the West Virginia Department of Environmental Protection (WVDEP) worked with the project team to break ground on an integrated AMD treatment/REE recovery plant at the A-34 site in Bismark, WV. The technology utilized the project team's patented staged precipitation process that simultaneously treats AMD and concentrates REEs. The solid product, denoted as hydraulic pre-concentrate (HPC), was shown to have an REE grade of 1%, and prior efforts at the laboratory and pilot-scale provided the insights and process knowledge needed to effectively handle and dewater the product. The plant was completed in September 2022, and within weeks of commissioning, was able to produce HPC, at scale, with purity specifications meeting or exceeding that of the laboratory projections. Throughout the course of the project, the plant generated over 115,000 gallons of HPC. Of this total, 23,000 gallons of HPC (containing over two tons of pre-concentrate material on a dry weight basis) was captured and utilized in subsequent testing and analysis.

In parallel to the upstream technology, the project team designed, optimized, constructed, and operated a pilot-scale acid leaching/solvent extraction (ALSX) plant co-located with the HPC production unit at the A-34 site. Uniquely, the process deployed in this project utilized acid leaching and solvent extraction in combination with novel stages of prestripitation and product purification to generate partially separated light rare earth oxide (LREO) and heavy rare earth oxide (HREO) products. Construction of the ALSX plant begin in June 2022, and the facility was fully operational by March 2023. Over the course of the project, the plant produced over 25,000 gallons of leach solution. Portions of this solution were further processed to generate 1.8 kg of LREO and 2.5 kg of HREO products with intermediate purities ranging from 55% to 90% REO. After applying the aforementioned purification processes, the team was able to generate more than 200 g of both HREO and LREO at purities exceeding 90% TREO.

Accompanying the experimental studies, the project team completed the technical and economic modeling needed to fully evaluate the viability of the technology in a larger REE/CM production ecosystem. Results from this study show that the process is highly profitable, with internal rates of return varying from 22% to 115% for the process configuration under consideration. Opportunities for further improvement included the addition of additional byproduct revenue (synthetic zeolite) or modifications to the process operation (higher pH leaching).

Overall, the pilot facility and the accompanying analysis validate that AMD is a viable and promising feedstock for REE/CM production.

Accomplishments

Task 1.0 – Project Management and Planning

Subtask 1.1 – Project Management Plan

Approach

The Recipient shall manage and direct the project in accordance with a Project Management Plan to meet all technical, schedule and budget objectives and requirements. The Recipient will coordinate activities in order to effectively accomplish the work. The Recipient will ensure that project plans, results, and decisions are appropriately documented, and project reporting and briefing requirements are satisfied.

The Recipient shall update the Project Management Plan 30 days after award and as necessary throughout the project to accurately reflect the current status of the project. Examples of when it may be appropriate to update the Project Management Plan include: (a) project management policy and procedural changes; (b) changes to the technical, cost, and/or schedule baseline for the project; (c) significant changes in scope, methods, or approaches; or (d) as otherwise required to ensure that the plan is the appropriate governing document for the work required to accomplish the project objectives.

Management of project risks will occur in accordance with the risk management methodology delineated in the Project Management Plan in order to identify, assess, monitor and mitigate technical uncertainties as well as schedule, budgetary and environmental risks associated with all aspects of the project. The results and status of the risk management process will be presented during project reviews and in quarterly progress reports with emphasis placed on the medium- and high-risk items.

Results and Discussion

Project management functions were preformed to ensure that the project team executed all tasks and subtasks to completion and maintained consistent communications while working towards project objectives. WVU managed and directed the project in accordance with a Project Management Plan to meet all technical, schedule, and budget objectives and requirements. WVU coordinated activities in order to effectively accomplish the work, ensuring that project plans, results, and decisions were appropriately documented, and that project reporting and briefing requirements were satisfied. Additionally, bi-weekly meetings were held throughout the course of the project to monitor researcher progress and allow for collaborative understanding.

Subtask 1.2 – Technology Maturation Plan

Approach

The Recipient will develop a Technology Maturation Plan (TMP) that describes the current technology readiness level (TRL) of the proposed technology/technologies, relates the proposed project work to maturation of the proposed technology, and describes known post-project work necessary to further increase the technology TRL.

Results and Discussion

Technology needed to recover Rare Earth Elements and Critical Minerals (REE/CM) from acid mine drainage (AMD) has developed to the point where it produced an economically attractive feedstock. Prior studies included: (1) a regional survey assessing the content, distribution, and form of REE/CM in AMD and the related treatment byproducts (DE-FE0026444); (2) the design, development, and testing of a bench-scale process to extract, purify, and concentrate REE/CM from AMD treatment byproducts (DE-FE0026927); and (3) the development and testing of preconcentrate REE/CM from raw AMD (DE-FE0031524).

The current project (DE-FE0031834) initiated a new REE/CM revenue stream that potentially improves environmental outcomes for many coal mining districts while creating new jobs that would support a domestic supply chain for REE/CM. The project team structured the new research program in an aggressive track that includes commercial vendors for full-scale application at a pace needed to fulfill USDOE/NETL commercialization objectives.

A preliminary Technology Maturation Plan for this project was submitted to DOE on March 16, 2020. A final draft was submitted August 8, 2023.

Subtask 1.3 – Workforce Readiness Plan

Approach

The Recipient will prepare and maintain a Workforce Readiness Plan (WRP) related to the technology being researched under the project. The Plan must describe the skillset and availability of the workforce needed for future commercialization and deployment of the technology, including whether any related apprenticeships, certificates, certifications, or academic training are currently available. If a workforce with the required skills is not readily available, or if the technology is so new that a trained workforce does not yet exist, the Recipient's plan shall detail how the needed workforce could be developed, for instance, through coordination with educational institutions such as community colleges, technical schools, and universities; company-led in-house training; union training, etc. The Recipient will monitor and update its assessment of workforce availability and development plans throughout the life of the project.

Results and Discussion

The project team monitored and assessed workforce availability and development needs during the project, especially amid shifting COVID-19 regulations. These activities helped build the final WRP. A draft WRP was submitted to DOE November 18, 2020, along with WVU's Continuation Application documents. A final draft was submitted August 8, 2023.

Task 2.0 – Financial Plan for Commercialization

Approach

The Recipient will develop and periodically update a Financial Plan for Commercialization. At a minimum, the plan should explain the economic feasibility demonstrated by the Recipient's Excel financial spreadsheet model and include a description of the Recipient's proposed business plan for developing and commercializing their technology to economically produce salable REEs and CMs from U.S. coal and coal-based resources. Information to be included is an explanation of the hurdles and risks for factors such as: supply of process inputs; process and technology development; capital, operating, and maintenance cost; process operation factors; life-cycle environmental, permitting, and other regulatory factors; market demand and quantity/price points for output products; offtake agreements; downstream supply chain for refining products; international demand, supply, competition, and other considerations; etc.

Results and Discussion

A preliminary Financial Plan for Commercialization was submitted to DOE on March 16, 2020. The Financial Plan for Commercialization was periodically updated throughout the project as new data became available. A final plan was submitted September 7, 2023.

Task 3.0 – Techno-Economic Assessment

Approach

The Recipient will develop and provide NETL a Techno-Economic Assessment (TEA) based on testing and operation of the REE/CM recovery system. The Recipient will develop a detailed TEA that estimates the cost and performance for scale-up to a commercial demonstration.

Results and Discussion

Analysis Scope and Operating Scenarios

The technology domain evaluated in the techno-economic analysis for this project includes the process circuitry needed to upgrade hydraulic pre-concentrate (HPC) to a mixed or partially separated rare earth oxide (REO). Herein, this process option is denoted as MREO production. The business case for this scenario envisions that the MREO production process would be deployed at medium to large scale AMD discharges where the REE production volumes are sufficient to justify the capital investment and fixed cost. The light and heavy REO products (LREO and HREO) from MREO production are considered non-saleable intermediates, which must be further refined to generate market-ready materials for manufacturing and other end uses. As such, products from the MREO production process would then be shipped to a central refinery where they are further processed to produce saleable materials, such as individually separated rare earth oxides, metals, or other salts. For smaller AMD discharges, HPC would be produced using a passive approach and later shipped to a regional MREO production unit or directly to the central refinery.

This strategy necessitates a specific design strategy, which has bearing on the assumptions and protocols utilized in the techno-economic analysis. Most significantly, the process design seeks to minimize fixed operating costs and capital costs. Modular or skid-mounted equipment is assumed in the CAPEX estimation, and as such, limited provisions are added for facilities, site improvements, and other non-equipment capital costs. Moreover, the facility is assumed to operate with minimal staffing, as engineering, laboratory analysis, management, and other non-operation labor would be provided through as-needed contract services or through a central provider.

For the purpose of this analysis, HPC acquisition costs, including production, generation, and transport, were not included. On the other hand, cost reduction credits resulting from the reduced sludge disposal requirements were also not included in the analysis. These assumptions are justified given the business case parameters described above. Since the MREO production process will be integrated into existing treatment systems, HPC production and transport are considered negligible. Handling costs will be similar to those that would be incurred had the sludge been disposed of as waste, as such, the cost and credits are assumed to be a wash. Application of this assumption also provides a mechanism to evaluate the MREO production process in isolation to identify major cost drivers and sensitive factors.

Given this background, one key objective of this techno-economic analysis is to identify the processing route, scale, and input parameters that result in a profitable outcome. As such, capital and operating cost estimates were generated for the following options:

1. Commercial implementation of the pilot circuit using the “as tested” conditions for material balance and product production, namely including: HPC feed rate = 19 t/day (dry basis), 0.6% solids, 0.6% TREE by weight, LREO and HREO products only. It should be noted, though that 0.6% TREE should be considered the floor HPC grade. Testing over the course of the project showed a mean HPC grade of approximately 1.5%. See the TEA sensitivity analysis for a more comprehensive discussion on the influence of grade.

2. An improved feed grade scenario. CAPEX and OPEX remains identical to scenario 1; however, LREE and HREE product production is increased to account for increased HPC feed grade (2.0% versus 0.6%).
3. An optimized operating approach, whereby leaching is conducted at a higher pH (5.0). The scenario eliminates the need for a neutralization circuit, reduces acid consumption, and slightly reduces REE recovery. In addition, the option does not provide an opportunity for zeolite recovery.
4. An additional revenue case, whereby zeolite is added as a value-added byproduct. CAPEX is identical to scenario 1; however, additional labor is added to account for the zeolite recovery.

Capital and Operation Cost Estimate Summary

A summary of the revenues, operating and capital cost estimates for various plant scenarios is presented as **Table 1.**

Table 1. Capital and Operating Cost Estimate Summary.

MM USD/YR	Base	Increased Grade	High pH Leach	Base w/ Zeolite
Raw Materials	$ 2.12	$ 2.12	$ 0.31	$ 2.12
Energy	$ 0.04	$ 0.04	$ 0.04	$ 0.04
Labor	$ 0.36	$ 0.36	$ 0.36	$ 0.71
Sustaining Capital	$ 0.07	$ 0.07	$ 0.07	$ 0.07
Total Operating Cost	**$ 2.60**	**$ 2.60**	**$ 0.79**	**$ 2.94**
Bare Equipment	$ 1.36	$ 1.36	$ 1.32	$ 1.36
Installation	$ 0.34	$ 0.34	$ 0.33	$ 0.34
First Fills	$ 0.05	$ 0.05	$ 0.05	$ 0.05
Other Direct	$ 0.75	$ 0.75	$ 0.72	$ 0.75
Indirect Costs	$ 1.10	$ 1.10	$ 1.07	$ 1.10
Total Capital Costs	**$ 3.60**	**$ 3.60**	**$ 3.49**	**$ 3.60**
Revenues	**$ 2.45**	**$ 8.01**	**$ 2.21**	**$ 3.61**

Economic Scenario Assumptions

The cost estimation data described in the preceding sections was used to support a life-cycle economic analysis to assess the overall project profitability with respect to common project indicators including net present value, rate of return, and discounted payback period. In addition, the economic analysis was used to determine the minimum product selling price needed to achieve a positive net present value. This analysis was repeated for the four facility options, namely: (1) base commercial case; (2) increased HPC grade; (3) reduced pH leaching; and (4) base with zeolite production.

Many of the economic assumptions, including those regarding the financing structure, escalation rates, tax calculations, and operating period were supplied by National Energy Technology Laboratory (NETL) in the RFP for this project. Key economic assumptions utilized in this study include:

- All amounts are in US dollars.
- The total operational period for the plant is 20 years.

- Inflation was applied to sales revenue and operating costs using a fixed rate of 3% per year.
- Capital costs are spread over a period not to exceed three years, and the allocation between those three years is 10%, 60%, and 30% for years one through three, respectively. Thus, the total analysis period (capital purchase plus operating) is not to exceed 23 years.
- During the capital expenditure period, capital costs escalate at a constant rate of 3.6% per year.
- The project is debt financed for 50% of the total overnight capital requirement; the remaining 50% is financed by equity.
- The debt repayment terms include: 6% interest rate, 10-year loan period, and no grace period on debt repayment. The repayment uses a standard amortization schedule with constant payments throughout the payoff period.
- Working capital is not included in this estimate and will instead be borne by the operating entity at no cost to the project.
- The combined federal and local tax rate is fixed at 26%.
- All capital is depreciable, using a 150% declining balance depreciation schedule over 20 years. The depreciation method was not changed to straight line when conditions favored the switch.
- The mineral depletion rate for REEs is 14%. Depletion is charged at the appropriate rate times the net sales revenue after deducting royalties and any severance tax, provided that the total amount calculated by depletion rates does not exceed 50% of the taxable income before depletion.
- The plant is part of a larger commercial entity with sufficient revenue to offset negative taxable income. Thus, losses are not carried forward and are instead calculated as a "negative tax" that indicates the reduction in tax burden required for overall entity.
- No royalties are charged for the productions of REEs.

Lastly, the data presented in this section provide a summary of the most salient outputs needed to interpret the findings.

Product Pricing

Pricing has been established for the project based on supplied price deck from NETL. The most recent update available to the project team was the July 2022 prices as included in FOA 2854. These prices are elevated from the original December 2016 prices supplied in FOA 2003; however, they better reflect current market conditions. Additional raw material prices were determined from USGS data for zinc carbonate and zeolite.

Table 2 shows the baseline product price deck used in the economic analysis. For comparison, the December 2016 prices are also included, but were not used in the analysis.

Table 2. Baseline Product Prices.

Product	Unit Price ($/kg)	
	Dec 2016 (FOA 2003)	July 2022 (FOA 2854)
Scandium Oxide	$ 4,200.0	$ 2,000.0
Yttrium Oxide	$ 6.0	$ 10.00
Lanthanum Oxide	$ 2.0	$ 1.00
Cerium Oxide	$ 2.0	$ 1.00
Praseodymium Oxide	$ 2.0	$ 100.00
Neodymium Oxide	$ 42.0	$ 125.00
Samarium Oxide	$ 2.1	$ 3.00
Europium Oxide	$ 150.0	$ 30.00
Gadolinium Oxide	$ 32.0	$ 50.00
Terbium Oxide	$ 400.0	$ 1,000.0
Dysprosium Oxide	$ 230.0	$ 300.00
Holmium Oxide	$ 53.0	$ --
Erbium Oxide	$ 34.0	$ 50.00
Thulium Oxide	$ --	$ --
Ytterbium Oxide	$ 28.7	$ --
Lutetium Oxide	$ 796.6	$ --
Zinc Carbonate	$ 2.00	
Zeolite	$ 0.10	

REE Prices listed in **Table 2.** are generally for high purity, individually separate oxides with a nominal grade of 99.5% to 99.9%. To utilize these prices in the current MREO production scenario, a 20% discount was applied to account for the downstream separation. This discount is lower than the standard discount (25% to 30%) applied to typical MREO production processes due to the partial HREO/LREO separation that occurs. Typical REE distributions of the LREO and HREO products were used in conjunction with the baseline product prices and discount to produce a final product basket price.

Economic Results

Table 3 shows the relative revenue contribution from each saleable product for the four TEA scenarios. As indicated, the largest fraction of the revenue in all cases is derived from the LREO product, primarily due to the elevated NdPr pricing and the high fraction of NdPr in that product. HREO provides a significant fraction as well, largely owing to Tb and Dy. In all cases, zinc carbonate revenues were insignificant; however, it should be noted that the zinc carbonate is a natural byproduct of the REE production process and thus incurs no additional incremental cost. Interestingly, the zeolite product has the potential to be a significant revenue component, providing nearly 1/3 of the revenue in the zeolite production scenario.

Table 3. Relative Revenue Contributions from each Product for Alternative Plant Scenarios.

Product	Base	Increased Grade	High pH Leach	Base w/ Zeolite
M-HREO	37%	38%	37%	25%
M-LREO	60%	61%	60%	41%
Zinc Carbonate	3%	1%	3%	2%
Zeolite	0%	0%	0%	32%

Table 4 summarizes the key financial indicators from the project for the four alternative scenarios. Given the assumptions and inputs described above, the project was found to be economically favorable for the three latter cases. While increased grade does have a pronounced impact on profitability (see supplemental sensitivity analysis below), the final two options also demonstrate a unique tradeoff, as they are mutually exclusive (i.e., higher pH leaching eliminates the ability to produce a zeolite byproduct). This analysis suggests that higher pH leaching is the more robust process option; however, it should be noted that the two options breakeven at a zeolite price of approximately $0.15 to $0.17 / kg ($0.10 / kg was used in the analysis). Current USGS data suggest zeolite prices as high as $0.30 / kg, thus suggesting that this option may be worth further exploration.

Table 4. Summary of Economic Indicators for Alternative Plant Configurations.

Parameter	Base	Increased Grade	High pH Leach	Base w/ Zeolite
REE Production (t/y)	46.0	153.5	41.4	46.0
Zinc Carbonate Production (t/y)	33.8	33.8	33.8	33.8
Zeolite Production (t/y)	--	--	--	11,655
Total Production (t/y)	79.8	187.3	75.2	11,735
Operating Cost ($/kg REE)	$56.44	$16.93	$18.95	$63.87
Operating Cost ($/kg Total)	$32.56	$13.88	$10.44	$0.25
Capital Intensity ($/(kg/yr REE)	$78.17	$23.45	$84.12	$78.17
Capital Intensity ($/(kg/yr Total)	$45.10	$19.22	$46.36	$0.31
Net Present Value$_{10\%}$ ($ mil)	$ (4.49)	$37.74	$8.02	$2.60
Rate of Return	N/A	115%	43%	22%
Discounted Payback Period	N/A	0.5 op years	2.5 op years	6.5 op years

Task 4.0 – Provide Split Samples

Approach

The Recipient will provide NETL with a single sample that reflects the highest achieved REE concentration generated during conduct of project effort. The quantity of material to be provided to NETL shall be no less than 3 grams. Material Safety Data Sheets (MSDS) are required to accompany material supplied to NETL. NETL reserves the right for DOE/NETL employees or agents to witness the sampling and splitting. Results of any analysis arranged by DOE/NETL will be documented in a Publicly Releasable Report accessible on the NETL website.

Results and Discussion

Two split samples per the above specifications were shipped to NETL on December 4,2023. While the original task calls for one single sample, the two samples are representative of process improvements that went above the expectations of the project. Through project-funded research, the team was able to split the mixed rare earth oxide sample into light and heavy mixed rare earth oxide samples respectively. These samples are representative of the two products that are generated at the pilot facility. Note that sample “WVWRI MLREO” on an oxide basis consisted of 94% mixed rare earth oxides and is primarily concentrated with light rare earth oxides. Sample “WVWRI MHREO” on an oxide basis consisted of 93% mixed rare earth oxides and is primarily concentrated with heavy rare earth oxides. Both samples exceeded the minimum project purity grade of 90% by at least 3%.

It should be noted that **Table 5** represents analytical results of subsamples of the samples sent to NETL. These samples were processed by WVU’s WISER Analytical lab. The lab uses a sodium peroxide fusion to digest all solid samples prior to analysis. WVU generated several MLREO and MHREO samples throughout the project of similar purity. These samples were sent on to Virginia Tech for further processing.

Table 5. Analytical results of split samples sent to NETL.

		WVWRI MLREO	WVWRI MHREO
Al	**mg/kg**	6,054.7	7,278.9
Ca	**mg/kg**	25,073.0	6,755.6
Co	**mg/kg**	68.2	6.3
Fe	**mg/kg**	1,578.0	900.4
Li	**mg/kg**	-	2,545.7
Mg	**mg/kg**	164.9	735.0
Mn	**mg/kg**	5,496.8	1,357.4
Ni	**mg/kg**	95.3	249.0
S	**mg/kg**	445.4	1,748.2
Si	**mg/kg**	735.2	528.0
Zn	**mg/kg**	2,615.7	252.9
TMM	**mg/kg**	42,327.4	22,357.4
Sc	**mg/kg**	8.1	0.6
Y	**mg/kg**	3,585.2	222,551.0
La	**mg/kg**	51,629.1	37.1
Ce	**mg/kg**	211,636.8	216.1
Pr	**mg/kg**	45,053.0	42.3
Nd	**mg/kg**	250,906.0	232.2
Sm	**mg/kg**	77,865.6	418.0
Eu	**mg/kg**	17,152.5	506.1
Gd	**mg/kg**	64,933.0	8,477.4
Tb	**mg/kg**	2,520.3	5,268.1
Dy	**mg/kg**	4,775.8	35,058.4
Ho	**mg/kg**	374.7	7,582.0
Er	**mg/kg**	708.3	20,059.1
Tm	**mg/kg**	25.4	2,185.6
Yb	**mg/kg**	302.3	9,275.3
Lu	**mg/kg**	35.3	1,116.9
TREE	**mg/kg**	731,511.3	313,026.3
REE Purity	**%**	94%	93%
Th	**mg/kg**	-	0.3
U	**mg/kg**	17.8	7.4

Task 5.0 – Feasibility Study

Approach

The Recipient will develop and provide NETL a Feasibility Study 30 days prior to the Go/No Go decision point. The Feasibility Study will provide NETL with information on, but not limited to, availability of the proposed feedstock; information on environmental impacts; process flow diagram(s); product yield and concentration; estimated system costs; etc.

Results and Discussion

Preliminary efforts for the feasibility study, including the initial data review and economic modeling, were initiated in late 2020. In early 2021, the project team requested pushing back the Go/No-Go

decision point, and consequently the Feasibility Study associated with it, to fall of 2021. DOE officially approved this request on March 17, 2021. The project team submitted its Feasibility Study on September 1, 2021. The team utilized techno-economic models originally developed in DE-FE0026927; however, these tools were updated with additional process knowledge gained from the laboratory testing and simulation studies conducted to date. Salient findings are provided below.

To assess the feasibility of recovering rare earth elements (REEs) and critical minerals (CM) from acid mine drainage, a detailed technical review and economic evaluation were conducted. The process evaluated in this study includes an integrated upstream water treatment and REE concentration step as well as a downstream REE purification and recovery process. In practice, the former would be conducted onsite at numerous existing AMD discharges, while the latter would be installed at a centralized processing location.

To facilitate the technical and economic review, the engineering team used a spreadsheet-based economic assessment tool that integrates technical, economic, and financial inputs to facilitate a systems-level optimization. The primary input data for this analysis consisted of experimental testing conducted at both the laboratory-scale and continuous bench-scale in earlier phases of the project. In addition to the experimental data, other inputs to the techno-economic analysis were derived from literature data and process engineering assumptions.

The actual cost analysis was conducted at a small industrial production scale of 1.81 metric tons per day of REE product (4.5 metric tons per hour of preconcentrated feed). Process performance and costs were assessed across five process modules covering onsite preconcentrate generation, leaching, neutralization, solvent extraction, and REE oxalate precipitation. The final saleable product was assumed to be a high-grade (>90%) mixed rare earth oxide.

Final economic indicators from this assessment are given in **Table 6** below. This data shows that under the baseline scenario, the process is economically viable with a positive NPV and a rapid payback period of three operating years. Subsequent sensitivity analyses and Monte Carlo simulations showed that preconcentrate grade, REE price, leaching % solids, and REE recovery were significant factors when tested under their anticipated range values. The model was particularly sensitive to feed grade, as an increase from 2% to 5% TREE prompted a 10-fold increase in NPV from $35 million to $350 million.

Table 6. Summary Economic Indicators.

Parameter	Unit	Value
Technical Results		
Plant Feed Rate	t/hr	4.5
Plant Feed Grade	ppm	20,000
Overall REE Production	kg/hr	75.3
Economic Results		
Overnight Capital Cost	$	12,937,311
Constant Dollar OPEX	$ / yr	22,497,552
(unit conversion)	$/ st feed	557.97
(unit conversion)	$ /kg REE	37.06
Constant Dollar Revenue	$ / yr	28,632,604
Net Present Value (@10% discount)	$	35,154,249
Internal Rate of Return	%	44.1%
Payback Period	Operating Years	3

Task 6.0 – Upstream Concentrator: Test Unit Construction

Approach

The Recipient will design and construct a scaled-down version of the staged precipitation process to be used in upstream concentration. Since the larger-scale concentrator will be installed in-line with an active AMD treatment process that must meet regulatory water treatment standards, the breadth of test conditions will be somewhat limited. Alternatively, this test unit will allow testing under extreme conditions and allow rapid optimization of various operational conditions.

This fully continuous, laboratory-scale test unit will be designed to match the form and function of the full-scale unit, with approximate capacity of 1 gpm of AMD feed. It will nominally consist of three mixers and three thickeners in series, each with independent pH control via staged base addition. The test unit will be housed in the Recipient's existing bench/pilot-plant facility, which includes an onsite analytical lab for rapid product analysis.

Construction of this unit will commence immediately upon project award to maximize the time available for testing before the full-scale system is commissioned. The Recipient will work with product vendors during startup to ensure that all equipment is installed to vendor specifications, and on-site visits may be requested from key equipment providers. A final safety review will be conducted after construction but before work is commenced.

Results and Discussion

Initial system testing plan

To design and operate the proposed system, a procedural plan was developed before the construction of the test unit. Feedstock characteristics vary with weather, which impacts the chemical demand needed to obtain the preconcentrate. To understand the feedstock inflow variation, raw AMD samples were collected from the host site, laboratory jar tests were performed, and outcomes were correlated to field measurements. The jar tests also generated data for optimization of gangue metals precipitation before preconcentrate generation, such as pH settling points, settling times, and the correspondent chemical dosages. In addition, an opportunity for a preliminary filtration study was identified and integrated into the process. With the procedural plan in place, the system was designed, and the piping and instrumentation diagram (P&ID) below simulates the full-scale treatment process, represented in **Figure 1**.

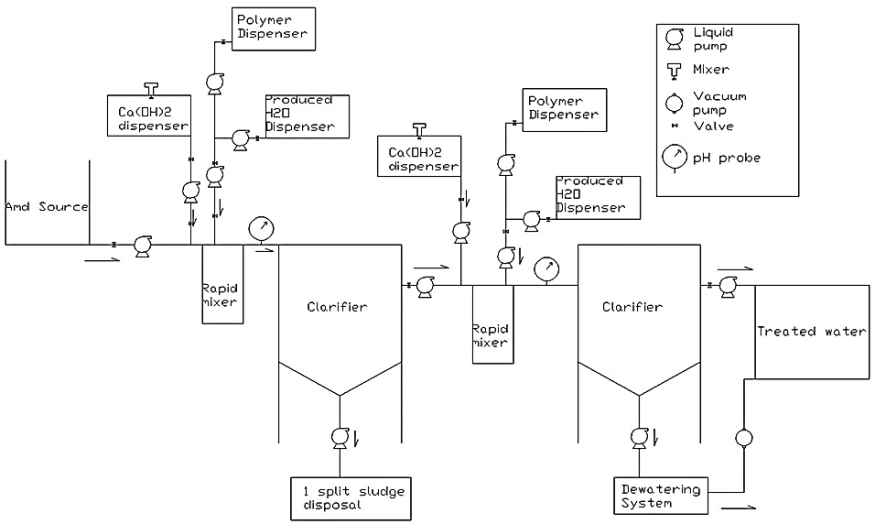

Figure 1. Bench scale clarifier P&ID flow process.

Assembly of the test unit

The two sets of bench scale clarifiers were ordered and delivered to the WVU-REE facilities in early January 2020. The clarifiers were cleaned for grease removal and assembled in place. Tubes, connections, and parts were purchased. The flowrate is controlled by peristaltic pumps and the chemical additions by diaphragm pumps. The flow from the rapid mixer to the clarifier is gravitational. An elevated platform was built adjacent to the test unit. The rapid mixer is composed of two units: the first unit is for the addition of the pH modifier and the second unit is for the addition of a flocculation agent. The Upstream Concentrator test unit assembly is shown in **Figure 2.**

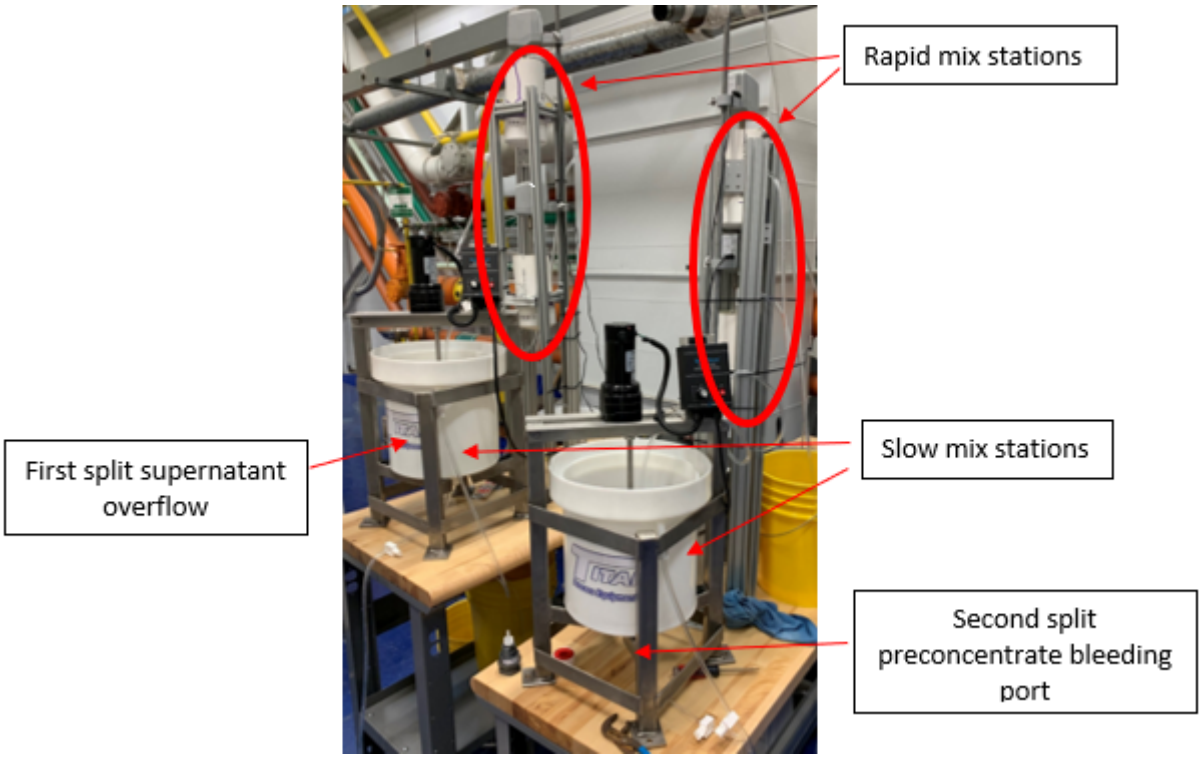

Figure 2. Upstream Concentrator (Bench Scale).

Task 7.0 – Upstream Concentrator: Test Unit Parametric Evaluation

Approach

In this task, the scaled-down upstream concentrator test unit will be evaluated in a series of parametric tests. Prior to testing, raw AMD from the host site will be procured and delivered to the Recipient facilities in 250-gallon totes. Upon receipt, the raw water will be evaluated for pH as well as major, trace, and REE metal content. These values will be compared with records from the current AMD treatment operator to ensure that water used in these tests closely resembles the typical discharge at the host site.

Data from prior laboratory and shakedown tests will be used to generate a detailed test matrix using a statistical experimental design. Nominally, the factors to be considered in these tests include the number of incremental pH steps needs (one, two or three), the type and concentration of pH modifier (e.g., lime, caustic soda, ammonium hydroxide, magnesium hydroxide), incremental pH set points (3 to 8 inclusive), and feed flow rate (design capacity -50%/+500%). Tests will be conducted over an eight-hour operating shift, with each experimental condition constituting a single shift. Experiments will be blocked and repeated to assess experimental error while mitigating the influence of covariates, such as sludge

heterogeneity and ambient environmental conditions. The tests will be repeated for any alternative host sites to be considered.

The results from this experimental design will be analyzed using a response surface methodology to identify the optimal conditions leading to the highest recovery and selectivity of REE/CMs. Initial efforts will focus on technical success criteria (i.e., grade, mass recovery, separation efficiency); however, economic factors (i.e., operating costs, value-based recovery) will also integrated into the performance objectives as testing continues. The REE preconcentrate precipitates from these tests will be analyzed with Scanning Electron Microscopy (SEM) and X-Ray Diffraction (XRD) to assess the form and structure of the REE/CM in the final product.

Results and Discussion

Material Mineralogical Analysis of Preconcentrate

An open top flat filter constructed using Solmax (previously Tencate) filter media was utilized to dewater HPC and explore the relationship between solids content over time. Over the course of several days, various HPC samples were taken with the resulting solids content beginning at approximately 1.5% initial solids by mass to 85% solids. A portion of the sample taken on the ninth drying day (85.2% solids by mass) was analyzed through X-ray Diffraction (XRD) (**Figure 3**). The analysis showed that the sample was fully amorphous, with no crystalline mineralogical phase observed.

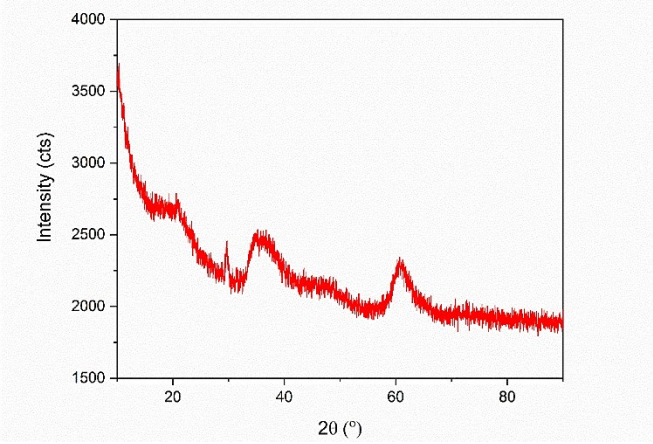

Figure 3. X-Ray Diffraction spectrum of an HPC sample after nine days of drying time.

Experimental Testing Phase

The test unit was operated inside the WVWRI research facility, and its purpose was to produce preconcentrate (both with and without polymer flocculation) for REE quality analysis and to evaluate the boundary limits of the clarifier. The raw AMD was treated using $Ca(OH)_2$ at 0.01 mol/liter. The floc that formed naturally under these conditions were light in weight and showed low settling velocities. The next phase was to produce preconcentrate using the previous pH splits with the addition of polymer flocculant. Because of operational restrictions, the stock solution of flocculant concentration was reduced to 0.1%. The dosages for each split were based on recommendations from previous jar test data. **Figure 4** shows a comparison of the un-flocked versus flocked second-split preconcentrate.

Figure 4. Operation of bench-scale clarifier (left) without addition of flocculant, and (right) addition of flocculant.

Optimization of Polymer Dosing and Estimated Sludge Mass

During operation of the bench scale clarifier, polymer addition was managed to control floc size and conform to system limitations while optimizing flocculation and precipitation. The flocculated precipitate underflow was collected by siphoning from the bottom of the two clarifiers. The dewatering/settling properties of the different flocculant doses were measured using specific resistance to filtration (SRF) experiments. It was determined that the average polymer stock solution addition resulting in a satisfactory settling velocity for the first pH split was 4.3 µL/L of raw water, and 8.1 µL/L of first split supernatant for the second pH split.

Underflow samples were also collected, weighed, and dried in an oven (103-105 °C) overnight. The obtained dry mass was then correlated to the total volume processed for a dry mass per unit volume ratio. **Table 7** lists the sludge production in dry mass(g)/vol (L) of A-34 AMD water using flocculent at 4 ppm for first split and 8 ppm for the second split. The sludge production is reported per volume of AMD water processed. These results aided in the estimation of sludge production rates for pilot-scale operations and became an important variable for the design of dewatering devices and downstream operations.

Table 7. Dry mass production rate using a bench scale system.

Treatment step: Sludge production w/ PE6070	Dry mass (g)/ vol (L)
1st Split (4.5, 4ppm)	0.262
2nd Split (8.5, 8ppm)	0.193

Performance Testing Phase

A small scale (1:10) rectangular clarifier (see **Figure 5**) was custom-built to evaluate the performance of HPC generation and settling under similar conditions to what would be in operation at A-34. This small-scale clarifier would generate HPC continuously over a period of eight hours or more. First-split feedstock for the 1:10 Clarifier was generated in 1000-gallon batches, using flocculant to assist with settling and hydrated lime for pH adjustment. This feedstock would then be pumped to the first compartment (rapid mix) of the 1:10 Clarifier at a constant flow, along with the addition of hydrated lime through a static mixer. The addition of the lime was calibrated using a peristaltic pump and pH was monitored in both the rapid mix and slow mix compartments.

With the addition of diluted polymer to the rapid mix compartment, the team was able to gather useful insights on the flow path behavior of the flocculated particles as well as optimize polymer consumption under continuous treatment conditions. These upgrades to the upstream concentrator test unit allowed the team to mimic the HPC generation process of the full-scale unit and process up to 5000 gallons of raw water per week. This provided an abundant generation of HPC for further evaluation, such as determining settling and filtration times and chemical consumption rates.

Figure 5. Photos (shown left to right) of 1:10 scale upstream concentrator test unit, 1000-gallon batch reactor for generating both first and second spilt pH, and full-scale upstream concentrator located at A-34.

Task 8.0 – Upstream Concentrator: Full-Scale Unit Construction

Approach

The West Virginia Department of Environmental Protection (WVDEP) will construct a full-scale AMD treatment plant with an integrated REE/CM recovery operation. The Recipient will provide technical input and guidance on the modifications and adaptations needed to integrate REE recovery with traditional AMD treatment. These alterations are expected to include: (1) staged precipitation using multiple clarifiers/thickeners in series; (2) independent pH control in each clarifier; and (3) additional materials handling and filtration units to recover and dewater the REE-enriched concentrates.

To augment the traditional AMD treatment system, the Recipient and Sub-Recipients will install a state-of-the-art automation and control system to remotely monitor key operating parameters.

This package is expected to provide real-time measurements of pump and mixer motor conditions, pH measurements, select ion concentrations, and other variables. These values will be logged in an archival data format and used for feedback loop control.

Specific activities associated with this task include (1) environmental review, including any updates, modifications or amendments to current permits, (2) engineering design and bid preparation, (3) materials and service procurement, (4) component fabrication and delivery, (5) on-site construction, and (6) commissioning and startup. All pertinent local, state and federal regulations will be followed by all participating subcontractors. Upon completion of the construction activities a safety analysis/review will be performed prior to equipment startup and shakedown.

Results and Discussion

Site Engineering

Meetings were held with WVDEP to discuss the layout of the treatment plant at A-34, along with the kW loading of the power system. WVDEP produced the preliminary drawings for the site (**Figure 6**) and prepared a bid package for construction. Drawings for configuration of the lime silo were also procured by WVDEP, which were provided to the vendor for fabrication. Once the contract for construction was

awarded, initial onsite work consisted of draining and cleaning the ponds as well as removal of the preexisting silos to facilitate placement of the new facility.

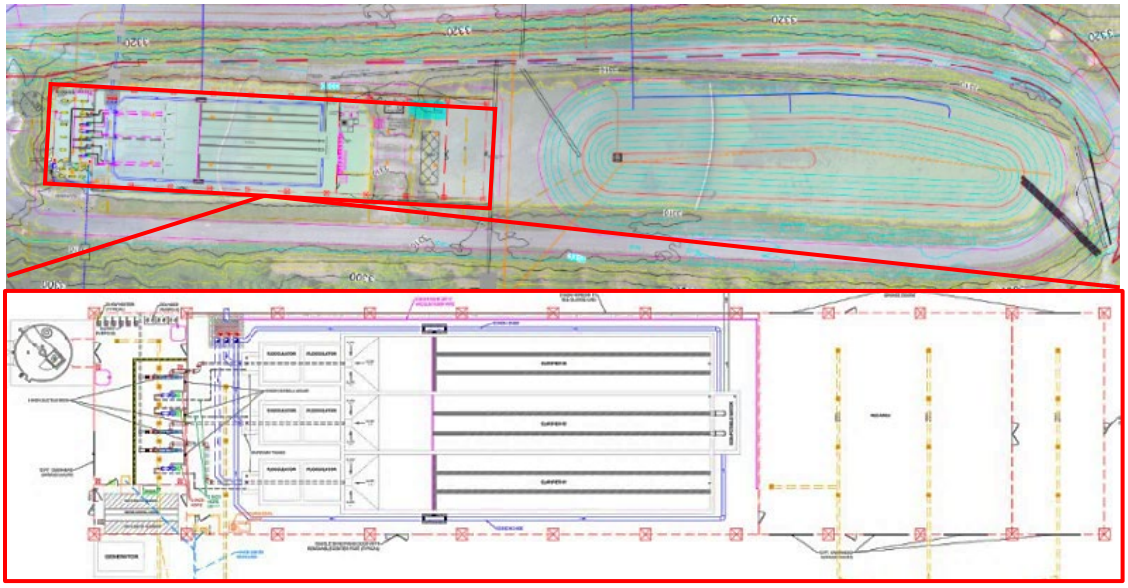

Figure 6. (top) Aerial view of site layout; pre-construction, and (bottom) plan view of proposed building construction.

Site and Clarifier construction

During early construction (November 2020), WVDEP's contractor installed a pipeline from the pre-existing ponds to the disposal pit to assist with the removal of sludge from the building site, which was also to be later used for sludge removal from the clarifiers. The contractors also established a chemial regime for treatment of the remaining ponds, as they were responsible for maintining water quality for the duration of construction. After the lower pond was cleared, the area was able to be reutilized for the pouring of the silo pad foundation and concrete forms for the clarifiers (**Figure 7**). While utilization of the former pond contributed to less excavation, fill dirt was required to expedite the earth filling around the clarifiers and under the plant building footprint.

Figure 7. Early construction of the A-34 site (formerly lower ponds). Construction utilized preexisting pond to pour concrete forms.

Construction of the building's foundation took approximately six months, largely due to the pour-in-place method of fabrication for the clarifiers. This process was conducive to a high demand for manual labor onsite. It should be noted that since the start of this project, technology has further developed to provide prefabricated clarifier forms. **Figure 8** shows the A-34 site before and after construction.

Figure 8. Before and after photos of the A-34 site.

While the foundations for the building were being set, drawings were finalized for the layout of the REE portion of the plant. Before building construction began, the sludge rakes and tube settlers for the clarifiers were installed. The building contractor was onsite by April of 2022, and WVU was able to move in July of the same year. By this time, WVDEP had electrical and automation installed and were ready to initiate shakedown testing (**Figure 9**).

Figure 9. (left) Control panels for WVDEP's treatment monitoring, and (right) First and second clarifiers on standby for shakedown testing.

Of the three clarifying "trains," all can accept incoming flows, which can be preferentially controlled by a series of gate valves at the source collection box. This allows for larger treatment capacity and a variety of treatment options. Trains #1 and #3 are identical in design; one train can act as the first stage clarifier for HPC capture while the other can be used for direct treatment or reserved as a backup during maintenance. While train #2 can also directly treat incoming flows, it is specifically designed for preconcentrate generation. It sits at a lower elevation so that it may be gravity fed first-cut treated AMD from one of the other two trains.

Automation and Controls

To easily manage the equipment and decrease the number of onsite working hours, the AMD plant was equipped with an automated system and control interface. This interface shows information for all equipment and controls, such as equipment status, inputs and outputs, sensor readings and trends, and applets for automation programs. The interface can also be used to remotely access monitoring and equipment control. From this interface (**Figure 10**), the operator can oversee treatment operation and make any adjustments automatically.

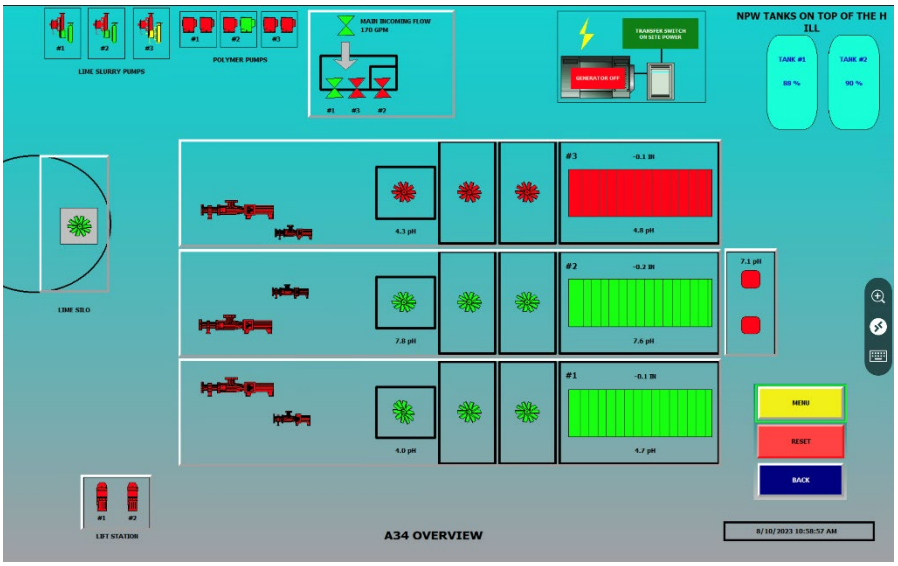

Figure 10. RD Client overview screen of A-34 site monitoring.

Subtask 9.0 – Upstream Concentrator: Full-Scale Unit Operation

Approach

This task includes all work associated with the evaluation, operation, and optimization of the upstream concentration unit. Prior to testing and operation, the Recipient will prepare a Sampling and Analytical Plan that will describe various components of the data collection activities associated with this unit operation. At a minimum, the plan will include: (1) the specific locations of sampling points within the system and expected consistency of those samples (liquid, solid, or slurry); (2) the specific procedures for obtaining, handling, transporting, and storing various sample types; (3) the expected frequency and extent of sample collection for both routine and intensive analysis; (4) the specific protocols for analyzing samples and interpreting the resultant data; and (5) the protocols for retaining and archiving samples.

After finalizing the Sampling and Analytical Plan, a test matrix will be developed to gather performance data under different operating conditions while ensuring that the final water discharge meets the National Pollutant Discharge Elimination System (NPDES) permit requirements.

The test matrix will be based on the results from the small-scale unit evaluation and will include expected variations in AMD flow and REE concentration that follow seasonal variations throughout the calendar year. These natural variations will be tracked over time and used to evaluate the robustness and resiliency of the REE/CM enrichment process.

After identifying and validating the optimal process operational parameters, the upstream concentrator will be operated continuously at those settings for the remainder of the project period. All REE/CM preconcentrates generated during this time will collected into 55-gallon drums or geotextile super sacks

and stored for future testing in the downstream processing units. All waste generated from the process will be retained by the WVDEP and disposed using standard approaches. During this operational period, various technical performance metrics and chemical consumption values will be routinely monitored and used in cost-benefit analyses and environmental impact studies.

Recipient technical personnel will be on-site during the project, from initial startup through detailed test work. These researchers will monitor the day-to-day operation of concentration process and provide expertise for the analysis and interpretation of the test data. WVDEP will also provide key assistance and technical labor throughout this phase as well as the longer-term operational phase.

Results and Discussion

By September of 2022, WVDEP's upstream concentrator was fully operational. Since startup, the plant has treated an average flowrate of 200-600 gpm of raw AMD. This flowrate fluctuates with the seasons and rainfall; historical flowrates have been seen as low as 150 gpm and as high as over 800 gpm. The upstream concentrator is capable of treating this range of volume and can be fully utilized for flows up to 1000 gpm.

The system follows a two-stage treatment plan, where the first stage primarily precipitates Iron from the raw AMD, and the second stage generates hydraulic pre-concentrate (HPC) for REE recovery. In conjunction with WVDEP, the setpoints of the pH splits have been slightly modified from the original process design. The first split pH was increased slightly to help aid in iron sludge settling, meanwhile the second split was lowered slightly. WVDEP hypothesized that higher pH in the second stage was causing Aluminum concentrations to be close to the NPDES-permitted discharge limit. Analytical results indicated that decreasing the second cut pH slightly had minimal effect on TREE recovery and grade.

The charts below in **Figure 11** elucidate the performance of the two-stage treatment on major metal removal, alongside REE capture performance. The treatment process effectively captures almost all TREE after the first stage and removes more than 90% of Iron, Aluminum, and Zinc before being discharged to the final settling pond.

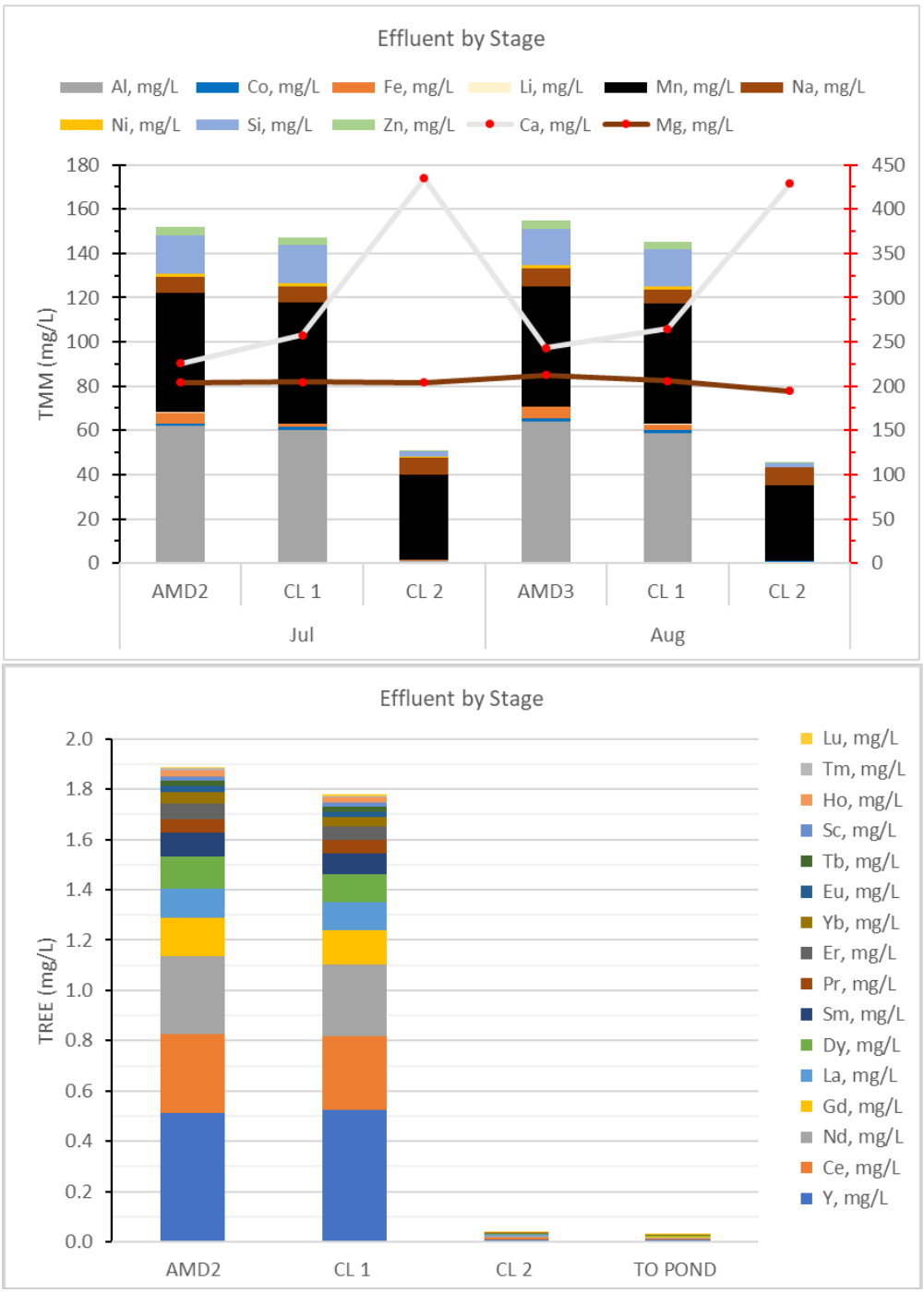

Figure 11. Major metal (TMM) (top), and (bottom) rare earth element (TREE) concentrations (in mg/L) throughout each treatment stage. Note, data marked in red indicates secondary axis.

To improve settling inside the second-stage clarifier, a constant dose of 1ppm emulsion polymer is supplemented to the rapid mix chamber. To further increase percent total solids and improve dewaterability, a secondary application point has been established by installing a polymer line directly to the suction side of the HPC transfer pump. Flocculation at the second application point only occurs when HPC underflow is pumped from the clarifier either to long-term storage or the REE treatment

portion of the plant. **Figure 12** and **Figure 13** compare the average monthly total solids content of HPC underflow with average inflow rates and solid assay summaries, respectively.

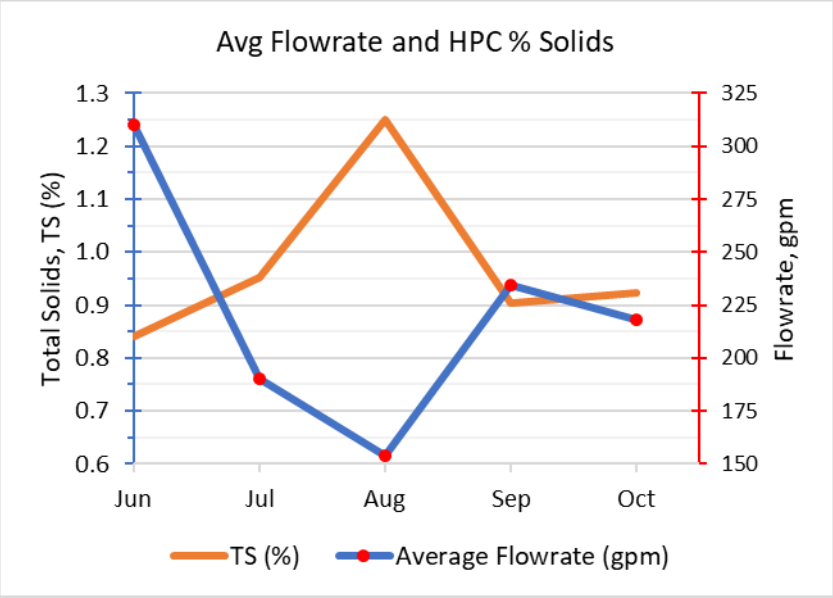

Figure 12. Comparison of 2023 monthly AMD flowrates and change in percent total solids of HPC collected. Note, data marked in red indicates secondary axis.

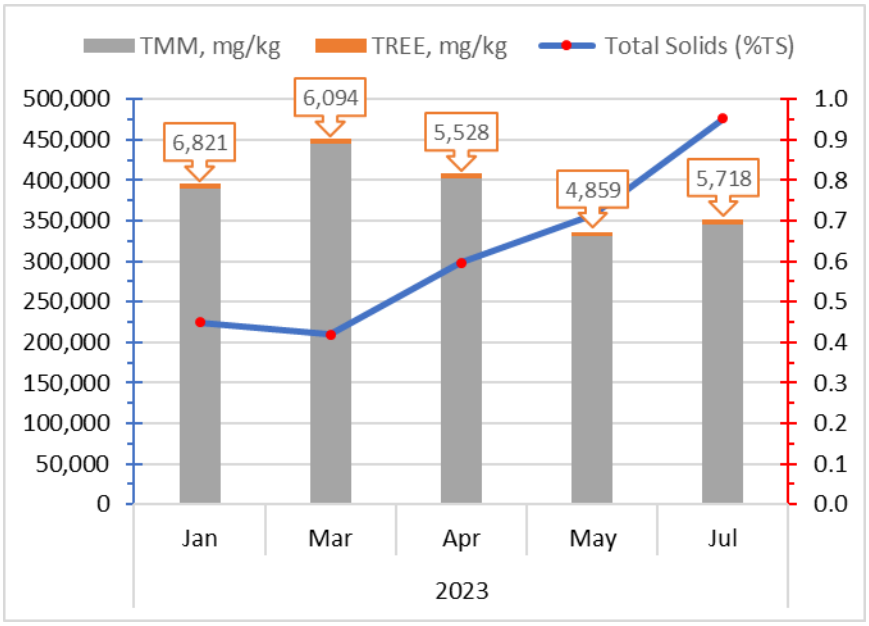

Figure 13. Monthly HPC solid assay results of TMM and TREE (in mg/kg), in conjunction with solids content of collected samples (as %TS). Note, data marked in red indicates secondary axis.

Subtask 10.0 – Acid Leaching/Solvent Extraction: System Design

Approach

This task includes all work elements needed to prepare a System Design Package for the pilot-scale acid leaching/solvent extraction (ALSX) unit. This system will be designed to process the preconcentrates generated from the large-scale upstream concentration unit. The final System Design Package will contain detailed information on the pilot-scale system components and specifically include: (1) a mass-

balanced process flowsheet, (2) piping and instrumentation diagrams, (3) a proposed facility layout, (4) a construction cost estimate based on vendor quotes, (5) a daily operational cost estimate, and (6) final engineering drawings of the pilot-scale plant.

Initial efforts in this task will focus on detailed flowsheet engineering. Bench-scale test work from prior studies will be used to guide design variables for specific unit operations, to include: leaching retention time, leaching acid type and expected consumption rates, leach residue filtration requirements, number and size of solvent extraction vessels, diluent type, extractant type and concentration, unit interconnections, and other miscellaneous items. A final internal design review will identify opportunities for process intensification and ensure that the bench-scale design will meet the specific project objectives itemized above. The Recipient will also conduct a fatal flaw analysis to identify factors that could preclude or severely impact the technical performance, economic feasibility, environmental impact, and/or worker health/safety of the proposed design.

The proposed location for the pilot-scale facility will be co-located with the upstream concentrator at the host site. This location has adequate access to water, power, and other utilities that will be required for the pilot-scale system. Only minimal changes to the facility will be required prior to system commissioning.

Results and Discussion

Pilot SX

The research team identified a vendor for SX equipment and commissioned initial design activities. For construction purposes, a generic configuration of four extraction, four scrubbing, and four stripping stages in series was used.

Batch SX

In designing the hydraulic pre-concentrate (HPC) dewatering circuit and acid leaching circuit, it was found that the pilot SX unit did not have enough capacity to meet the demands of the upstream process. Even if configured into three solvent extraction cells, the pilot SX only had a capacity throughput of 180 gallons per hour (gph). With this knowledge, the team sought to design a unit at low cost but with high throughput. In bench top lab testing, the team either utilized beakers or circular mixer settlers with small fins to promote mixing. Based on the parameters of the upstream process, the team sought to design a unit that could have a throughput of at least 400 gph. Using the desired operational parameters and modeling the unit off of the lab scale test unit, the team created the Batch Solvent Extraction Unit (BSX). The BSX acts as a mixer and settler. It is capable of processing 550 gph of PLS at O:A zero to 15%. It is equipped with sensors and flow meters to monitor the tank inputs and outputs as well as the organic extractant level to ensure it never reaches the aqueous outlet point. The mixer impeller is to be the same as the one in the pilot SX or benchtop SX units but scaled to fit the BSX unit.

HPC Dewatering Circuit

Using data from laboratory acid leaching, the team found that HPC had to be of at least 1% solids to facilitate HPC processing to PLS. Given the fact that PC in a Hydraulic form offered decreased CapEx costs for filtration and acid leaching downstream, the team sought to increase total solids coming from the clarifier at 0.2% to at least 1%. Given flocculation and settling results found in Task 19, it was found that, with proper flocculation, a 1000-gallon cone tank could be settled to 250 gallons of HPC at 1 to 1.5% solids in one to two hours. The team designed a dewatering circuit of five (5) 1000-gallon cone tanks. The circuit could be filled in an hour and a half and then fully decanted in a total of 3.5 hours.

Each tank was designed with a series of automated valves to fill, drain, and transfer HPC from the tanks. The tanks were also designed to be easily automated in the future with the addition of level sensors.

Acid Leaching Circuit

Bench scale laboratory testing indicated the need for an acid leaching reaction vessel and a PLS neutralization vessel to generate PLS acceptable for solvent extraction. Given the upstream design of the HPC dewatering circuit, 1600-gallon tanks were selected for both reaction vessels. Each tank was designed with appropriate pumps, valves, and educators to allow for proper mixing of the reaction vessel, settling of residuals, and removal of PLS supernatant.

The acid leaching tank was designed to autonomously add acid to the tank via a chemical metering pump. This pump was controlled by pH monitoring equipment. Additionally, to aid in residual settling, a flocculation system was designed to deliver flocculant to the tank at the completion of acid leaching. The neutralization tank was designed in a similar manner to the acid leaching tank but delivers base to the tank instead of acid.

The acid leaching circuit was also designed to dispose of its respective residuals (Leaching residual and Synthetic Zeolite) via the bay area of the plant. These residuals could either be pumped to a disposal box that returned them directly to clarifier 1 or to hanging geosynthetic bags for further filtration.

It should be noted that under optimal conditions the initial design for the acid leaching circuit was to have two trains to generate PLS. Owing to financial restrictions (primarily large increases in supply costs due to inflation following the pandemic), only one PLS train was installed.

Stripping Circuit

With the pilot SX unit intended to be entirely utilized for solvent extraction, a new stripping circuit was designed. This circuit was designed to perform each process step in a batch sequence. Laboratory data indicated that a prestripitation process would separate mixed rare earth oxides into light and heavy rare earth oxides (LREO and HREO, respectively). Each process step in the stripping circuit takes several hours to complete. Due to this, the tanks were sized at a minimum of 600-gallon total capacity so that a single strip cycle could handle all of one process week's loaded organic if the plant were running under optimal conditions. The circuit was designed with two vessels for stripping, one vessel for reagent preparation, and one precipitation tank to generate HREOs from strip liquor.

Both stripping vessels were designed with multiple valves and flow meters to send material to appropriate processing locations as well as to promote hydraulic mixing via educators. The valves were all designed so that they could easily be automated or locally controlled by an operator. Additional considerations were taken due to the use of concentrated acid to ensure a proper unit would be installed to capture any fumes.

Both the reagent preparation tank and the precipitation tank were designed with an automated pH control that would meter appropriate amounts of base into solution without the need of an operator. Both tanks were also designed with automated valves and pumps that were capable of mixing or sending material to the correct area of the process.

Optimal Design

The optimal design was completed by the team in May of 2022, but the electrical and automation contractor had still not finished their design for install at that time. Upon receipt of their quote to automate the system in August of 2022, it was determined that insufficient funds were available to automate and staff the plant if the full design were implemented. Supply chain issues and increasing inflation also made it unlikely that the project could be completed on schedule if the initial design were

implemented. Due to this, much of the design criteria above was installed but at a lower efficiency. All automated valves and tanks were installed except for a second PLS processing train. Despite this, all valves and pumps were set up to be locally controlled instead of using a Programmable Logic Controller (PLC). The team installed the final design to be capable of being upgraded to achieve the optimal specs below. Had the original design plans been implemented with the plant running four days per week, 20 hours a day, the plant would have had the capacity to hit the production goals in **Table 8** below.

Table 8. Optimal Plant production estimates.

Daily Mixed Rare Earth Oxide production@ 90% Purity	4.5	Kg/day
Yearly Mixed Rare Earth Oxide production @ 90% purity	1.6	t/yr
Yearly HPC capture (without plant operation)	266.0	Dry t/yr
Yearly MREO capture (without plant operation)	3.5	t/yr

Task 11.0 – Acid Leaching/Solvent Extraction: System Procurement, Construction, and Installation

Approach

The final system design will be used to prepare bid packages for key pieces of equipment, fabricated components, and services needed to complete the installation of the pilot-scale facility. These bid packages will be reviewed by project personnel prior to submission, and the final vendor selection will be based on the overall cost, availability, and suitability for the proposed duty.

Prior to equipment delivery, the Recipient will begin site preparation activities. This task may include clearing unnecessary equipment, reinforcing foundations or structures, and/or adding mechanical and electrical utilities. These initial preparations will ensure that equipment installation and assembly can be completed in a timely manner after delivery.

Fabricated components and final equipment will be shipped directly to the host site. Upon receipt, the Recipient will inspect all purchased items to ensure that the materials of suitable workmanship and quality. As equipment is delivered, the Recipient will retain important operational, maintenance, and worker safety manuals to create an in-house technical library for future reference. This documentation will be used to generate detailed protocols for start-up and shut down operations as well as other unique operational configurations.

Field construction activities will begin as materials are received on site. This work task will include the installation of foundations/buildings, process and ancillary equipment, chemical storage and secondary containment, and instrumentation and controls. The Recipient will work with subcontractors to ensure that all construction activities follow all pertinent regulations. After installation, all equipment will be appropriately plumbed, and the instrumentation will be properly calibrated. A final safety review will be conducted after construction but before work is commenced.

Results and Discussion

General Procurement

Given the designs developed under Task 10, the project team built out those designs with the most cost-effective and commonly available supplies. Most common supplies came from WVU partners Grainger, Lowes, or McMaster Carr. These suppliers would commonly be compared to find the best price for needed material. With the exception of chemical inlet lines and the pilot SX, the entire plant was designed to be built with schedule 80 two-inch PVC pipe due to its compatibility across a wide variety of harsh chemicals. All plumbing and tanks were securely attached to the surrounding structure of the

building or the floor using standard mounting brackets and Unistrut.

All of the plastic process tanks to be utilized in the process were either sourced from closed mining operations or from Go To Plastics, which had the best price and availability of tanks. The project team attempted to use as many tanks from previous mining operations as possible to both save money and be more environmentally friendly in building the plant. In particular, the stripping tanks had to be stainless steel as plastic tanks were not compatible with the extractant. The three stainless steel tanks procured for the process were used tanks bought from a regional supplier.

The pumps utilized across the project were selected based on the following: (1) having a maximum flow rate of 60 gpm and (2) their given chemical compatibility. The project team attempted to find standardized pumps that could be used across the plant. Two primary pump styles were selected: magnetic drive or impeller driven, with two pump suppliers selected for each style due to supply chain shortages on pumps. Spare pumps were procured that could be easily swapped out in the event of failure.

Once agreement was reached on the final design, automated valves were consequently needed for the project. The project team selected Heyward actuating valves due to their availability and competitive price. Each valve had a standard actuating unit and appropriate seals to handle the material with which it would come into contact. Each valve was equipped with PVC unions so that they could easily be replaced if a failure occurred.

Electrical Procurement

Due to the existing partnership between project partner Rockwell Automation and Mon Valley Integration (MVI), MVI was selected to perform the electrical and automation install at the plant. As previously mentioned, due to rising costs and supply chain issues regarding automation equipment, the project team ultimately chose not to have it installed as originally designed. Instead, MVI designed and installed a 480V and 120V panel with various connections that powered all the electrical equipment locally within the plant. With future upgrades in mind, they installed the electrical equipment with capacity for future automation.

Analytical Monitoring Equipment

The project team chose Endress+Hauser as the supplier for all analytical monitoring equipment onsite due to the partnership that they developed with WVU during the R&D phase of the project. Endress+Hauser project engineers were both familiar with their equipment and install and provided great customer service. The project team chose to install several liquiline CM448 units that were capable of locally controlling pumps via an OFF and ON function that was based on pH targets or conductivity readings.

Plant Construction and Installation

To facilitate cost savings, WVU assembled a team of engineers that could mobilize and construct most of the plant (excluding electrical) themselves. WVDEP gave the project team permission to move into the REE side of the plant in June of 2022. In the months prior to this, the project team had composed an AutoCAD drawing that detailed many of the pipe measurements and tank locations for the given floor space. The team spent much of the first month onsite placing and installing all the process tanks in the exact locations specified in the drawings. They then moved forward by first installing the HPC dewatering system. This system was completed just after the AMD treatment plant started operation in September of 2022. It was immediately water tested and used after that date. In November of 2022, the acid leaching circuit was completed; the team began testing the circuit upon its completion. Due to

supply chain issues in procuring the mixer for the main BSX unit, the solvent extraction and stripping circuits were not completed until March of 2023. During this time, the acid leaching circuit operated but the PLS was stored in its entirety.

It should be noted that electrical install was not completed until late December 2022. It was not until this time that shakedown testing could begin in earnest at the plant. To utilize the acid leaching portion of the plant prior to electrical completion, automated valve actuators were removed and equipped with manual handles. Each tank was equipped with a localized control panel for its associated valves and all valves were electrically operational by March of 2023. Furthermore, each tank or process area ran on its own electrical circuit so that individual areas could be powered down without interrupting the entire plant operation.

Specialized Equipment Procurement and construction

Pilot SX

The pilot SX was built according to the design in Task 10 by SX Kinetics. The unit was delivered to WVU on May 28, 2020, where it underwent water testing to ensure that all the tanks were liquid tight. The system was not installed until June of 2022, wherein it was retrofitted with internal recycle pumps to operate in the way desired by the project team.

Batch Solvent Extraction Unit (BSX)

The BSX, which was designed in house by WVU engineers, was built by Mow Money, LLC. WVU and Mow Money partnered together to find recycled materials from abandoned coal mine facilities to fabricate the unit. The main mixier/settler chamber is a recycled drainage pipe. The pipe was outfitted with various ports that were welded into place. The base features a recycled steel plate that is both welded and bolted onto the pipe. The unit was delivered to WVU prior to the commencement of plant construction. The mixer and plumbing to operate the vessel were completed in March of 2023; completion was hindered by supply chain issues that made it difficult to acquire parts to operate the mixer safely. A picture of the completed BSX can be found in **Figure 14** below.

Figure 14. Installed BSX unit.

As equipment was delivered and installed, the team developed operational, maintenance, and safety manuals that contain the necessary protocols for safe use and operation. These were compiled into a technical library for reference by current staff as well as future researchers.

Task 12.0 – Acid Leaching/Solvent Extraction: System Shakedown, Training, and Troubleshooting

Approach

Coincident with shakedown activities, the Recipient will work with the appropriate officials to develop a detailed chemical hygiene plan and waste management plan specially addressing the pilot-scale ALSX plant. While the proposed system has been purposefully designed to exclude unsafe and dangerous components, the scale of the effort and the paramount importance of laboratory safety necessitate a well-formulated safety plan. As such, the chemical hygiene plan will describe all engineering controls, personal protective equipment requirements, standard operating procedures, and waste handling procedures needed to ensure safe operation of the facility throughout the duration of the project.

While other issues may be addressed during the safety certification, the primary safety hazard is the use of strong acids in the leaching and solvent extraction units. At a minimum, the chemical hygiene plan

will specify the use of acid resistant gloves and gowns and adequate ventilation in the testing area. In addition, all researchers will be required to receive laboratory safety training as well as hazardous waste management training prior to work and once annually during employment. These policies will be strictly enforced per the chemical hygiene plan developed under this task.

The chemical hygiene plan will be combined with the technical library developed in Task 11 to formulate an Operational Training Plan. All researchers working on-site will be required to complete this task training prior to initiating any research work. This plan will describe all the appropriate work protocols associated with specific tasks and duties.

After finalizing the appropriate training protocols, a series of shakedown tests will be conducted to identify and resolve operational issues that may arise during the detailed system testing. Shakedown testing provides an opportunity to mitigate these issues while providing key operational data that can support a detailed test campaign. The specific goals of this testing program are: (1) verify vendor specifications on capacity and power; (2) ensure the sufficiency of various ancillary equipment and utilities; (3) identify the operational limits to be used in detailed system testing. Shakedown testing will be conducted by operating all unit operations under "water-only" conditions to first ensure the structural integrity of the process units. After water-only testing, solids will be slowly incorporated into the test regimen to ensure the adequacy of valves, pumps, and other fittings. Strong acids and other chemicals will be added only after the system has been proven in these more benign conditions.

During the water-only, the Recipient will install and deploy a state-of-art real time monitoring and control system. Like the system for the upstream concentrator described in Task 8, this system will provide real-time measurements of pump and mixer motor conditions, pH measurements, select ion concentrations, and other variables. These values will be logged in an archival data format and used for feedback loop control. This task will also include all troubleshooting needed to ensure consistent and safe operation of the pilot-scale system.

Results and Discussion

Acid Leaching Circuit Shakedown Testing

Upon startup of the acid leaching circuit, the team sought to acid leach HPC from the cone tank dewatering process to the pH designated by bench scale results. The first trial of acid leaching analytical results indicated that the resulting PLS only contained approximately 30 mg/L of TREE. This was lower than the 60 to 100 mg/L TREE in bench scale tests. Initial solids content testing showed solids contents coming from the cone tank to be at acceptable levels for PLS generation. However, low PLS concentration is typically indicative of low solids content. After investigation, the team found that the solids contents were not representative of the entire HPC cone tank as any water not decanted from the tank would not drain until near the end of the charge to the PLS tank. To obtain accurate data, the team chose to take one solids content measurement from the acid leaching tank prior to adding acid since it would be more representative than a random sample taken from a pipe tap.

Sample data, once corrected, indicated low solids content coming from the HPC dewatering system. Due to low solids content in the clarifier, the cones were not filling with HPC to the 250-gallon outlet point. Therefore, unwanted water was being transported to the acid leaching system. To rectify this issue, two steps were taken. First, a cone tank would be recharged with HPC if the settled HPC was below the 250-gallon outlet port. Secondly, upstream flocculation was evaluated to find the source of the low solids content generated in clarifier 2. Over the course of this investigation, it was found that the polymer line to clarifier 2 was clogged and HPC was not being flocculated at all. These two changes resulted in solids content entering the cone tank going from less than 1% solids to greater than 1.5% solids. PLS

concentrations were subsequently at a minimum of 60 mg/L TREE after the process improvements.

Upon startup, further observations noted that, due to the cone design of the tank, much of the PLS supernatant in both the leaching tank and the neutralization tank was going to the filtration area. The goal of the project team was to filter as little volume as possible by allowing residuals to settle. Both residuals settled in the process tanks more effectively than results indicated at the bench scale. To make the overall leaching process more efficient, the team utilized two extra tanks that were procured for the original design as settling tanks for Leaching Residual and Synthetic Zeolite. These tanks were equipped with sump pumps that an operator could lower or raise to the interface of the supernatant and residual. By implementing this additional infrastructure, the filtered volume of slurry was reduced on average from 400 gallon to 150 gallons. A picture of the leaching residual settling tank can be found in **Figure 15** below.

Figure 15. Leaching Residual Settling Tank.

In addition to the described issues above, over the course of multiple acid leaches it was found that the tank mixing had decreased from startup. Upon dissembling of the pump, the team found the impeller to be clogged with debris and leaching residual. Upon rebuilding the pump, it was found to have the same issue soon after. While the pump was not replaced during this project, the team intends to switch both the acid leaching and neutralization tank pumps to magnetic drive to avoid residuals becoming caught in the small fins of the impeller, avoiding pump failure and system downtime.

Solvent Extraction Shakedown Testing

Upon startup, the scale at which the BSX operated was much larger than any previous testing. Due to this, the mixing speed had to be carefully evaluated to sufficiently mix the extractant while also not mixing it so quickly as to cause emulsification. Since the organic extractant had a yellow hue, the project team was able to visually watch the mixing in the top of the reactor to see when the extractant became fully mixed into the aqueous layer. Despite this, emulsification could not be observed until after mixing ceased and the layers had separated. Despite the group's attempts to mix the unit at the lowest speed

possible, emulsification occurred during the first cycle of the BSX process. This caused a solid gel-like material to form in the organic layer that had to be filtered out via gravity bag filtration. Further evaluation of the process identified four factors that the team hypothesized led to the emulsification. First, high mixing speed promoted emulsification. Secondly, the O:A ratio that was chosen added too much organic to the reaction vessel. The PLS contained 30 mg/L TREE while comprising a large amount of Calcium. The amount of extractant in the tank had a greater capacity that allowed for full extraction of the REE while also allowing for a large extraction of the calcium. An additional factor impacting this issue was the use of six contacts; by the third contact, so much calcium had been extracted that it began to back extract from the organic. This was indicated by the negative recovery of calcium seen in **Table 9**. This, in combination with high mixing velocity, was hypothesized to cause the emulsification with solid precipitation.

Table 9. Recovery from Initial BSX cycle.

	Raffinate Out of BSX Contact 1	Raffinate Out of BSX Contact 2	Raffinate Out of BSX Contact 3	Raffinate Out of BSX Contact 4	Raffinate Out of BSX Contact 5	Raffinate Out of BSX Contact 6
	% Extracted from PLS	% Extracted from PLS	% Extracted from PLS	% Extracted from PLS	% Extracted from PLS	% Extracted from PLS
Al	29%	23%	22%	21%	25%	23%
Ca	33%	6%	-7%	-15%	-20%	-15%
Co	-1%	-11%	-8%	-11%	-11%	-7%
Fe	0%	0%	0%	0%	0%	0%
Li	0%	0%	0%	0%	0%	0%
Mg	0%	0%	0%	0%	0%	0%
Mn	1%	-11%	-8%	-8%	-10%	-6%
Na	8%	53%	52%	55%	57%	52%
Ni	-1%	-11%	-7%	-9%	-9%	-5%
Si	-2%	-10%	-11%	-15%	-16%	-12%
Zn	32%	40%	53%	54%	47%	47%
TMM	10%	26%	26%	27%	26%	26%
Sc	93%	93%	81%	73%	70%	73%
Y	100%	100%	99%	99%	99%	99%
La	79%	66%	59%	52%	41%	40%
Ce	90%	84%	84%	83%	73%	72%
Pr	92%	88%	88%	87%	78%	77%
Nd	93%	89%	90%	89%	80%	79%
Sm	97%	95%	95%	93%	88%	88%
Eu	98%	96%	96%	95%	91%	91%
Gd	98%	97%	96%	95%	93%	93%
Tb	99%	99%	98%	98%	97%	97%
Dy	100%	99%	99%	99%	98%	98%
Ho	100%	100%	99%	99%	99%	99%
Er	100%	100%	99%	99%	99%	99%
Tm	100%	100%	99%	99%	99%	99%
Yb	99%	99%	99%	98%	98%	98%
Lu	99%	99%	98%	98%	98%	98%
TREE	95%	92%	92%	91%	86%	86%

Despite the poor results from the first cycle of the BSX, results from **Table** 9 indicate an average recovery of 90% TREE. The team sought to maintain high REE recovery while preventing emulsification. To obtain these results, three changes were made for the second trial. First, operators adjusted the

mixing speed in small increments and visually inspected the unit to discern the point at which little to no organic extractant could be seen on top of the vessel. By doing this, the team established the VFD only needed to run at around three quarters of the speed of the first test. Secondly, to prevent calcium loading, the O:A ratio was decreased by 1.3%. The third change was to reduce the total contacts in the cycle from six to four. The other factor that aided in the second test, which was independent of the BSX operation, was that the incoming PLS concentration had increased to 60 mg/L due to upstream optimization. This improvement meant that there was more TREE to load into the organic extractant (**Table** 10).

Table 10. Recovery from second BSX cycle.

	Raffinate Out of BSX Contact 1	Raffinate Out of BSX Contact 2	Raffinate Out of BSX Contact 3	Raffinate Out of BSX Contact 4
	% Extracted from PLS	% Extracted from PLS	% Extracted from PLS	% Extracted from PLS
Al	29%	6%	6%	94%
Ca	11%	-7%	-12%	-33%
Co	-7%	-11%	-8%	99%
Fe	0%	0%	0%	0%
Li	0%	0%	0%	0%
Mg	0%	0%	0%	0%
Mn	-7%	-11%	-8%	83%
Na	2%	0%	0%	96%
Ni	-7%	-10%	-7%	100%
Si	-9%	-10%	-7%	93%
Zn	23%	50%	55%	85%
TMM	1%	-2%	-2%	70%
Sc	89%	68%	73%	87%
Y	100%	99%	99%	99%
La	46%	44%	42%	31%
Ce	73%	79%	80%	73%
Pr	79%	86%	86%	80%
Nd	83%	89%	88%	83%
Sm	95%	95%	92%	93%
Eu	96%	95%	93%	94%
Gd	97%	95%	93%	95%
Tb	98%	98%	97%	97%
Dy	99%	99%	98%	98%
Ho	99%	99%	99%	98%
Er	100%	99%	99%	99%
Tm	100%	99%	99%	99%
Yb	100%	99%	98%	99%
Lu	100%	98%	98%	99%
TREE	88%	89%	89%	86%

Results from **Table** 10 indicate that the lower O:A ratio and number of contacts were able to sufficiently extract an average of 89% TREE. This is only a 1% decrease from the initial trial. Results still indicated a back extraction of Calcium. Upon visual inspection, no emulsification or solid precipitant occurred. Due

to the favorable results of this trial, the mixing speed and number of contacts were maintained throughout the rest of the project.

Aside from extraction and emulsification issues, operation of the BSX unit revealed a few design flaws that were corrected after the first few trials. First, the long mixing shaft combined with the mixing disc caused the shaft to move back and forth when mixing. This caused the mixing disc to contact the fins within the unit. Even after reducing mixing speed, operators reported that this issue persisted. The team identified that two of the fins sat closer to the mixing blade due the mixer having to be set slightly off-center by design. To prevent downtime and damage to the equipment, the team removed the two fins that were being struck by the mixing disc. This modification proved to have no effect on extraction of TREE as it never decreased from an average of 89% across four trials without the fins. Secondly, during operation, the team found that solely relying on one flow meter to remove raffinate from the tank presented operational difficulties. To ensure that a proper amount of raffinate was removed from the tank, the team installed a secondary flow meter and a conductivity probe that would shut the pump off if the extractant reached a level too low in the tank. These changes allowed for more confident and efficient processing of the BSX unit by the operator.

Stripping

Upon startup of the plant under sub-optimal conditions as well as very limited staffing time due to budgetary constraints, the team chose to install a secondary scaled-down stripping unit in order to generate multiple batches of LREO and HREO. To use the originally installed reaction vessels, the team needed to run a minimum of four BSX cycles to have enough organic to strip in the large units. In order to generate LREO and HREO to meet project objectives, the team installed two BSX-style 55-gallon reaction vessels to conduct stripping. Startup of these vessels went as anticipated, and stripping results were similar to those found in laboratory testing. Owing to this, no substantive changes were made until the parametric testing phase (Task 13). A picture of the scaled-down reaction vessels can be seen in **Figure 16.**

Figure 16. 55-gallon capacity stripping circuit.

To ensure safety at the plant, the team compiled a document outlining necessary controls, protective equipment, waste handling protocols, as well as codified other standard operational safety procedures into a Chemical Hygiene Plan. This plan, combined with the Technical Library, serve as the Operational Training Plan to be reviewed by all personnel before initiating work onsite.

Task 13.0 – Acid Leaching/Solvent Extraction: System Parametric Testing

Approach

This task encompasses the primary operational test campaign to be completed during the project. Using feedstocks produced from Task 9, acid leaching and solvent extraction tests will be conducted over an extended operating period. Nominally, each experimental condition will require at least 64 hours of continuous testing, and the SX operation is anticipated to run continuously for 24 hours per day. The specific items to be analyzed during this test campaign may include but are not limited to: (1) the influence of SX extractant type and concentration; (2) the influence of SX solvent type and ratio; (3) the influence of extracting and stripping acid type and pH; (4) the number of extracting and stripping stages needed to reach the target purity level. Other objectives are to explore pathways to remove non-target impurities and optimize the process with regards to separation efficiency, solvent recycling, and waste minimization. The test matrix will be generated using a statistical design of experiments, and specific conditions will be blocked and repeated to assess experimental error while mitigating the influence of covariates, such as ambient environmental conditions. The results from this experimental design will be analyzed using a response surface methodology to identify the optimal conditions leading to the highest recovery and selectivity. Initial efforts will focus on technical success criteria (i.e., grade, mass recovery, separation efficiency); however, economic factors (i.e., operating costs, value-based recovery) will also

be integrated into the performance objectives as testing continues. The REO concentrate precipitates from these tests will be analyzed with SEM and XRD to assess the form and structure of the REE/CM in the final product.

Results and Discussion

Acid Leaching

Over the course of the project, the acid leaching circuit at the plant produced more than 25,000 gallons of PLS. Due to the intense study of the leaching circuit in the lab prior to mobilization to the plant, the project team did not alter the leaching pH or neutralization pH The major variable that changed over the course of the project was the incoming solids content. This ranged from 0.8% to 2.1%. This allowed PLS to be generated between approximately 30 to 100 mg/L TREE. An average assay of all the PLS and Neutralized PLS assays can be found in **Table 11** and **Table 12**, respectively, below.

Table 11. Average PLS assay.

Average PLS Assay		
Al	**mg/L**	1,291.7
Ca	**mg/L**	579.7
Co	**mg/L**	29.6
Fe	**mg/L**	0.9
Li	**mg/L**	0.2
Mg	**mg/L**	503.3
Mn	**mg/L**	450.7
Na	**mg/L**	154.7
Ni	**mg/L**	26.8
Si	**mg/L**	299.9
Zn	**mg/L**	103.0
TMM	**mg/L**	3,440.4
Sc	**mg/L**	0.3
Y	**mg/L**	14.5
La	**mg/L**	3.3
Ce	**mg/L**	7.6
Pr	**mg/L**	1.5
Nd	**mg/L**	7.5
Sm	**mg/L**	2.4
Eu	**mg/L**	0.6
Gd	**mg/L**	3.6
Tb	**mg/L**	0.6
Dy	**mg/L**	2.9
Ho	**mg/L**	0.6
Er	**mg/L**	1.5
Tm	**mg/L**	0.2
Yb	**mg/L**	1.0
Lu	**mg/L**	0.1
TREE	**mg/L**	48.3

Table 12. Average Neutralized PLS assay.

Average PLSN assay		
Al	**mg/L**	155.3
Ca	**mg/L**	537.6
Co	**mg/L**	28.2
Fe	**mg/L**	0.4
Li	**mg/L**	1.1
Mg	**mg/L**	484.3
Mn	**mg/L**	420.6
Na	**mg/L**	3291.1
Ni	**mg/L**	25.0
Si	**mg/L**	58.5
Zn	**mg/L**	100.8
TMM	**mg/L**	5103.1
Sc	**mg/L**	0.1
Y	**mg/L**	14.5
La	**mg/L**	3.2
Ce	**mg/L**	7.5
Pr	**mg/L**	1.5
Nd	**mg/L**	7.3
Sm	**mg/L**	2.3
Eu	**mg/L**	0.6
Gd	**mg/L**	3.4
Tb	**mg/L**	0.5
Dy	**mg/L**	2.9
Ho	**mg/L**	0.5
Er	**mg/L**	1.4
Tm	**mg/L**	0.2
Yb	**mg/L**	0.9
Lu	**mg/L**	0.1
TREE	**mg/L**	46.9

Results from the testing indicated an average total recovery of rare earths in the acid leaching system to be greater than 80%. Results in **Table 12** indicated average removal of 80% of Silica and Aluminum through Neutralization and less than 5% loss of TREE.

Solvent Extraction

Following the initial setup of the BSX unit described in Task 12, the team sought to run the BSX at steady conditions. The O:A ratio was maintained in a tight range throughout the testing. While a higher ratio was found to work well in initial testing, the team found that that pushing it slightly lower promoted equal extraction with less extraction of gangue elements. The team ran 22,000 gallons of PLS through the BSX through the course of the project campaign. The average recovery across all the cycles excluding the first trial is indicated in **Table 13** below. Note that negative extraction typically indicates back extraction of the element. **Table 13** indicates an average 89% recovery of Total Rare Earths and a low recovery of total major metals.

Table 13. Average Elemental Recovery of BSX unit.

Average Elemental Recovery	
Al	10%
Ca	5%
Co	-12%
Fe	0%
Li	-24%
Mg	-11%
Mn	-11%
Na	3%
Ni	-14%
Si	41%
Zn	36%
TMM	1%
Sc	81%
Y	99%
La	41%
Ce	78%
Pr	85%
Nd	87%
Sm	95%
Eu	96%
Gd	96%
Tb	98%
Dy	98%
Ho	99%
Er	99%
Tm	99%
Yb	99%
Lu	99%
TREE	89%

Stripping

During testing of the stripping circuit using laboratory-developed methods found in Task 16, LREO purity was between 55 and 71%. This large range was primarily due to the amount of Calcium extracted in the solvent extraction circuit. Laboratory testing developed an acid washing method that was able to easily wash the Calcium out of the solid to generate an LREO of at least 90% purity regardless of the initial purity from the stripping circuit.

During initial testing of the stripping for HREO, results indicated a solid of only 30% purity with the major impurity being Zinc. Test work developed in Task 16 indicated that an intermediate low concentration HCl strip would be needed to remove the Zinc from the loaded organic prior to HREO stripping. Lab testing indicated that inputting this additional process step would result in an HREO purity of greater than 90% TREE.

A third BSX-style 55-gallon reactor was installed to do the intermediate strip. While the organic was only able to be intermediately stripped with low concentration acid once during this project, results subsequently indicated a HREO solid downstream of 90% TREE.

Task 14.0 – System Decommissioning

Approach

After the conclusion of all testing campaigns, including validation testing and/or any follow-on testing requested by project participants or DOE, the system will be decommissioned.

All residual solutions, including organic and extractant, will be drained from the SX plant and disposed according to Recipient waste handling protocols. The mixer-settler units will be acid washed, and any remaining wear parts or other waste will be landfilled. Final disposition will follow Federal Financial Assistance Regulations at the conclusion of the project.

Results and Discussion

The REE recovery pilot plant was not decommissioned at the conclusion of the project. Funding was received under DE-FE0032296 that requires further production of LREO and HREO products to develop downstream elemental separation. Owing to this need, a portion of the budget has been dedicated to paying for further operations at site A-34. Furthermore, the need for HPC is needed and therefore justifies leaving the HPC storage systems in place. At the time of this report, the plant is running a minimum of two days per week and is anticipated to run four days/40 hours per week during summer 2024.

Task 15.0 – Alternative Feedstock Testing

Approach

After meeting the project objectives using the preferred AMD feedstock, other feedstocks may be evaluated in the ALSX pilot plant. Specific examples include: AMD treatment sludges, coal refuse and under clays, fly ash and gasification char, and other REE-enriched coal byproducts. The Recipient will coordinate these activities with the DOE federal project manager.

Results and Discussion

The team evaluated an alternative site to determine how well the process developed for A-34 could be translated to the other AMD sources. The Omega mine site in Morgantown, WV was chosen for the initial test work. Approximately 50 gallons of raw Omega AMD was gathered from the site and returned to the WVU laboratory where it was subject to the staged precipitation water treatment process being implemented at A-34. Testing was conducted using established first and second pH cuts utilizing titration via lime slurry. Following staged precipitation, the solid preconcentrate was leached and neutralized using established processes.

Due to sample volume restrictions, intermediate assays of the PC could not be performed. Rather, the process start- and endpoints (i.e., raw water and PLS concentration, respectively) were compared against those of the A-34 site to evaluate similitude. **Figure 17** shows the comparative graph REE distribution in the A-34 and Omega raw water, while **Table 14** shows a side-by-side comparison of the PLS concentrations. Results from this evaluation show that similar PLS compositions are produced from both sites, particularly with respect to REE content. Major metal composition (particularly Ni and Co) showed much greater variability, which merits further evaluation.

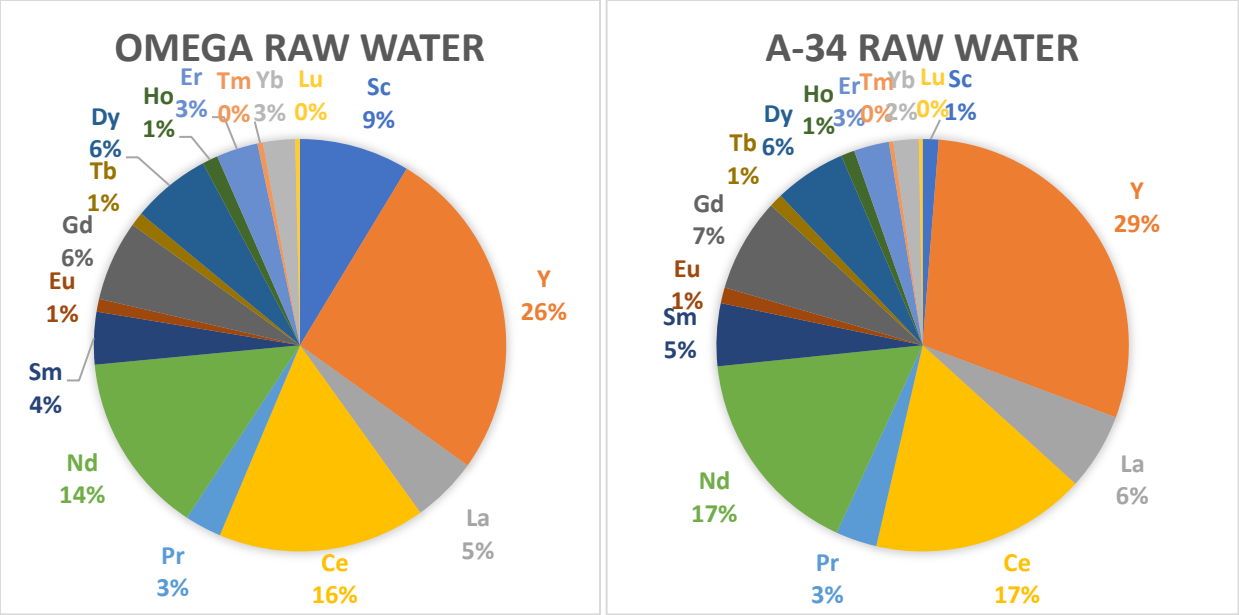

Figure 17. REE Distribution in the raw water of the Omega (L) and A-34 (R) sites.

Table 14. A-34 vs Omega Neutralized PLS.

		A-34 Neutralized PLS	Omega Neutralized PLS
		aqueous	aqueous
		22'0506	22'1153
Al	mg/L	199.3	349.0
Ca	mg/L	641.1	622.2
Co	mg/L	53.6	6.4
Fe	mg/L	0.4	1.0
Mg	mg/L	387.2	74.3
Mn	mg/L	433.2	28.4
Na	mg/L	24.8	46.1
Ni	mg/L	48.1	11.8
Si	mg/L	177.3	57.6
Zn	mg/L	228.8	249.2
pH*		4.1	4.0
MMT	mg/L	2193.6	1,446.0
Sc	mg/L	0.1	0.1
Y	mg/L	34.2	30.0
La	mg/L	7.1	5.2
Ce	mg/L	15.4	14.5
Pr	mg/L	3.7	3.3
Nd	mg/L	18.7	15.8
Sm	mg/L	5.8	5.0
Eu	mg/L	1.5	1.3
Gd	mg/L	8.5	7.4
Tb	mg/L	1.3	1.2
Dy	mg/L	6.5	6.8
Ho	mg/L	1.3	1.4
Er	mg/L	3.2	3.5
Tm	mg/L	0.4	0.5
Yb	mg/L	2.2	2.5
Lu	mg/L	0.3	0.4
TREE	mg/L	110.2	98.8
Th	mg/L	0.0	0.0
U	mg/L	0.3	0.5

Since the project team was focused on completing project objectives at pilot plant A-34, no other alternative sources were investigated throughout the project

Task 16.0 – Laboratory Support and Testing

Approach

Both aqueous and solid samples will be routinely analyzed for REE/CM, major gangue metals, trace gangue metals, and CMs. REE aqueous concentrations will be determined using inductively coupled plasma-mass spectrometry (ICP-MS). Solid samples will be digested by sodium peroxide (Na2O2) fusion and re-dissolution in hydrochloric acid. This method appears to be comparable with the United States Environmental Protection Agency's (USEPA's) total digestion method 3052 (microwave digestion) for

total REE/CM. Resulting aqueous analysis will then be undertaken using ICP-MS. Major ions such as iron (Fe) and aluminum (Al) will be determined by inductively coupled plasma optical emission spectrometry (ICP-OES).

While ongoing work has emphasized recovery of REE, cobalt enrichment has also been identified in the feedstock. However, the Recipient's current ALSX circuit is not optimized for either cobalt or scandium recovery. It is clear that a need to develop independent ALSX circuits for cobalt and scandium exists. Using the rare earth extraction facility (REEF), the Recipient will develop protocols for incorporating those elements into the recovery process. In addition, the Recipient will initiate a broad scan of its feedstocks to identify other CMs and, if economically attractive, ensure that the ALSX process is modified for their recovery. In addition, the Recipient may initiate ad hoc laboratory experiments to further evaluate unexpected phenomena or outcomes observed during pilot-scale testing. These laboratory tests will be used to troubleshoot problems and expand the process knowledge base for the integrated system.

Results and Discussion

Acid Leaching Circuit Development

Leaching Temperature and pH experimentation

To optimize the leaching pre-concentrate (PC), a series of laboratory-scale acid leaching tests were conducted on the PC generated from the mobile production plant. Previous work has shown that leach pH and temperature significantly affect the leachability of REEs from the feed material; thus, an experimental plan was designed to examine their effects on REE and gangue metal recovery.

The solution was mixed until homogenized with an acid under constant temperature. When the leach solution maintained the target pH for at least 30 minutes, the solution was taken off the hot plate and was filtered through a Millpore Pressure Filter with nitrogen gas pressurizing the filter. Once filtration was completed, the residue left on the filter was mixed with an equal volume of DI water and re-filtered through the pressure filter, while the PLS was stored for later. The mass of both the residue and the PLS were recorded.

Once the second filtration was complete, the solids mass was recorded and dried overnight. The mass of the wash solution was recorded, and it was then combined with the pregnant leach solution (PLS) from the first filtration. Approximately 30.8 grams of dried residue was collected, indicating that the dry mass of PC dropped by 38%. The decrease in mass can be attributed to the material being dissolved into solution and small losses during testing (i.e., transfers between vessels). Samples of the PC, dried leach residual, and combined PLS and wash solution were sent for analysis. **Figure 18** shows the stages of the residue after each stage of testing. **Figure 19** shows the wash solution before filtration and **Figure 20** shows the PLS and Wash solutions before combining them.

Figure 18. (Top Left) Initial Wet PC (Top Right) Residue after first filtration (Bottom Left) Solid residue after second filtration (Bottom Right) Dried residue.

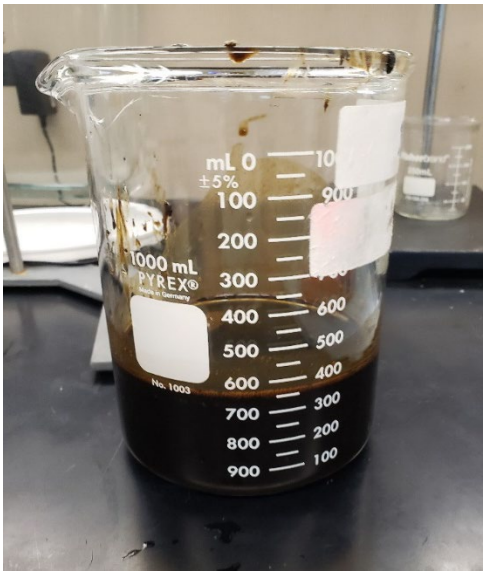

Figure 19. Wash Solution before Filtration.

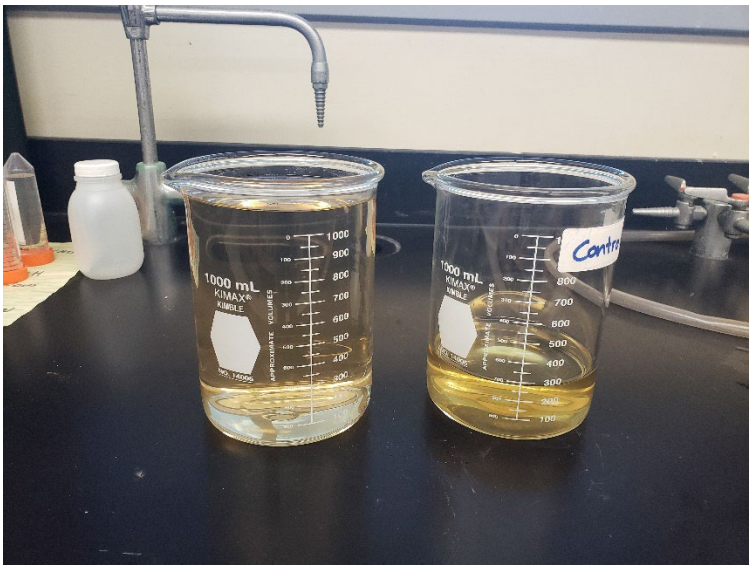

Figure 20. PLS after the first filtration on the left and the wash solution after the second filtration on the right.

Analytical results indicated the recovery of TREEs by the leach solution to be approximately 89% based on the PLS assay. The assay also indicated that significant quantities of gangue metals were not leached from the PC feed. Notably, almost no iron and half of the aluminum were leached. These elements can cause serious issues in the SX plant as noted in previous work. However, small adjustments to the moisture content of the PC feed can cause significant changes in recovery. For example, a 0.5% change in moisture content led to a 5% change in TREE recovery. **Table 15** shows the assays of the PC feed, PLS, and the percent recovery of major metals and REEs. The indicated recovery from the PLS sample showed that a high recovery of REEs was possible with a relatively high pH and at slightly above room temperature.

Table 15. Assay of Samples and Estimated Recoveries.

Stream	Feed	PLS+W	Feed	PLS+W	Leach % Basis
(mL or g)	50.0	1,258.1			Aqueous
Element	Assay (mg/L, g/L, g/t)		Mass (mg)		%
Fe	2584.69	0.10	129.23	0.13	0%
Ca	20549.01	102.26	1027.45	128.66	13%
Mg	25969.31	135.01	1298.47	169.86	13%
Co	4871.59	17.15	243.58	21.57	9%
Al	134403.2	2383.26	6720.16	2998.49	45%
Mn	64466.09	1444.05	3223.30	1816.83	56%
Ni	1044.08	132.34	52.20	166.50	319%
Si	59891.96	361.50	2994.60	454.82	15%
La	409.23	14.16	20.46	17.81	87%
Ce	973.15	28.59	48.66	35.97	74%
Pr	186.40	6.46	9.32	8.13	87%
Nd	930.78	30.94	46.54	38.93	84%
Sm	285.06	9.92	14.25	12.48	88%
Eu	76.80	2.57	3.84	3.23	84%
Gd	451.01	15.49	22.55	19.49	86%
Tb	66.77	2.09	3.34	2.63	79%
Dy	348.83	11.90	17.44	14.97	86%
Ho	66.19	2.09	3.31	2.62	79%
Y	1335.30	59.68	66.76	75.09	112%
Er	165.19	5.56	8.26	6.99	85%
Tm	19.78	0.65	0.99	0.82	83%
Yb	112.31	3.70	5.62	4.65	83%
Lu	15.78	0.53	0.79	0.67	85%
Sc	35.86	0.21	1.79	0.26	15%
Th	0.34	<0.007	0.02		
U	24.88	0.49	1.24	0.61	49%
TREE	**5478.44**	**194.53**	**273.92**	**244.75**	**89%**

Due to the high TREE recovery of 89% from the experiment above, the conclusion was drawn that higher temperature test were not necessary. Later testing focused on evaluating pH as the only independent variable, using finer pH steps to provide better resolution of data.

Leaching pH optimization at room temperature

Prior data and analyses have shown that feed moisture content can have a large influence on the recovery calculation. Due to the manner in which error propagates in the recovery calculation, a small 0.5% or 1% error in the moisture measurement may propagate to high errors in calculated recovery, particularly for materials with a starting moisture greater than 80%. Based on this analysis, a detailed protocol for feed sampling, handing, and analysis was developed and validated by repeat laboratory analysis. The final method showed suitable reproducibility and thus validated the experimental integrity of the leaching tests.

For each leaching test, approximately 480 grams of wet PC was used. After homogenizing the bucket, multiple representative splits were recovered for both the actual leaching test and the determination of a representative feed assay. During leaching, the feed PC was mixed with 1000 grams of DI water and the appropriate amount of acid needed to reach the target pH. During leaching, the pH was measured incrementally, and additional acid was periodically added to maintain the desired pH. The leaching reaction was assumed to be complete when the pH remained at the desired value for greater than 30 minutes.

Following leaching, the PLS was filtered using either vacuum filtration or centrifugation. After the initial filtration, the leach residue was washed and filtered again to ensure all residual leachate was removed from the residual solids. **Figure 21** shows an example of both the filtered and unfiltered PLS. This result indicated that much fewer solids remains in the solution after filtration. The leaching residue was then dried in an oven for eight hours at 100°C to obtain moisture content. The leaching residue, solid feed, and PLS combined with the wash was then sent to the analytical lab for assay via ICP.

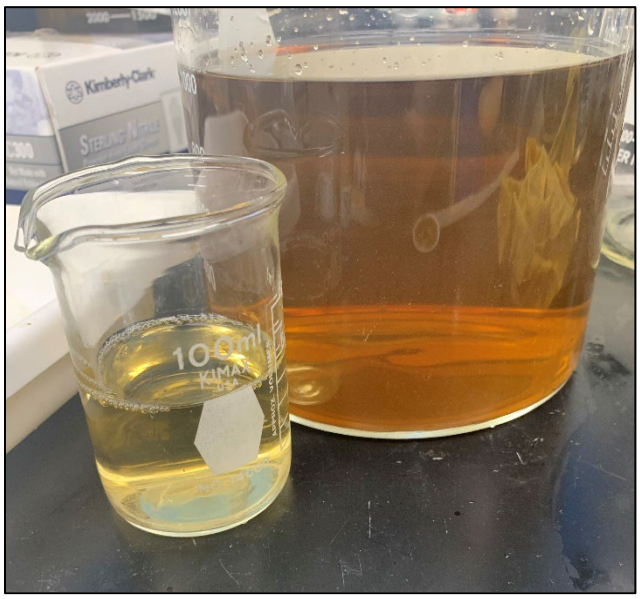

Figure 21. PLS filtered (right beaker) PLS unfiltered (left beaker).

One challenge observed during the leaching tests was the duration needed to adequately filter the PLS from the leach residue. While the time did vary between tests, results showed that filtration times of over 24 hours were typical using the Millipore Nitrogen pressure filter. This result was both an impediment to progress in the laboratory testing and a process design issue to be addressed. To this end, the team considered three options to hasten the filtration time and improve the pace of laboratory testing. Initially, efforts evaluated methods to reduce the filtration volume. An initial experiment was conducted to determine if the leaching residue would adequately settle to the bottom of leach reactor to allow siphoning of the bulk of the PLS before filtration. This test was performed by simply halting the mixer at the conclusion of the leaching tests and observing the settling characteristics of the particulate residue. This approach was ineffective for higher pH target points. After a week of settling, very little separation occurred between the particulate phase and the aqueous phase. For intermediate pH target points, settling occurred in approximately 16 hours, and at the lowest acceptable pH target point, settling occurred in approximately one (1) hour. This discrepancy was likely due to the decrease in silica remaining in the leaching residue at lower pH points. At higher pH points, the particulate silica stayed mixed in solution and exhibits poor settling behavior. A correlation was also found between filter time

with the pressure filter and pH. At the lowest pH, the pressure filter required less than 10 minutes to complete. At higher pH target points, significantly longer times were needed.

Centrifugation of the leachate was explored as a second option for hastening the filtration time. The optimal centrifuge conditions were determined to be 20 minutes at 8500 RPM, and these values were adjusted for cases where poor separation as achieved. Like the pressure filtration testing, the centrifuge showed adequate performance for lower pH values; however, it was not successful in prompting solid-liquid separation at high leaching pH values. In these cases, after centrifugation, the material became completely unfilterable by the pressure and vacuum filters. Due to this result, the centrifuge was ruled out as suitable method for laboratory testing. As a final method, a bench scale plate and frame filter were used on the leaching solution. This approach yielded good filtration; however, the results were not superior to that of the pressure filtration.

Leaching of Pre-Concentrate generated with Lime (Ca(OH)2)

A modification of PC generated using lime instead of caustic produced a notable change in the dewatering characteristics of the PC leaching residue. Prior tests showed that the leaching residue from the caustic-based PC was difficult to filter, often several hours when leached at an intermediate pH and several days when leached at high pH values. The change to lime-based PC reduced this filtration time to under 10 minutes regardless of leaching pH. Moreover, the PLS filtrate contained no residual solids and did not need to be prefiltered to remove fine particles as was the case for the caustic-based PC.

Starting Material (HPC) solids content vs recovery at constant leaching PH

After optimizing the leaching pH, the team shifted focus from the leaching conditions to the solids content of the PC. Solids content has a direct influence on TREE recovery, contaminant recovery, and TREE concentration in the PLS solution. To evaluate these relationships, leaching tests were conducted on PC varying in moisture content from 1 to 10%. In all cases, leaching was performed at constant pH to ensure consistent results.

Several pre-processing steps were needed to produce PC of varying moisture contents for testing purposes. First, PC was settled in a processing vat similar to the second clarifier at the A-34 site. The resultant PC was then placed into a laboratory-scale cone bottom tank where it was allowed to settle. Over time, additional PC was added to the cone tank, which led to further consolidation of the solids in addition to clarified overflow. This process removed a substantial amount of water and increased the solids content of the PC to approximately 1.5% by weight.

To further increase the solids content of the PC, a few filtration methods were evaluated. First, PC underflow from the cone tank was passed through a standard bag filter house. This process produced a PC filter cake with approximately 4% to 6% solids by weight in a short period of time. Despite this improvement, the bags introduced notable materials handling challenges, which were not optimal for the process. Subsequent tests instead used a flat filter This approach was successful, as the filter was able to dry materials to a wide range of solids content in little amounts of time. The filter box also obviated the materials handling challenges, as the material was easy to remove. Over time, material in this filter was able to air dry to 85% solids, a notable improvement over the prior 10% target. For this testing, the material was dried to a maximum of approximately 10% solids, so the PC remained mixable for acid leaching. While this filtration produced desired solids contents, the flat filter would require large amounts of space in the plant at A-34, as well as create additional labor challenges. For these reasons experiments to dewater PC continued.

Leaching tests were conducted on the PC materials generated from this process. During PC preparation, the dewatering time was altered for different experimental runs to produce different solids

concentration. Leaching was then conducted consistently with acid to a constant pH. For this experimental set, no wash cycle of the residual after filtration occurred as the team sought to exclude this step for ease of processing and reduced economic costs.

Table 16 shows the raw data from these trials presented as PC % solids vs. TREE recovery and TREE concentration in the PLS. **Figure 22** and **Figure 23** show these same results graphically. Overall, this data showed a clear inverse relationship between PC solids content and leaching recovery, as higher solids content led to lower recoveries. Alternatively, higher solids content led to higher PLS concentrations due to the lower dilution from the feed water. These two datasets showed competing objectives, as high leach recovery and high PLS concentrations were desired simultaneously. Further fundamental work is needed to identify the mechanism causing reduced leach recovery; however, one cause may be increased mineral crystallinity imparted by increased water removal. This crystallinity may be locking up some of the REEs in a more difficult to leach phase. Additional work is needed to determine if adjustments are needed to ensure high recovery at high PC solids contents.

Table 16. Experimental Results from PC Leaching Tests at constant pH.

PC Feed Solids Content (%)	TREE Leaching Recovery (%)	PLS Concentration (mg/L)
0.8	87	58.5
1.5	90	138.4
1.5	85	133.8
1.6	92	71.0
4.7	78	400.6
5.5	68	425.9
5.7	83	430.4
8.1	67	454.6

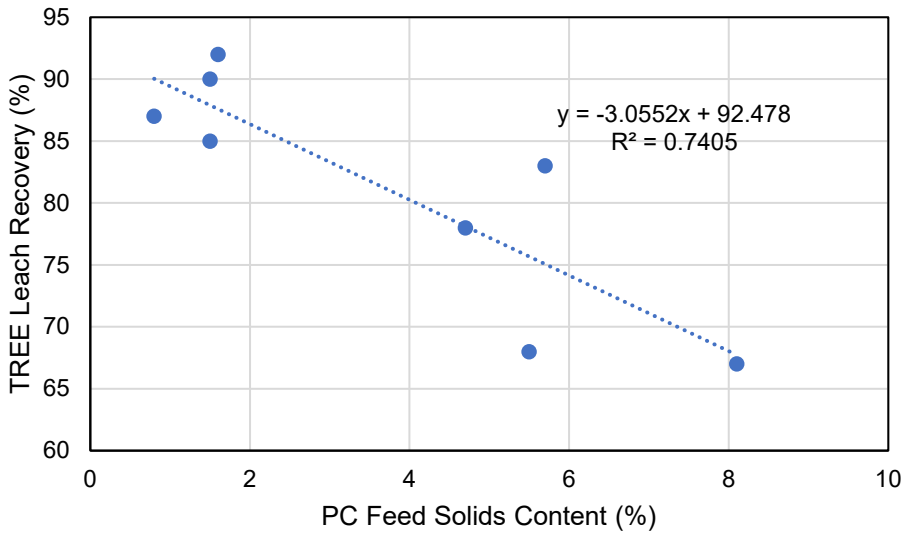

Figure 22. TREE leaching recovery as a function of PC Solids Content from PC leaching tests. Nitric Acid, pH 3.0.

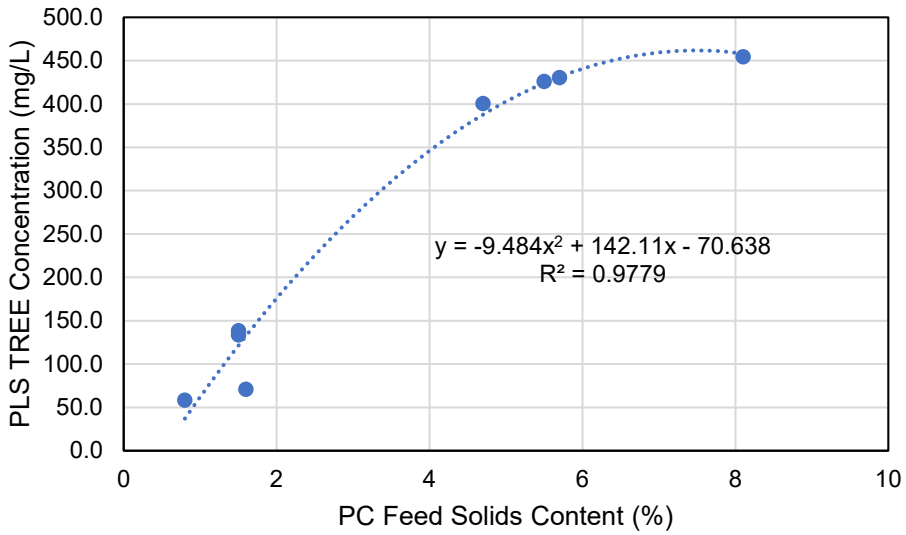

Figure 23. TREE concentration in PLS as a function of PC Solids Content from PC leaching tests.

Leaching retention time vs recovery at constant leaching pH

In a second major test campaign, the team evaluated the influence of extended leaching time (extending over multiple days) on leaching recovery and solution concentration. In total, four tests were conducted to simultaneously evaluate the influence of mixing (agitation vs. no agitation) and acid addition (continual addition vs. no addition after initial reaction). All tests were performed at a constant pH acid as the lixiviant. Throughout the trial, PLS samples were taken at intervals of one hour, one day, two days, three days, and seven days. To limit outside variables, the reaction chambers were sealed to prevent evaporation and stored in the same location away from sunlight.

The REE recovery values from this test campaign are shown in **Table 17** and **Figure 24**. In all cases, recovery generally increased over time, reaching a peak at approximately three days and declining during the latter days of the test. Many curves followed sinusoidal pattern, which was somewhat unexpected for this material. The results did not follow a clear trend with respect to stirring condition and acid addition, suggesting that other confounding variables may be influencing the results.

Table 17. Experimental Results (REE Recovery) from Extended Leaching Tests.

Leaching Time	REE Recovery (%)			
	Test 1 (Not stirred/No acid addition	Test 2 (Stirred/No acid addition)	Test 3 (Stirred/Acid addition)	Test 4 (Not stirred/ Additional acid)
1 hr.	66	60	51	73
1 day	76	65	55	67
2 days	69	79	63	75
3 days	77	74	67	79
7 days	69	71	61	73

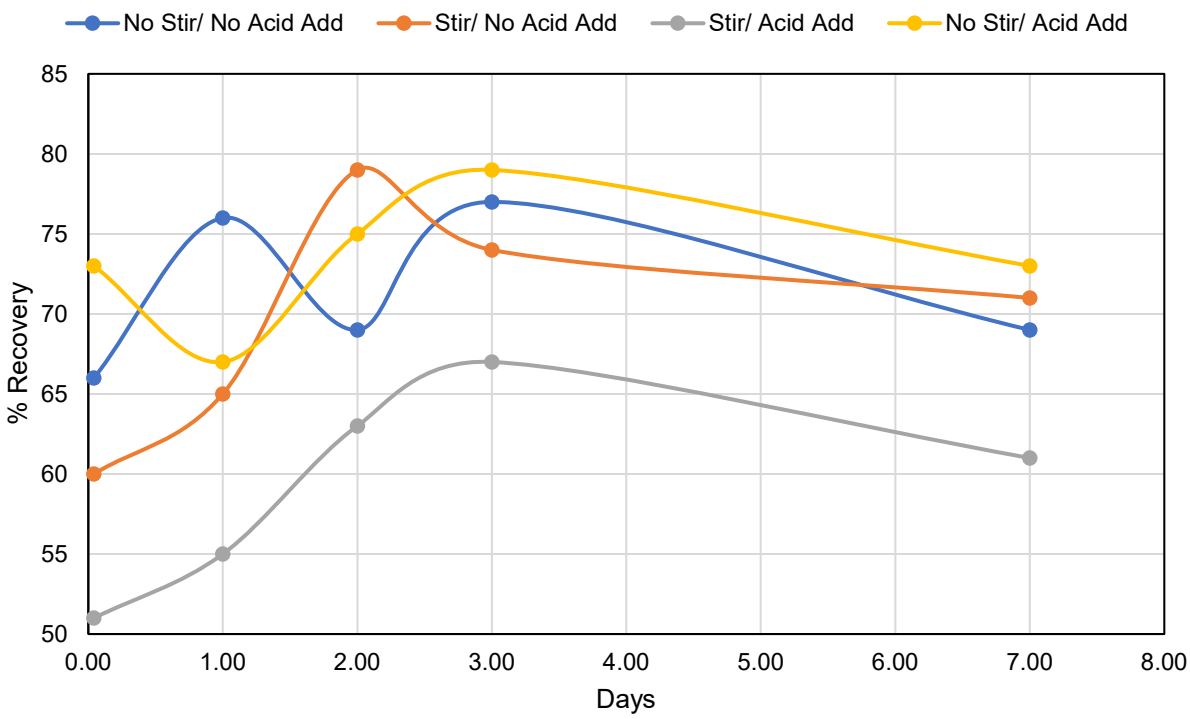

Figure 24. Leaching kinetics for extended leaching time. Nitric acid, pH 3.

Table 18 and **Figure 25** show additional data from this test, namely the total major metal (TMM) concentration as a function of time through the seven-day trial. These data followed a similar sinusoidal trend; however, they did show a net decrease over time. Overall, these data suggested that prolonged storage of the PLS after leaching may lead to changes in solution concentration due to slow precipitation of some insoluble species.

Table 18. Experimental Results (TMM concentration) from Extended Leaching Tests.

Leaching Time	TMM Concentration (mg/L)			
	Test 1 (Not stirred/No acid addition	Test 2 (Stirred/No acid addition)	Test 3 (Stirred/Acid addition)	Test 4 (Not stirred/ Additional acid)
1 hr.	13,713	13,798	14,094	14,353
1 day	13,916	12,464	12,761	12,853
2 days	12,625	14,684	14,688	13,599
3 days	13,708	13,584	15,215	13,540
7 days	11,988	13,285	14,140	12,049

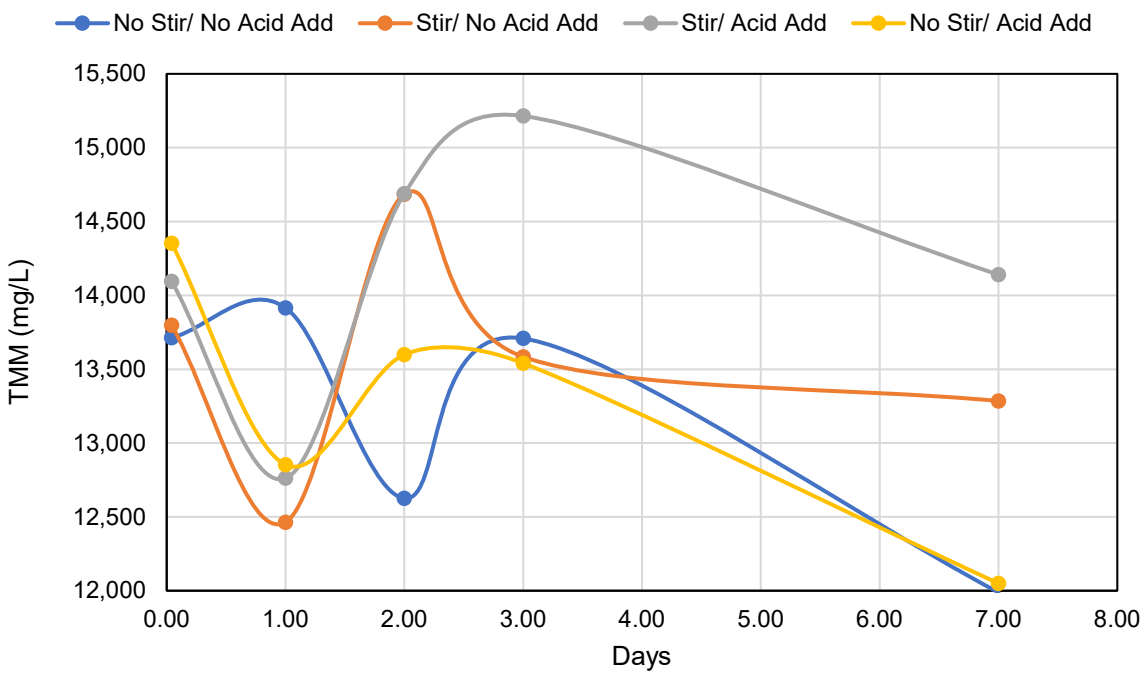

Figure 25. TMM Concentration vs Time Graph.

Leaching Residual Filtration vs solids content

Filtration of the leaching residuals from PLS became a large priority throughout the project. Scale up tests performed on one-gallon buckets of approximately 5% solids HPC yielded unfilterable PLS at optimal leaching pH's. The team evaluated several options, including pressure filtration and vacuum filtration, but found that neither were suitable given the budgetary constraints of the project. As an alternative, the team considered leaching dilute HPC, as prior batch tests indicated that this material was easy to filter. The drawback is that it produced PLS with low REE concentrations (typically 60 to 80 mg/L), which would increase downstream reagent utilization costs. Efforts to increase the REE concentration after leaching (e.g., evaporation) were shown to be technically viable but cost prohibitive.

After balancing the project objectives, physical and budgetary constraints, and commercial viability, the team concluded that leaching cone bottom HPC would be best for the success of the project. This material would simplify the leach residual filtration operation, and while sub-optimal, the low PLS concentrations could be compensated by optimizing the O:A ratio in solvent extraction.

Leaching Residual Filtration optimization via flocculation

With the growing need for an efficient method to separate leach residuals from solution, flocculation was explored as a way to aid in filtration. Experiments were implemented to floc both the leaching residuals and the neutralization residuals. At a polymer input of 6 ppm, the leaching residuals at both two desired pH points flocculated and settled in under 20 seconds. The particle sizes were large enough that residuals could be filtered easily with an 8-micron vacuum filter via vacuum or gravity. An example of the large flocs can be seen in **Figure 26.**

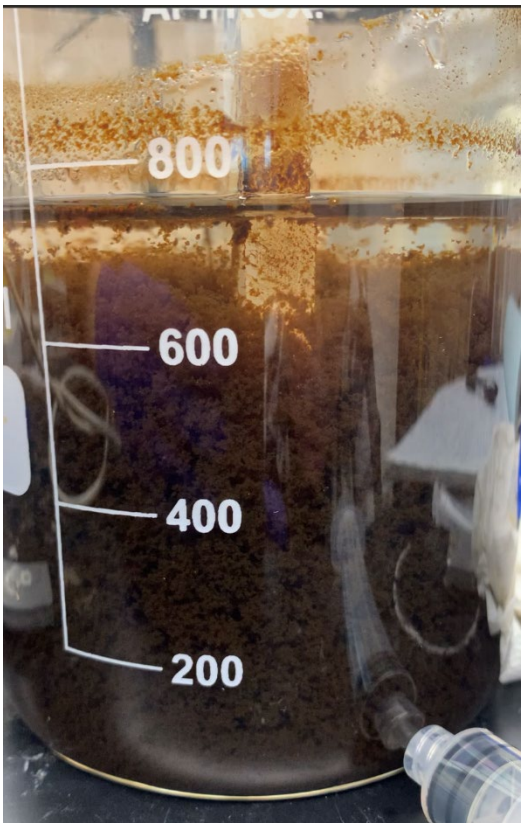

Figure 26. Acid leaching flocculation.

Observations from neutralizing the PLS indicated that the neutralization residual was much more difficult to floc. The team hypothesized that the neutralization residuals could not floc due to the large amount of aluminum in the material. The flocculent used is an aluminum-based floc and therefore may not work due to the similar charges. To help solve this problem, the team consulted Phoenix Solutions to test various polymers on the neutralization residual. Testing of anionic and neutral polymer solutions did not yield any flocculation of the residual. Further testing indicated that the neutralization residuals would floc with the original flocculent, but the mechanics were critical for success. The typical rapid and slow mix process used by the team for flocculation sheered the neutralization floc. Due to this, Phoenix Solutions proposed mixing in the polymer solution at a very slow speed. This resulted in residual that flocked and settled in less than 20 minutes. It also was able to filter on an 8-micron filter easily.

Scale-up Leaching tests

Upscaled experiments were conducted to ensure lab scale procedures were suitable for pilot scale operation. This began by successfully leaching, neutralizing, and oxalic precipitating in 10-gallon batches. These tests successfully produced 10-gallon batches of PLS that were near 100 mg/L REE and had little gangue elements after neutralization. The oxalic precipitation yielded nearly 1 kg of solid from 10 gallons of PLS. It should also be noted that these processes were able to be done successfully using automated pH controllers to meter in neutralizing and leaching reagents while achieving steady target pH values in one (1) hour. The experiments also indicated the neutralization and residuals could settle out to 30% of the original volume in under 15 minutes. Results also indicated in larger scale leach batches; the sulfuric acid usage rate decreased from the rate found in bench top tests. Furthermore, the team decided to leach a 70-gallon batch of HPC. The apparatuses used for this experiment can be seen in **Figure 27**. This test proved that with proper flocculation of the leaching residual, the PLS could be filtered out cleanly using a standard 1-micron bag filter. The neutralization residual was also able to be

filtered in this manner but not under pressure. The team hypothesized that the floc input needs to be changed in the neutralization PLS in order to produce larger and stronger neutralization residual particles.

Figure 27. Left: Filter house and pump used to separate PLS from leaching residuals. Right: Vat, pumps, and automated pH controller used to leach HPC and neutralize PLS.

Pregnant Liquor Solution (PLS) Neutralization

Neutralization pH and reagent vs recovery

Prior data and observations indicated that gangue elements, especially Iron, Aluminum, Silica, were detrimental to downstream solvent extraction. To avoid downstream complications, the team sought to remove these elements from solution prior to solvent extraction. To remove the aluminum and silica, the team proposed neutralizing the PLS with a base. **Figure 28** indicated that neutralizing PLS effectively allowed the solution to have a greater number of rare earths by mass and far less gangue elements excluding calcium.

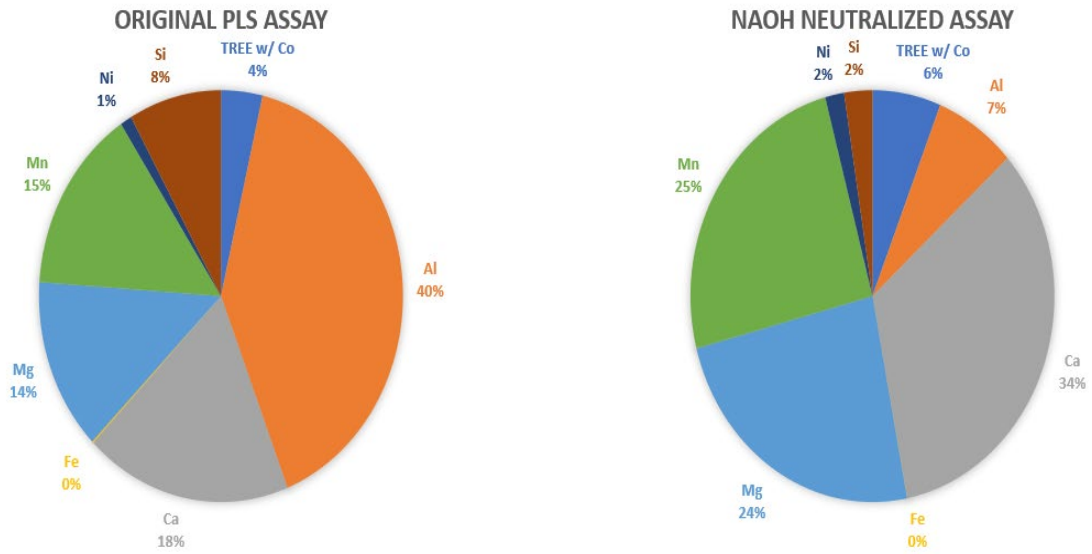

Figure 28. Post Neutralization: PLS vs Original.

Hydraulic Pre-concentrate (HPC) generation

Batch generation via pretreated A-34 starting AQ solution.

Laboratory efforts prior to A-34 becoming operational focused on the leaching of surrogate PC material produced from the Spring 2020 mobile plant campaign. These tests provided useful information on critical design parameters and expectations for the REE recovery and leachate contamination that could be anticipated from the leaching process. However, the surrogate PC material utilized in these tests had some characteristics that distinguished it from the actual PC anticipated from the plant operation at the A-34 site.

Efforts were made to modify the feed preparation process to generate PC that would more closely reflect the material anticipated during on-site operations. Over the course of the period, several thousand gallons of first split treated acid mine drainage from A-34 were transported to the WVU high-bay research center. This partially treated water was then precipitated at the specified second split pH and dewatered to various solids contents. This process entailed two major distinctions from the original PC generation process used in the mobile plant. First, the AMD from A-34 was treated with lime rather than caustic to mimic the process being employed by WVDEP at the A-34 AMD treatment plant. Second, flocculent was added during the pH adjustment step to promote faster dewatering kinetics. The A-34 plant would likely use flocculent in one or both pH adjustment steps.

Further laboratory efforts focused on increased production of PC material for the various laboratory activities. The initial experiments utilized a labor-intensive batch process to generate the material needed for subsequent lab testing. To improve this process, the team utilized existing equipment to construct an automated system for PC generation. First, the PLC intended for the automated leach circuit was repurposed for creating PC. Once the proper cards were installed, the PLC was able to add lime to a batch of AMD at a slow rate autonomously to the desired pH point. This aided in creating a PC that was extremely similar each batch as well as eliminated most of the labor needed to create PC.

Hydraulic Pre-Concentrate Dewatering

Significant effort focused on increasing solids prior to leaching. In a separate test campaign, the kinetics of open air drying of PC on the geosynthetic flat filter was investigated. As noted previously, preliminary tests showed that this process produced very high solids content, as high as 80% to 85% in some trials.

Figure 29 shows the results from a more detailed kinetic study. Results indicated the rate of drying was fairly slow for the first three days but increased substantially between day four and day seven. The high solids content achieved after seven days produce an enriched material that would promote high leaching concentration and easier materials handling.

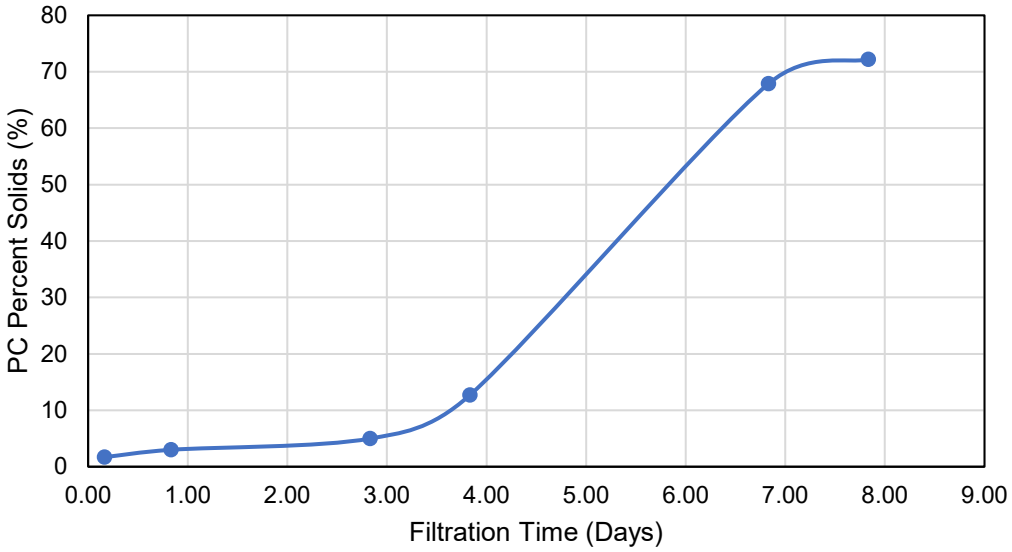

Figure 29. Graph of Time vs solids content of material on the flat filter.

Continuous HPC Generation (A-34 Mini)

Despite the improvements in PC generation, the team desired to simulate an autonomous process closer to what would happen at A-34. To do this, the team designed and constructed a scaled down version of the A-34 site equipment, herein denoted "A-34 Mini." **Figure 30** shows the system installed in the WVU high-bay research facility. A-34 mini consist of an inline pH up adjustment with lime slurry, a rapid mix polymer tank, a slow mix polymer tank, and a clarifier. Using flow rates found from the batch process, lime slurry and polymer inlet rates were found that made the process automatable. The purpose of this model was to allow high-rate production of hydraulic pre-concentrate (HPC) in a manner that closely resembled the future process at the A-34 site. This HPC could in turn be used as feedstock for laboratory-scale process development testing.

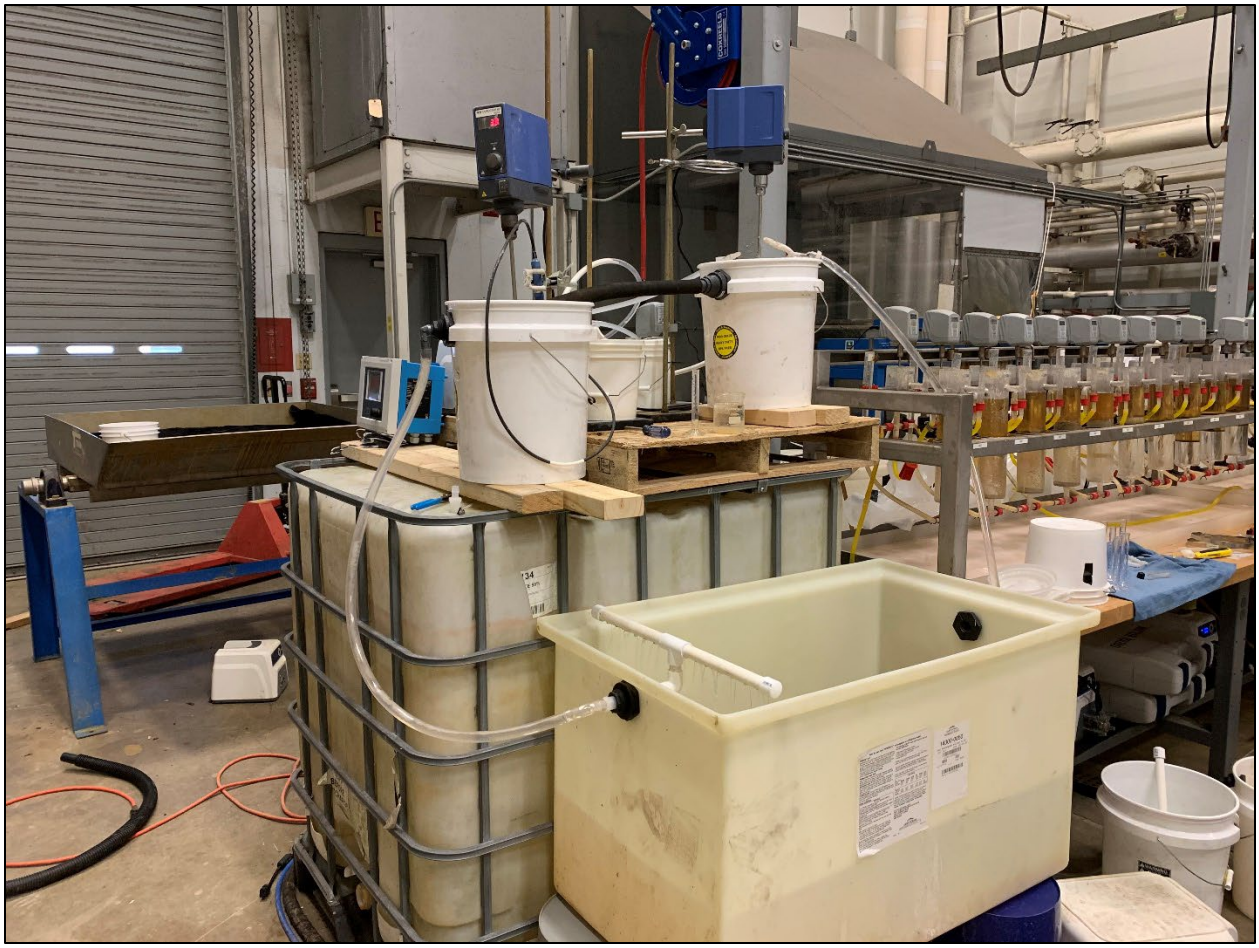

Figure 30. A-34 mini system installed in the WVU high-bay research facility.

Once constructed, the team began shakedown testing of A-34 mini. One issue that was discovered during the initial testing was the generation of “pin” flocs during the pH adjustment. The HPC generated in this manner consisted of extremely fine particles that were not able to filter at high efficiency. Prior experience from the batch precipitation tests led the team to conclude that the contact time in the rapid mix and slow mix reactors was the root cause for the poor flocculation of HPC. In the initial design of the rapid mix reactor, the vessel feed and the vessel product lines were positioned at the top of the cell. This location of the exit port did not allow the constituents to mix in the reactor at a rapid rate for a long duration. To resolve the problem, the exit port was moved to the bottom of the reactor as seen in **Figure 31**. The exit port at the bottom allowed the constituents to mix for approximately 5 minutes before exiting to the slow mix tank.

Figure 31. Improved polymer mix tank reactors.

Despite the improvements to the reactor, the pin floc persisted as it entered the clarifier. Further observations of the system showed that the HPC would quickly settle to the bottom of the slow-mix reactor, rather than flowing over the top. To resolve this issue, the team redesigned the slow mix reactor to match that of the rapid mix reactor with the product port on the bottom.

Installation of the new reactors resulted in larger floc flowing into the mini clarifier. Despite successful flocculation, the team still was challenged to maintain a steady second split treatment pH. The equipment available to use was not capable of adjusting the lime slurry input rate based on pH. This resulted in the pump having to be constantly maintained to obtain the correct pH when operating A-34 mini. To rectify the issue, the team installed a static mixer on the lime slurry line. In previous experience, chemicals were added in line and mixed via a series of pipes that changed direction as seen in **Figure 32**. This mixer resulted in an efficient mixing of lime slurry and first split treated AMD to create a more consistent pH in the second split.

Figure 32. Static Mixer.

Despite these system design changes, operational challenges persisted, the most problematic being poor settling of floc in the clarifier. After consulting the design of the A-34 plant, the team identified that the settling time in the clarifier was not sufficient due to the short length of the clarifier (approximately 2 ft). The team further modified the A-34 mini design to more closely resemble a 1:10 scale mockup of the clarifier to be installed onsite. The design includes a rapid mix and slow mix tank built to match the ones at A-34. These tanks were critical to properly flocking the HPC. The modified design of A-34 mini also had the benefit of having a cone style sump that allowed the team to test how HPC will be removed from the clarifier. The modified A-34 mini is shown in **Figure 33.**

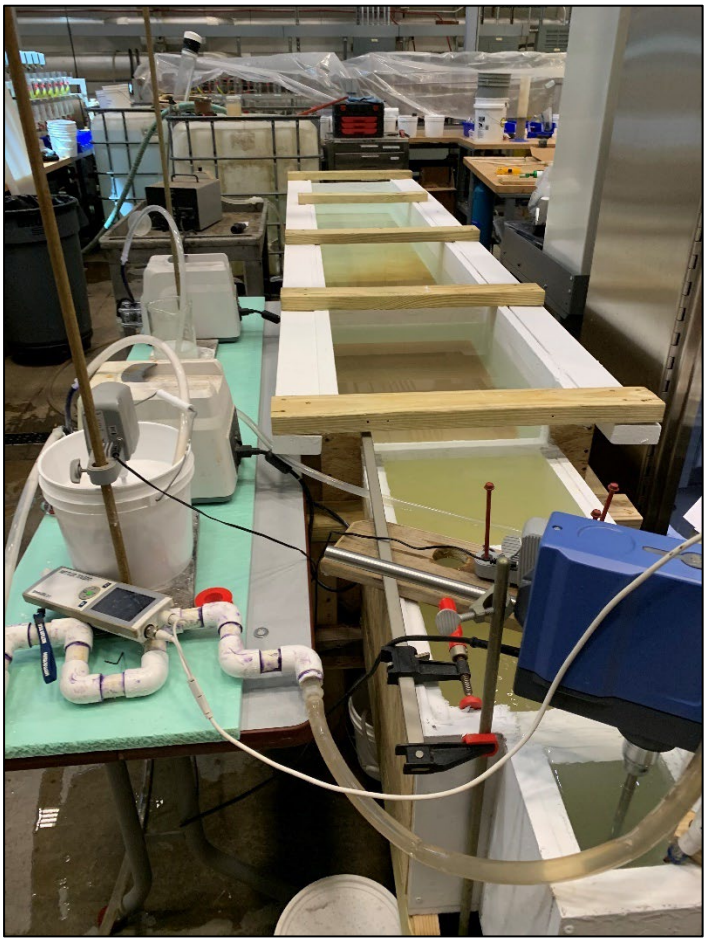

Figure 33. Modified A-34 mini.

The new design for A-34 mini was successful upon installation. Throughout shakedown testing, the team continued to make improvements to further automate the unit. Particularly, the team modified the lime slurry input to maintain a tight pH control of the HPC without having to constantly monitor the pumps. The team installed an Endress-Hauser liquiline PLC with two pH probes to monitor both the rapid mix and slow mix reactors. The pH probe in the slow mix tank was tied to a pump that automatically adjust the pH based on the desired pH needed to generate HPC This allowed the slow mix tank to act as a polishing tank to consistently obtain the target pH. The liquiline can be seen in **Figure 34** and **Figure 35** below.

Figure 34. Liquiline PLC.

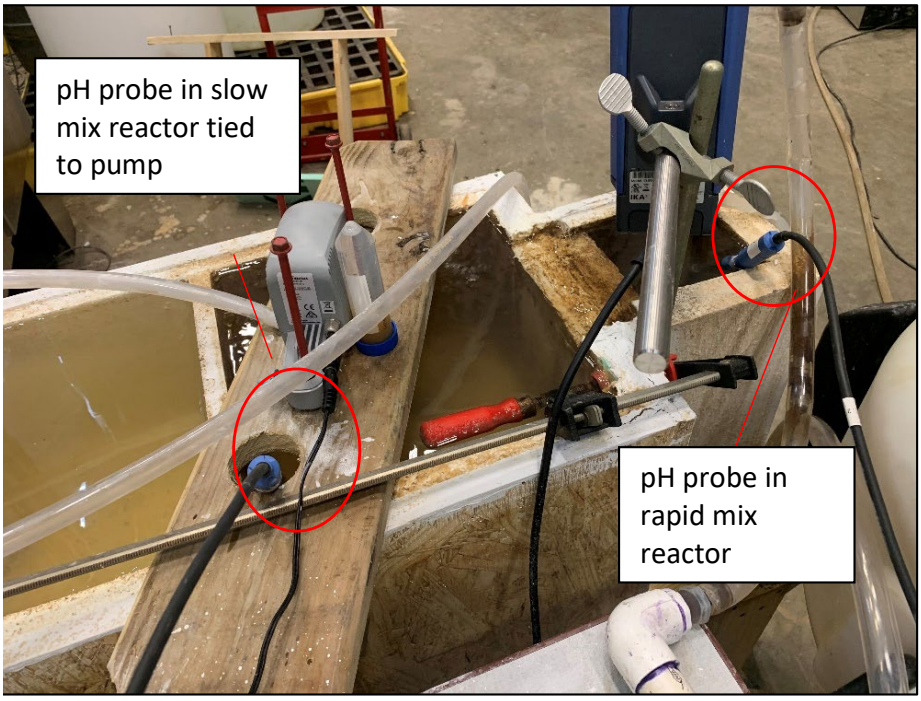

Figure 35. pH probe placement in A-34 mini for liquiline.

With the liquiline installed, the team successfully ran A-34 mini continuously for extended periods. In initial tests, for example, the team ran A-34 mini for several days to generate over 20 gallons of HPC. Further modifications to the system attempted to resolve materials handling issues, such as the collection of HPC from the discharge line. For example, the team observed that upon draining the sump in the clarifier, the material "ratholed" in under 30 seconds. Ratholing is when a vortex forms from the sump and pulls water through the sump instead of HPC. Water is a large issue for downstream processing; therefore, a solution must be found to prevent ratholing. An example of a "rathole" can be found in **Figure 36** below. The team proposed several tests to help identify a solution to ratholing

including studying the effect of polymer concentration and the effect of agitation in the cone near the sump on the clarifier.

Figure 36. "Rat holing" to sump on A-34.

HPC generation upscaling to 1000-gallon batches

With the need for a more consistent stream of PLS, the team sought to prepare larger amounts of HPC in a more efficient manner than A-34 mini. To do this, a 1000-gallon tank was placed in the high bay laboratory equipped with a large mixer as shown in **Figure 37.** This tank was also equipped with a PLC that allowed a pump to automatically adjust the pH to the desired cut points for the rare earth pre-concentrate. Once optimized, the system could treat up to 3000 gallons of raw or pH 4.5 water in one day. With an average raw water off load of 6000 gallons, the team could produce an average of 70 gallons of HPC at 1.2% solids in as little as a week. A-34 mini could only treat a maximum of 480 gallons per day without the first pH cut yielding an average of 15 gallons of 1.2% solids HPC in one week. A-34 mini often had operational issues that caused water production to be far less than 480 gallons per day.

Figure 37. HPC generation tank.

Critical Mineral Extraction

pH and oxidation selective precipitation of REE Solvent Extraction Raffinate

After solvent extraction, the raffinate contains critical elements (cobalt, manganese, nickel) as well as other metals (aluminum, calcium, zinc) and Group I (Na, K) and Group II (Mg, Ca) metals. The focus of this effort was to selectively remove the three critical elements from the mixture through control of solution pH and oxidation/reduction potential (ORP).

The experiment protocol consisted of three stages. In Stage 1, the acidic raffinate was titrated to an intermediate pH with base to remove aluminum as a precipitant. In Stage 2, sodium hypochlorite was added in a 1:1 mole ratio with respect to the manganese to the filtrate of Stage 1 and the pH was adjusted to a target pH point. The purpose of this state was to oxidize Mn(II) to the insoluble $Mn(IV)O_2$. In Stage 3, the filtrate from Stage 2 was titrated to a high pH target point with base. The purpose was to precipitate the remaining cobalt. A synthetic raffinate was prepared with a composition to a real raffinate (**Figure 38**). A major difference between the two solutions was the presence of silicon in the real raffinate.

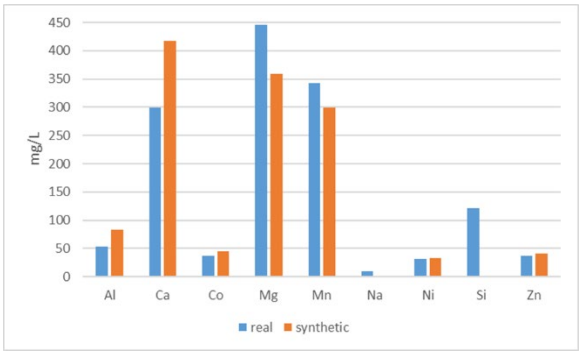

Figure 38. Compositions of a real and a synthetic raffinate, both at pH 1.9.

In **Figure 39**, the masses of elements in 400 mL of raffinate (both real and synthetic) and in the filtrates of Stages 1, 2 and 3 are shown for the real raffinate. The synthetic raffinate behaved as expected. Most of the aluminum was removed in Stage 1 while the amounts of the other elements remained nearly constant. Measurements of pH and ORP in Stage 2 confirmed that manganese should be converted to MnO_2 and that cobalt(II) should not be oxidized. However, cobalt did co-precipitate with the manganese. Stage 3 conditions effectively removed the nickel along with the zinc.

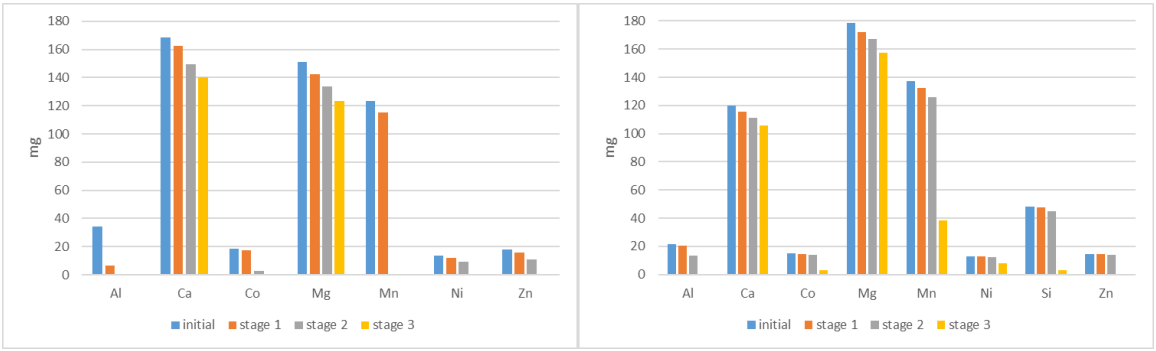

Figure 39. Masses of selected elements in synthetic (left) and real (right) raffinate in the original solution and in the filtrates of the three stages of treatment.

However, the real raffinate did not behave as expected. Stage 1 only slightly lowered the mass of aluminum in the filtrate. Stage 2 only slightly lowered the mass of manganese and cobalt in the filtrate. Stage 3 conditions resulted in removal of most of the cobalt and zinc and a large portion of the manganese and nickel. The reason for the different behaviors of synthetic and real raffinates was unknown.

Next, tests were conducted to remove manganese from solution by manipulation of the oxidation-reduction potential. After several unsuccessful tests with hydrogen peroxide, the team evaluated ozone as a possible oxidant. The initial test shown in **Figure 40** below yielded visual results of a dark brown solid forming when the raffinate was in the presence of Ozone. Despite the success, the analytical assay of the solid yielded less than 15% manganese was removed from solution. Also, 10% of the Cobalt in the solution coprecipitated out with the Manganese. An assay revealed a solid containing only 16% Manganese while silica was the dominant element in the solid which can be seen fully in the pie chart in **Figure 41**.

Figure 40. Ozone precipitating solid from neutralized raffinate solution.

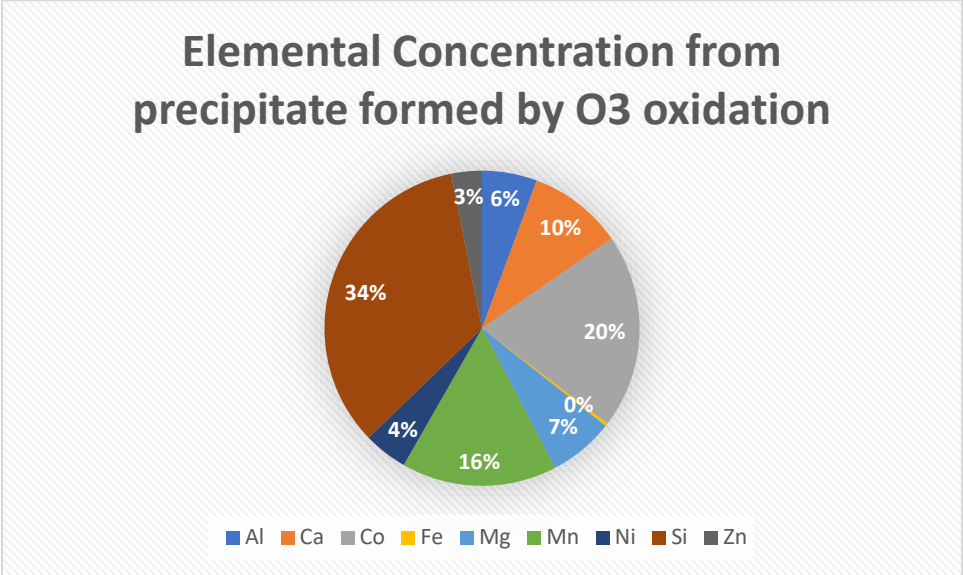

Figure 41. Solid assay from the solid created by Ozone oxidation.

With the precipitation of manganese through oxidation leading to no positive results, the team also tried to precipitate manganese in the presence of FeOOH with the hypothesis that manganese would coprecipitate with iron if the oxidized around pH 6. This test also yielded an assay where no manganese was removed from solution.

Critical Material Solid Generation and Leaching

Critical materials from raffinate generated from Rare Earth Element Solvent Extraction were investigated. The current extractant used did not have the capability to extract Cobalt, Nickel, and most of the Manganese from the PLS solution generated through acid leaching of HPC. Previous testing concluded that raising the pH of the AMD precipitated nearly all the Cobalt, and Nickel reported to the HPC solid. The team hypothesized the same process would work on the raffinate solution.

To obtain the critical material solid, raffinate at low was obtained and titrated using a base to the same pH used to generate HPC. The titration yielded poor results, only precipitating approximately 34% of the Cobalt and approximately 14% of the Nickel from the solution. Despite this, approximately 99% of the aluminum, approximately 99% of the Zinc, and approximately 86% of the Silica were precipitated from the solution. This indicated that it may be possible to use a multi-step precipitation on the raffinate to remove most of the impurities from the solution prior to precipitating the critical materials. Full results from this test can be found in **Table 19** below.

Table 19. Analysis of Raffinate Pre and Post neutralization with recovery to solid from liquid concentrations.

		Raw Raffinate	Neutralized Raffinate	% Precipitated to solid CM product
		aqueous	aqueous	
		22'2132	22'2133	
Al	**mg/L**	55.5	0.4	99.4%
Ca	**mg/L**	490.1	487.3	0.6%
Co	**mg/L**	43.1	28.6	33.6%
Fe	**mg/L**	2.5	0.0	99.4%
Li	**mg/L**	0.1	0.3	-348.5%
Mg	**mg/L**	820.7	815.3	0.7%
Mn	**mg/L**	502.9	416.0	17.3%
Ni	**mg/L**	42.3	36.6	13.6%
Si	**mg/L**	227.2	31.1	86.3%
Zn	**mg/L**	29.7	0.3	99.1%
pH*		2.2	8.3	
TMM	**mg/L**	2214.2	1815.8	18.0%

Despite the poor results from the titration described above, an analytical analysis was still performed of the solid precipitant generated from the titration. The results (**Table 20**) indicated a 21.9% purity of critical materials in the solid. **Figure 42** indicates that a large portion of the impurity in the solid is Silica. Using this data, subsequent testing focused on removing Silica prior to precipitating the critical materials.

Table 20. Solid Fusion Analysis of resulting solid from neutralization of raffinate.

		CM solid
Purity		**21.9%**
		22'2136
Al	**mg/kg**	55,375.5
Ca	**mg/kg**	46,591.0
Co	**mg/kg**	17,459.7
Fe	**mg/kg**	3,260.5
Li	**mg/kg**	2,075.9
Mg	**mg/kg**	16,029.1
Mn	**mg/kg**	84,641.9
Ni	**mg/kg**	10,197.9
S	**mg/kg**	22,201.1
Si	**mg/kg**	237,148.2
Zn	**mg/kg**	31,633.6
TMM	**mg/kg**	526,614.4

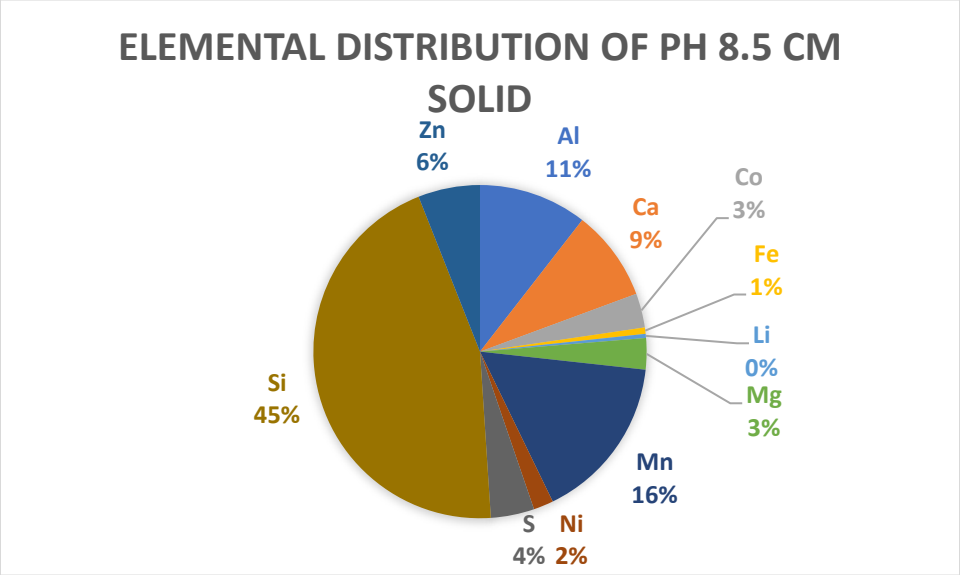

Figure 42. Elemental Distribution of Critical Material Solid made by neutralizing raffinate to pH 8.5.

With the goal of trying to recover as much of the critical materials as possible from the raffinate, a test was executed to first remove most of the Aluminum and Silica from solution by titrating to a neutral pH using a base. The solution was then filtered to remove the gangue precipitant. Once filtered, the solution was titrated to a higher pH to remove Cobalt, Nickel, and Manganese.

Table 21. Aqueous assay and recovery to solid from two step raffinate neutralization.

		Raw Raffinate	Neutralized Raffinate (First pH cut)	High pH neutralized Raffinate (Second pH cut)	% Precipitated to neutralized Solid (First pH cut)	% Precipitated to high pH solid (Second pH cut)
		aqueous	aqueous	aqueous		
		22'2132	22'2150	22'2151		
Al	mg/L	55.5	0.7	0.2	98.7%	1.0%
Ca	mg/L	490.1	480.3	478.5	2.0%	0.4%
Co	mg/L	43.1	41.6	2.3	3.4%	91.2%
Fe	mg/L	2.5	0.0	0.0	100.0%	0.0%
Li	mg/L	0.1	0.3	0.5	-352.9%	-297.1%
Mg	mg/L	820.7	822.0	816.2	-0.2%	0.7%
Mn	mg/L	502.9	501.3	261.2	0.3%	47.8%
Ni	mg/L	42.3	41.0	13.3	3.1%	65.5%
Si	mg/L	227.2	74.0	2.1	67.5%	31.6%
Zn	mg/L	29.7	12.6	0.0	57.7%	42.3%
pH*		2.2	6.8	8.0		
TMM	mg/L	2214.2	1,973.9	1,574.2	10.9%	18.1%

Results in **Table 21** indicated that by titrating the raffinate to a neutral pH, approximately 99% of the Aluminum and approximately 67% of the Silica was removed from the solution. Approximately 3% of both Cobalt and Nickel and nearly no manganese was removed from the solution at neutral pH. By titrating the raffinate to a high pH target point, approximately 91% of the Cobalt, approximately 65% of the Nickel, and approximately48% of the manganese was precipitated from the solution. Despite this, the remainder of the silica in the solution did coprecipitate with the critical materials. This silica led to most of the impurity issues in the solid, as shown in **Table 22** and **Figure 43.**

Table 22. Solid Assay of solids generated by two-step raffinate neutralization.

		Neutral pH solid (First pH cut)	High pH CM solid (Second pH cut
Purity		**6.3%**	**44.1%**
		22'2154	**22'2155**
Al	**mg/kg**	65,367.8	1,240.7
Ca	**mg/kg**	94,215.2	8,261.5
Co	**mg/kg**	3,176.0	58,177.8
Fe	**mg/kg**	3,421.8	125.9
Li	**mg/kg**	2,139.0	1,737.5
Mg	**mg/kg**	12,321.7	21,622.8
Mn	**mg/kg**	22,551.4	45,359.4
Ni	**mg/kg**	3,133.7	33,266.0
S	**mg/kg**	52,587.8	1,333.1
Si	**mg/kg**	236,452.8	119,770.0
Zn	**mg/kg**	21,978.1	23,180.2
TMM	**mg/kg**	517,345.1	314,074.9

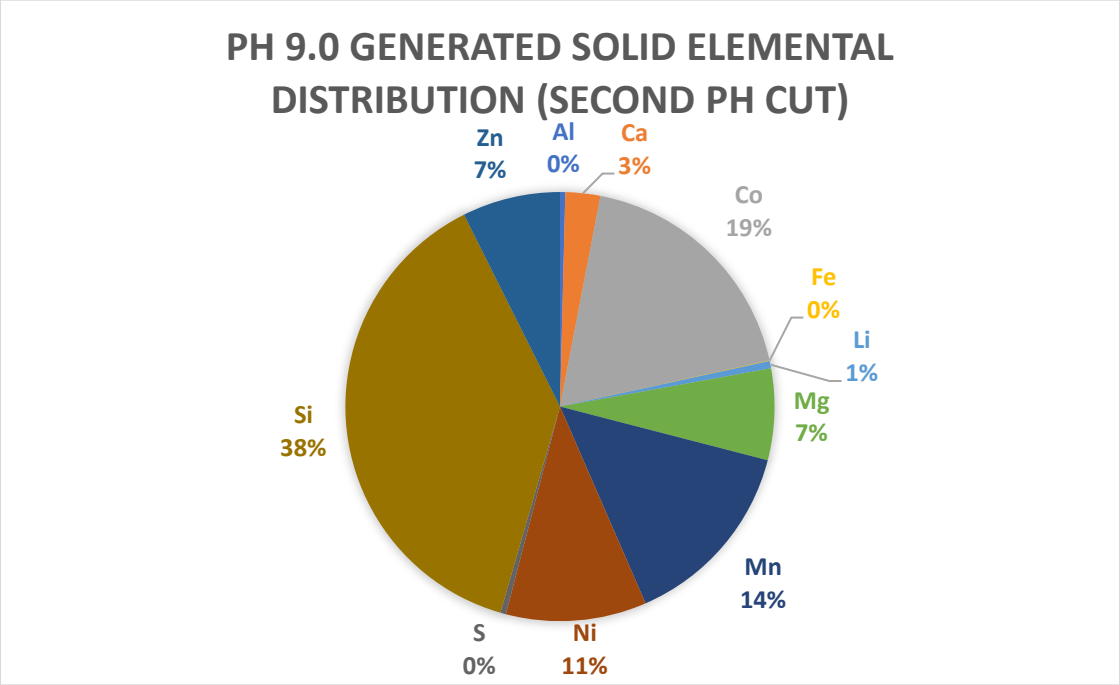

Figure 43. pH 9.0 raffinate neutralization solid elemental distribution.

The resulting solid from the high pH titration of the raffinate yielded a solid with a 44.1% purity of critical materials (Co, Mn, and Ni).

The leach of the resulting high pH solid yielded a critical material PLS that was made up of over 85% of critical materials by concentration. An assay of the liquid indicated that approximately 67% of the

solution comprised manganese as shown in **Figure 44.** The solution also comprised mainly Cobalt, Magnesium, and Zinc. The leach of the solid also was successful in selectively not leaching silica out of the solid as it now comprised approximately 1% of the solution concentration.

Table 23. Analytical assay of Brick Leachate.

		Brick Leachate
Theoretical Purity		**85.1%**
		22'2152
Al	**mg/L**	82.8
Ca	**mg/L**	455.6
Co	**mg/L**	1,861.2
Fe	**mg/L**	2.0
Li	**mg/L**	0.0
Mg	**mg/L**	1,092.3
Mn	**mg/L**	10,792.5
Ni	**mg/L**	1,016.4
Si	**mg/L**	107.5
Zn	**mg/L**	654.4
pH*		1.0
TMM	**mg/L**	16,064.8

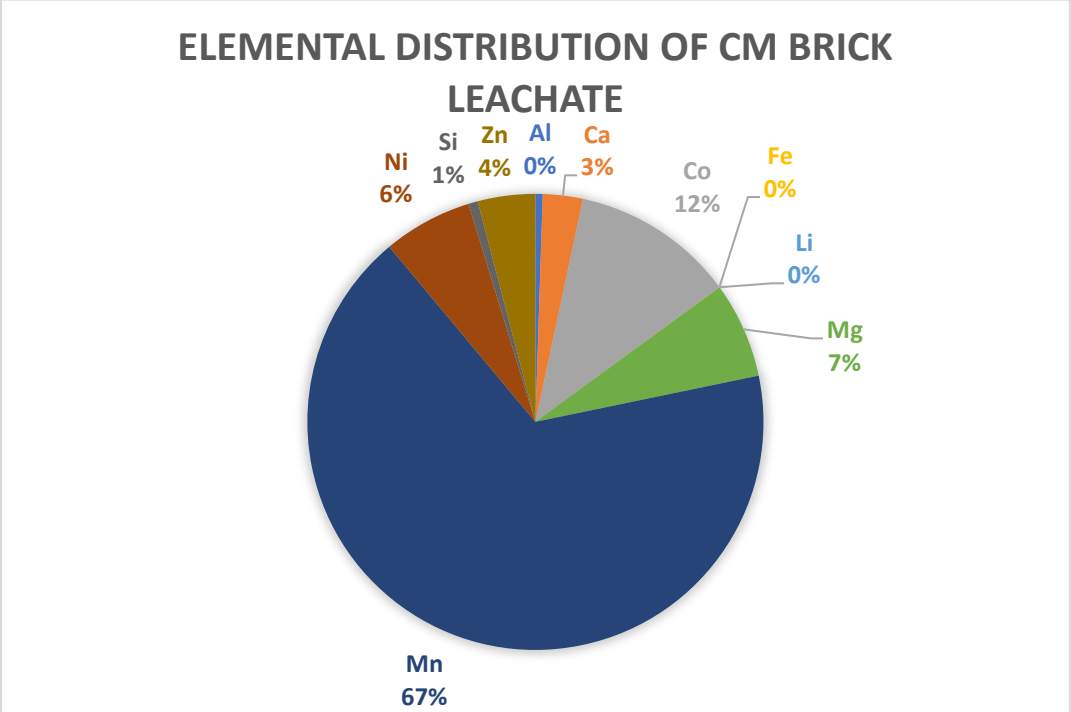

Figure 44. Elemental Distribution of Critical Material Brick Leachate.

Table 23 indicates that in a liter of solution, approximately 10.7 grams of manganese, approximately 1.8 grams of Cobalt and approximately 1 gram of Nickel were present. Due to these high concentrations, it was hypothesized that an oxalic acid precipitation similar to the one used for heavy rare earth strip liquor could generate a high purity critical material solid.

This resulting precipitation, precipitated approximately 99% of all the critical materials present in the solution while also precipitating nearly all the gangue elements, as shown in **Table 24.**

Table 24. Oxalic Acid Precipitation Liquid phase analysis and recovery.

		Brick Leachate	Oxalic Precipitation Raffinate	% Recovery to Solid phase
			aqueous	
		22'2152	22'2271	
Al	mg/L	82.8	0.0	100%
Ca	mg/L	455.6	5.0	99%
Co	mg/L	1,861.2	11.0	99%
Fe	mg/L	2.0	0.0	100%
Li	mg/L	0.0	4.3	
Mg	mg/L	1,092.3	303.2	72%
Mn	mg/L	10,792.5	198.1	98%
Ni	mg/L	1,016.4	28.2	97%
Si	mg/L	107.5	1.5	99%
Zn	mg/L	654.4	0.0	100%
TMM	mg/L	16,064.8	551.4	97%

Table 25. Assay of Oxalic Acid Precipitation generated solid.

		Oxalic Precipitation generated Solid
Purity		**68%**
		22'2272
Al	**mg/kg**	3,384.8
Ca	**mg/kg**	19,911.8
Co	**mg/kg**	81,593.1
Fe	**mg/kg**	222.8
Li	**mg/kg**	2,646.6
Mg	**mg/kg**	35,065.9
Mn	**mg/kg**	87,164.0
Ni	**mg/kg**	46,208.0
S	**mg/kg**	7,334.1
Si	**mg/kg**	4,832.4
Zn	**mg/kg**	32,153.8
TMM	**mg/kg**	320,517.3

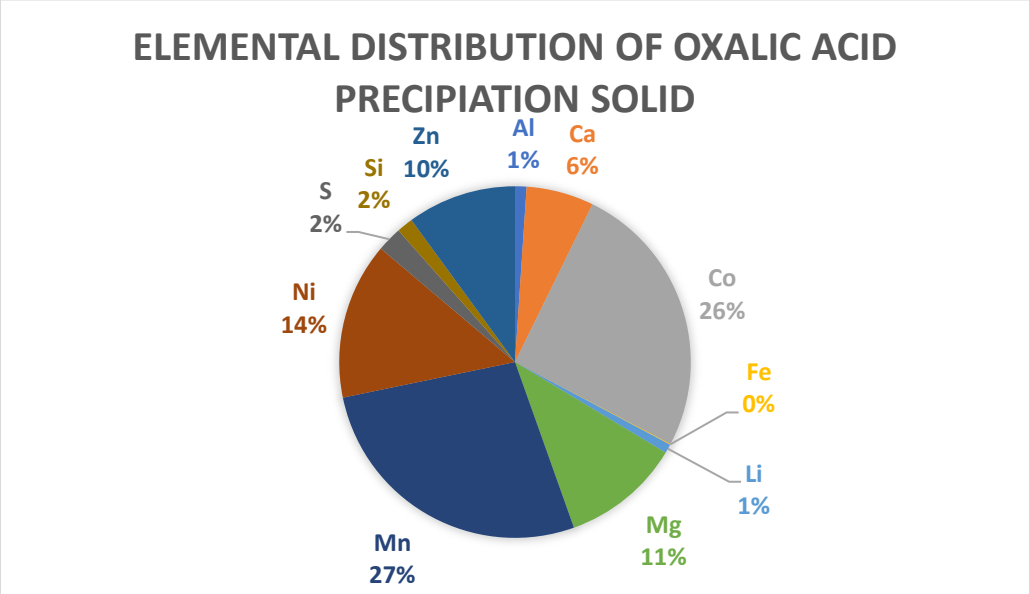

Figure 45. Elemental Distribution of Oxalic Acid Precipitation solid.

Results from **Table 25** indicated the solid produced from oxalic acid precipitation yielded a 68% purity of critical materials with the major impurities being Magnesium, Zinc, and Calcium. Results in **Figure 45** indicated that, even though manganese made up much of the solution concentration, the solid concentration was nearly even with Cobalt, while Nickel made up a slightly smaller portion of the solid.

Task 17.0 – Technical System Analysis

Approach

The raw test data generated from the project will be compiled and analyzed by the Recipient using standard mineral industry approaches. Test data will be assessed to examine transient behavior in the integrated flowsheet and confirm that steady state conditions have been achieved. Upon reaching steady state, the experimental data will be reconciled using a standard mass balancing approach. The reconciled data will then be used to determine numeric indicators of process performance including yield, recovery, grade, throughput capacity, and separation efficiency. This technical assessment will be distributed to all project team members for technical review and critique. The final performance data will be used to generate, refine, and validate detailed process models using standard mineral-industry approaches.

These models will be integrated into an in-house or commercial flowsheet simulation software to evaluate flowsheet alternatives or investigate options for flowsheet reduction/intensification. These models may also reveal opportunities for novel circuit configurations, particularly in the SX operation.

Results and Discussion

Preconcentration Data Analysis

Data from prior laboratory-scale selective precipitation test work was analyzed to determine the content of REEs and major metals in the preconcentrate product. This prior data can be used to predict the relative distribution of metals in the PLS after leaching of the preconcentrate, which in turn can be used to develop synthetic solutions for laboratory-scale solvent extraction tests. The justification for this approach of initially using synthetic solutions is based on the low mass yields of the laboratory-scale preconcentrate process. Laboratory-scale selective precipitation tests do not generate sufficient preconcentrate mass for the numerous downstream SX tests required for a full system evaluation. Using synthetic solutions will streamline the execution of the initial solvent extraction test work. After the commissioning of the A-34 site, these synthetic solutions were generally replaced by solutions with leached HPC.

The selective precipitation dataset included 14 tests with an experimental design that varied the first pH set point and the flocculent used in each step. Overall, the experimental parameters showed little influence on the composition of the second split precipitate with most of the results falling within one standard deviation of the mean. One notable exception was that the no-floc condition tended to produce higher REE concentrations and lower major metal concentrations for both pH set points. The average assays from all 14 tests for both major metals and REEs are shown in **Figure 46** and **Figure 47**, respectively. As shown, the average REE concentration was just under 2%, with critical REEs Y and Nd having the highest individual assays. Primary gangue elements included Al, Mg and Si.

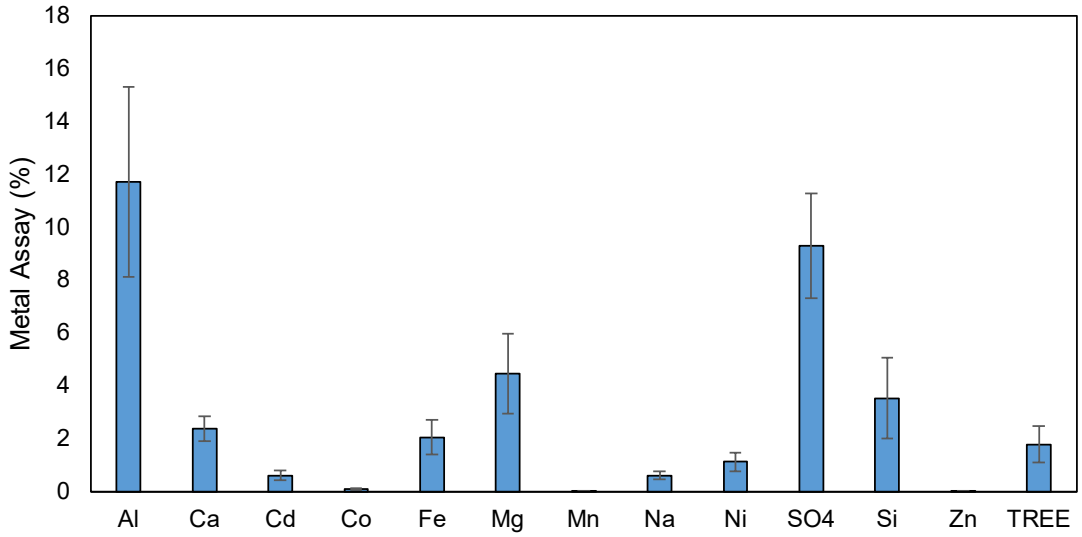

Figure 46. Average Major Ion Composition in the second split precipitate from various laboratory scale tests.

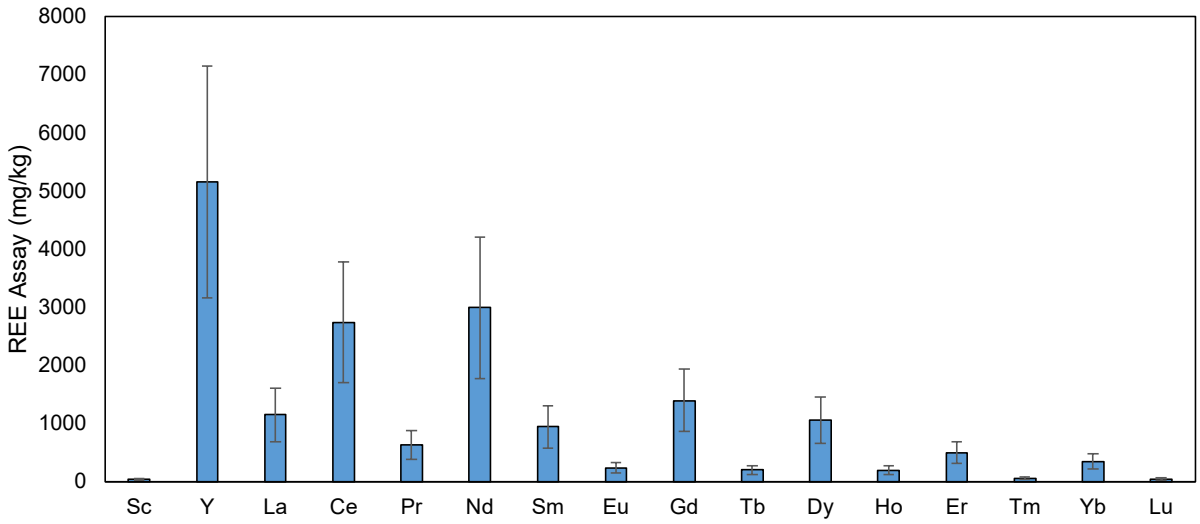

Figure 47. Average REE Composition in second split precipitate from various laboratory scale tests.

Preconcentration Data Analysis from Field Demonstration

In April of 2020, a mobile pilot plant for the preconcentration process was deployed at the A-34 site. At the time, site operations at the A-34 site used multiple settling ponds to progressively raise the pH from the inflow value to the NPDES permit condition. During the trial, the pH exiting the first pond was set to the first split target pH to simulate the first pH set point in the REE recovery process. The mobile pilot plant then intercepted a portion of the first pond discharge and raised the pH to the desired set point for the second split, thus simulating the second pH set point in the preconcentration process.

The purpose of this pilot testing was to (1) validate the processing approach in a field setting and (2) generate sufficient preconcentrate for laboratory testing of the downstream refining process. Following an initial installation, shakedown, and troubleshooting period, the pilot plant was operated continuously for 5 days including 10 process runs. During this period, the plant treated approximately 7,000 L of AMD,

producing more than 15 kg of preconcentrate (**Figure 48**). The pilot plant confirmed the metallurgical performance of the preconcentration process, as the rare earth recovery values exceeded 99% and the product grade averaged 0.55% TREE and 0.94% TREE+Co throughout the test runs (Table 1). Note, this result exceeds our proposed preconcentrate target grade in terms of TREE and CM, (cobalt) which was 0.5%. **Table 26** summarizes analytical results from the 10 test runs. The results indicate high degree of consistency (per 95% Confidence Interval) in the grade and proportion of critical (Y, Nd, Eu, Tb, Dy) REEs. The residence times in the mobile plant are much shorter than will be realized in the full plant operations and grade performance is expected to increase with scale up. It is also of interest to note that, in our previous REE project, a preconcentrate grade of 0.1% yielded a final MREO product averaging 95% after solvent extraction.

Figure 48. Mobile Plant at WVDEP site A-34 April/May 2020.

Table 26. Pre-concentrate produced at the mobile plant.

Process Run	TREE g/t	TREE+Co g/t	% Critical REEs
1	5,589	8,561	51.4%
2	3,634	5,298	52.2%
3	5,594	10,669	53.3%
4	6,444	12,056	53.1%
5	7,440	13,029	52.3%
6	6,884	12,446	53.1%
7	4,139	4,419	56.0%
8	5,478	10,350	50.4%
9	4,507	8,405	53.9%
10	5,258	8,832	55.4%
mean	5,497	9,407	53.1%
$CI_{95\%}$	815	1,967	1.2%

Figure 49 further expounds on the results from the mobile plant testing by showing the metal content of the mobile plant feed (i.e., the first pH split as a function of time throughout the five-day test.

Interestingly, the Al content experienced an unexpected increase approximately halfway through test, improving from 10 mg/L to approximately 25 mg/L. The REEs followed a similar, albeit less intensive, trend, increasing from approximately 800 µg/L to nearly 1,200 µg/L during the same period.

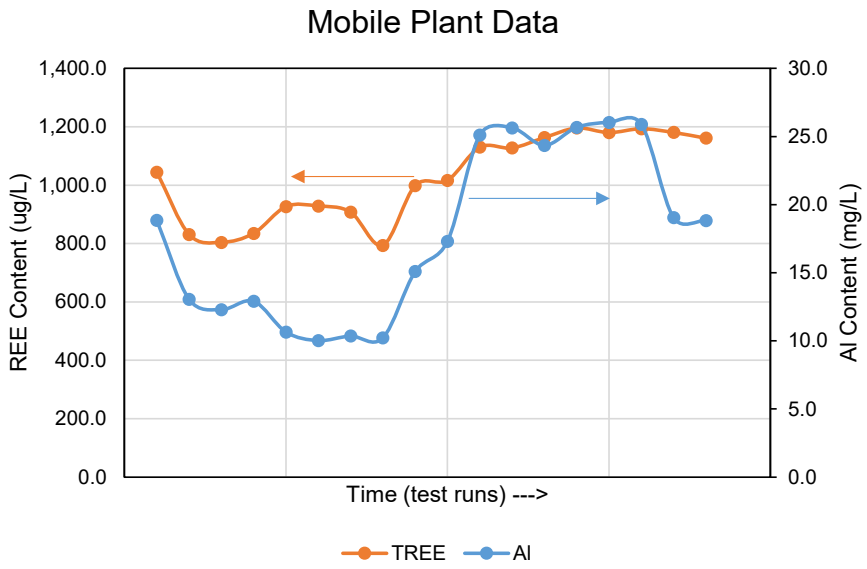

Figure 49. TREE and Al content in mobile plant feed (i.e., pH 4.5 effluent) as a function of time throughout five-day plant trial.

Figure 50 shows the same data as TREE concentration vs. Al concentration for both the pilot plant data as well as batch laboratory data with tests conducted at two pH set points. The TREE vs. Al concentration follows a very consistent trend for both datasets, thus suggesting that similar precipitation mechanisms are controlling the Al content and the TREE content in the first pH set point effluent.

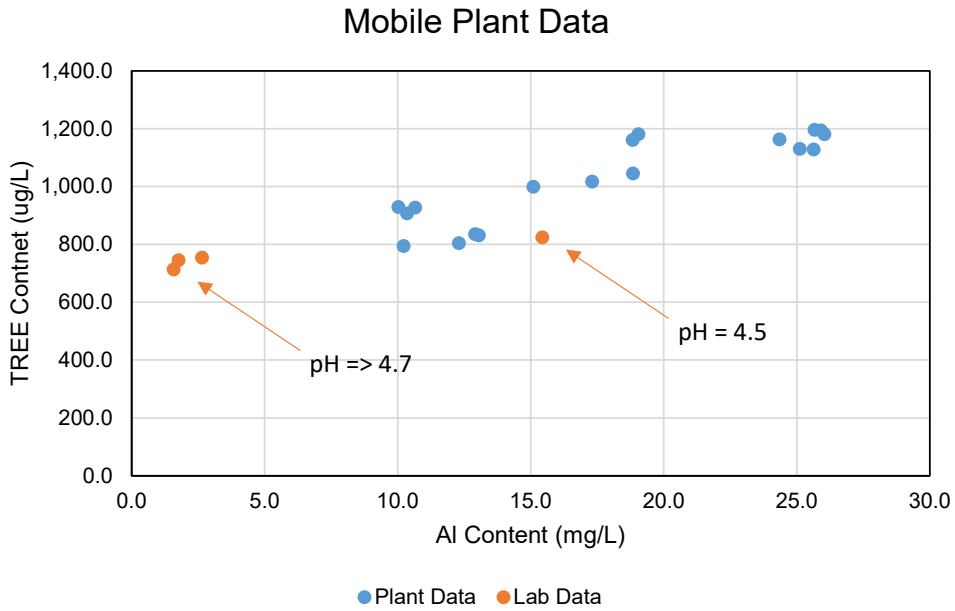

Figure 50. TREE versus Al content in mobile plant feed (i.e., pH 4.5 effluent) throughout five-day plant trial. Also shown is similar effluent produced from batch laboratory testing at different pH set points.

Despite the changes to the feed water conditions, the metallurgical performance of the mobile plant was very consistent throughout the trial. The element-by-element recoveries were very high, often in excess of 99%, and the quality of the preconcentrate product did not appreciably change, even with a nearly 2.5 increase in feed aluminum concentration (see CI values in **Table 26**). These observations suggest that the recovery in the second pH step and the grade of the PC product are independent of the inlet water conditions. Despite this finding, the REE flux and overall system recovery are dependent on feed conditions, as higher REE loading in the feed water will ultimately lead to higher REE production in the PC.

In addition to the analysis of metallurgical performance with respect to feed conditions, a second analysis was conducted to assess the inner correlation of major metals in the PC product. **Figure 51** shows a correlation matrix of the assay each major metal in the analytical suite for the 10 PC products collected during the run. Interestingly, this data shows a positive correlation for nearly all major metals, implying that an increased grade of any one metal will correlate to an increased grade of every other metal. This result indicates that some other compound, such as bound water, may be the primary "impurity" influencing the grade.

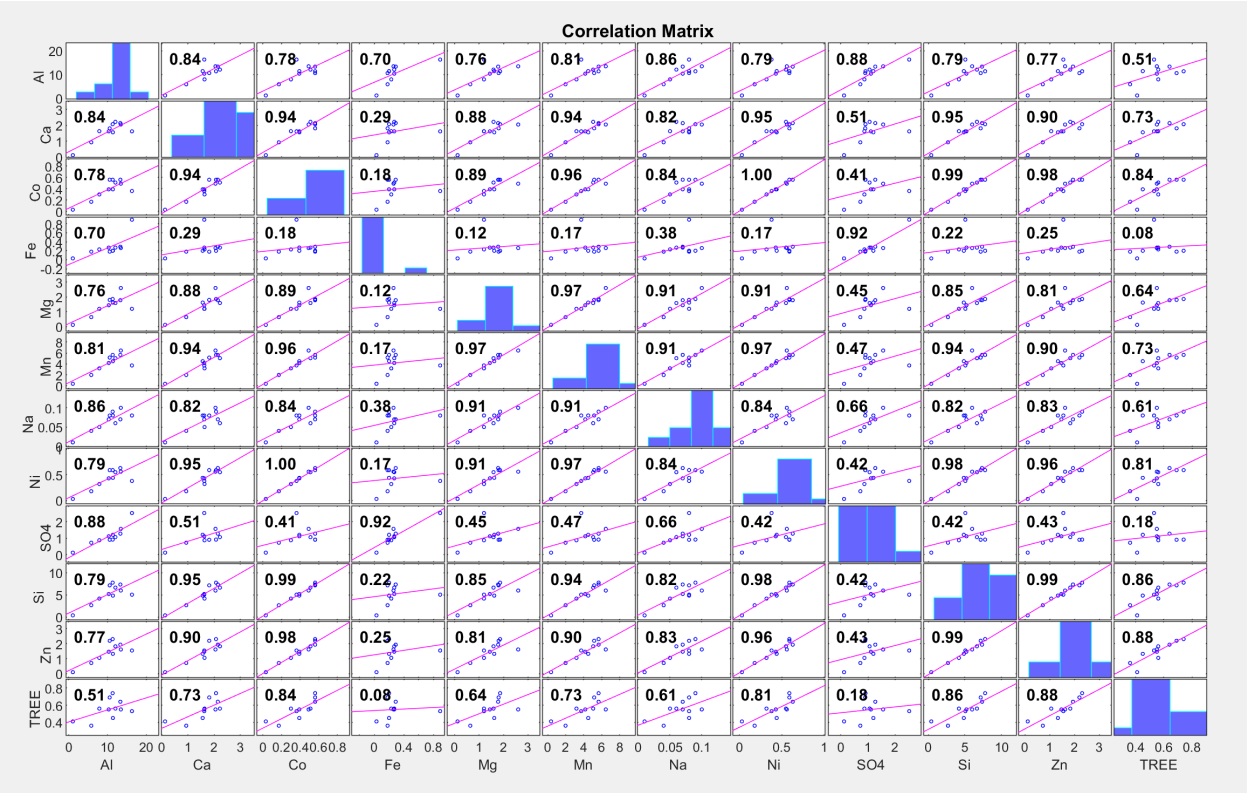

Figure 51. Correlation matrix showing assay values for major metals and REES for 10 preconcentrate samples recovered from mobile plant testing.

XRF Evaluation

Process monitoring is a valuable tool that can be used to ensure a system is operating as designed. Deviations from the norm which are quickly detected, can be quickly corrected. During the operational stage of the current project, samples from the process will be collected on a periodic basis and shipped to an offsite analytical lab for the determination of major metal and REE content. The lag between the sample collection and sample analysis may be as high as seven to ten days, which creates challenges in

properly controlling the process and adapting to changes. As a result, the team is explored low-cost options for in field measurements, which can augment the higher precision (but slower) ICP-MS analysis.

One technique evaluated was X-Ray Flourescense (XRF). XRF is a common analytical technology can be deployed in a handheld device to obtain a quick assay for solid samples in the field. For this project, researchers evaluate this technology could be used to detect trace levels of Y for process monitoring. Concentrations of Y are strongly correlated with concentrations of most other REEs during both the generation of PC and in many parts of an SX system, so a system that can adequately detect Y may serve as a suitable field instrument for process adjustments. For testing purposes, researchers used a Thermo Scientfic Niton XL2 Goldd (**Figure 52**), housed at the Virginia Tech Mining and Minerals Research Facility.

Figure 52. XRF analyzer in use at the Virginia Tech Mineral Processing Laboratory.

As an initial experiment, dried portions of a single PC sample were analyzed in incremental masses to estimate the minimum mass of PC required for detection. Sample masses used were 0.432 g, 0.1689 g, 0.0735 g, 0.0365 g, 0.0173 g, 0.0071 g, and a control test of 0 g. XRF spectra data was recorded for statistical analysis. The spectral peak for Y is at 15 keV. A larger mass of Y should correspond to a stronger peak at 15 keV. While the assay for this particular PC sample is unknown, a single sample was used. Therefore, it can be assumed that the expected Y content for a given subsample is proportional to the sample mass analyzed, allowing for sample mass to serve as a surrogate for Y mass in this exploratory test.

Simple linear regression was conducted on the data. Hypothesis testing, at the 0.05 level, provided evidence that mass is a predictor of signal strength. **Figure 53** shows the results of the linear regression with prediction intervals and the observed data. It should be noted, the prediction interval for signal strength extends into negative values, which is nonsensical. This phenomenon is a result of the small sample size and the variability of the data.

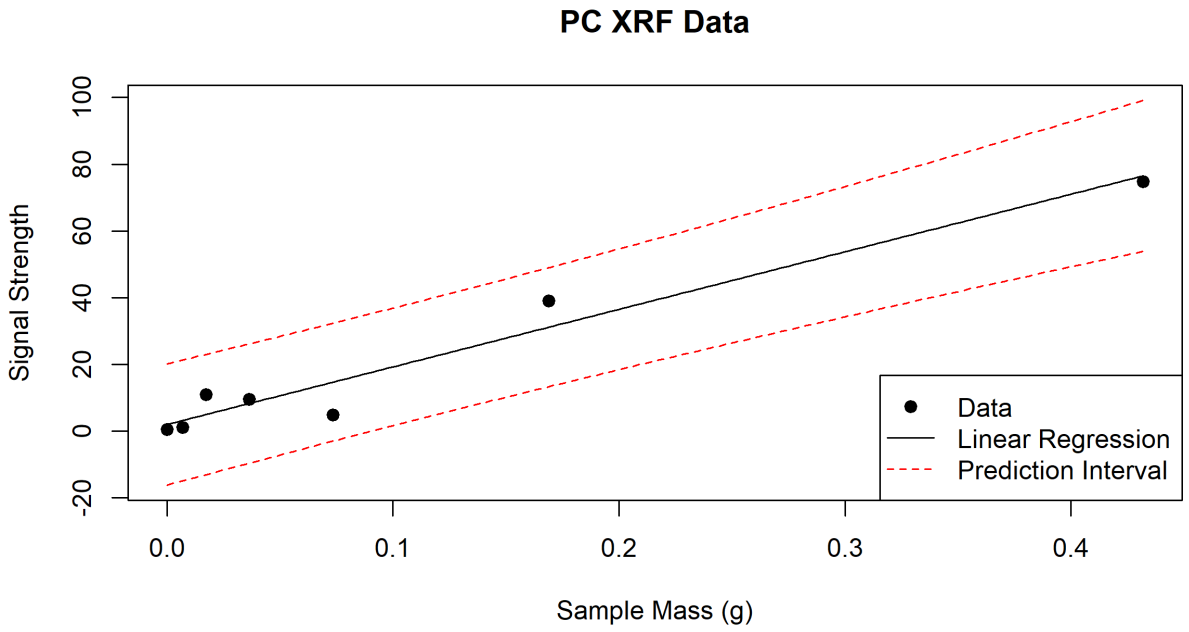

Figure 53. XRF spectra data, linear regression, and prediction intervals for dry PC.

For some tests, a very small mass of PC was used, so small that it did not properly cover the sample window on the XRF instrument. Furthermore, the dry PC sample was not completely homogeneous There were grains which were of different color. These are both causes of potential variability in the observations. Given these anomalies, a second test was conducted. In this case, a standard Y solution of known concentration was obtained. A piece of filter paper was cut out so that it covered the entire sample cup viewing window for the XRF instrument. After scanning the clean filter paper as a control test, a specified volume of the standard solution was pipetted onto the filter paper. Capillary action dispersed the aqueous solution giving a much more uniform mass of Y per unit area within the viewing window than the previous tests with dry PC material. The filter paper was air dried for 24 hours, and then analyzed using the XRF device. Additional tests were run by pipetting additional Y volumes onto the previously used paper.

The analysis was conducted for cumulative Y masses of 0 µg, 40 µg, 100 µg, 140 µg, 180 µg, and 220 µg. Linear regression was conducted on the obtained data, with a dummy variable included for the control test. A p-value for the null hypothesis of the slope of the line was computed and rejected, meaning signal strength likely changes for a change of Y mass. The dummy variable was also tested to be significant at the 0.05 level. The data, regression, and prediction intervals were plotted in **Figure 54**.

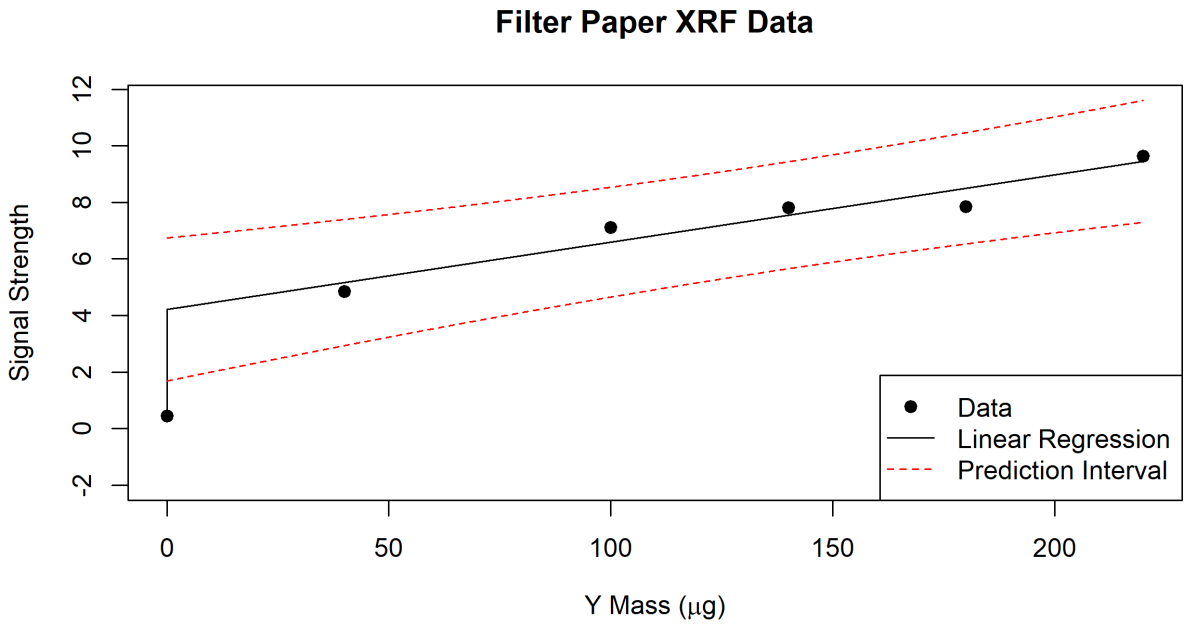

Figure 54. XRF spectra data, linear regression, and prediction intervals for Y standard on paper.

The linear fits to the data in **Figure 53** and **Figure 54** give strong evidence that the relationship between sample mass and signal strength is linear. However, with the small data sets obtained, variability in the regression is large, as indicated by the wide prediction intervals. Nevertheless, controlling for some variability produced favorable results. Quantifying this variability and estimating the minimum mass that can be measured with reliability will requires more data and complex statistical methods.

Thermogravimetric Analysis of PC

Obtaining an accurate assay of the pre-concentrate (PC) solid material has challenges. The material does not reliably fully digest in nitric acid or properly dissolve in lithium tetraborate heated to 1000˚ C as part of a fusion procedure. It was hypothesized that there may be organic material in the samples, leading to a difficulty in conducting some analytical procedures. Thermogravimetric analysis (TGA) data on PC was available, as the TGA device is used on samples prior to lithium tetraborate fusion. To get a better understanding of the components of the sample, the TGA data was examined. Approximately five grams of three wet samples were loaded into the TGA instrument and change in mass as temperature increased was recorded.

Figure 55 shows the first derivative of mass with respect to temperature. The large decrease in mass around 115˚ C is likely due to unbounded water within the samples, while the decrease in mass around 240˚ C is likely due to water bound within crystal lattices, but could be related to bicarbonates, which decompose at the same temperature. Between 400˚ C and 700˚ C the change in mass for an increase in temperature is negligible. Settings for the program used in these TGA runs used too steep of a ramp for the temperatures below 400˚ C, and it is probable that with a shallower ramp $\partial \mathrm{m}/\partial \mathrm{T}$ would have been equal to zero by 300˚ C. No definitive conclusions on the presence of organic matter were drawn from the TGA data.

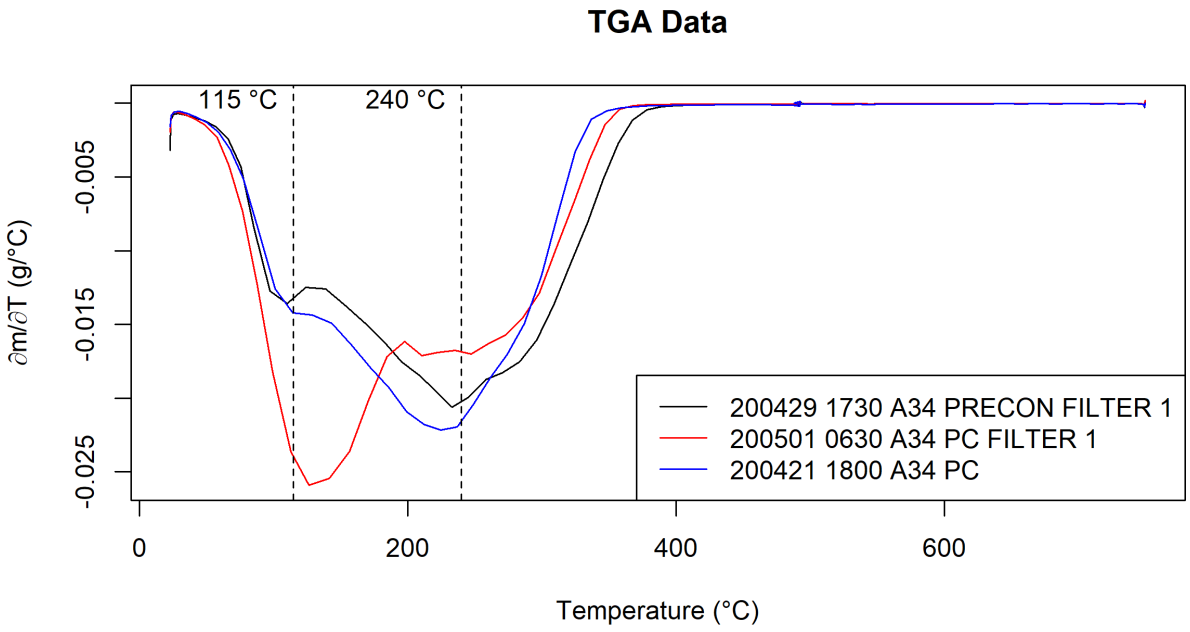

Figure 55. First derivative of mass with respect to temperature approximated from TGA data.

Data Collection for Calibration of METSIM

An SX simulation using METSIM software can be calibrated using distribution coefficients and separation factors from lab scale data and provide accurate results (Larochelle and Kasaini 2016). The distribution coefficient, D_{A}, of element A and separation factor, $\alpha_{\mathrm{A}}^{\mathrm{B}}$, between elements A and B is defined in Gupta and Krishnamurthy (1992) as Equations (1) and (2), respectively:

$$D_{\mathrm{A}} = \frac{C_{\mathrm{A1}}}{C_{\mathrm{A2}}} \qquad (1)$$

$$\alpha_{\mathrm{A}}^{\mathrm{B}} = \frac{D_{\mathrm{A}}}{D_{\mathrm{B}}} \qquad (2)$$

where C_{A1} is the concentration of element A in phase 1, and C_{A2} is the concentration of element A in phase 2. The separation factor is a ratio of distribution coefficients between elements A and B. Data used in the METSIM model were taken from the appropriate pilot and laboratory data sets included in Tasks 13 and 16, respectively.

Task 18.0 – Economic Systems Analysis

Approach

Experimental results from the various testing campaigns as well as model results from the system design optimization will be compiled into a techno-economic analysis (TEA). The analysis will report costs and performance at the existing scale and project those costs to the next design scale and/or a commercial implementation using standard scaling factors and itemized costs as appropriate. All analyses will use guidelines and assumptions provided by NETL, and results will be presented in accordance with NI 43-101 reporting standards for disclosing mineral projects. At a minimum, this analysis will include: a clear statement of the assumptions; cash forecasts on an annual basis; a discussion of potential NPV and IRR; a summary of the tax structure imposed; and a sensitivity analysis with respect to grade, price, and other significant input factors.

Results and Discussion

In addition to the economic results included in Tasks 3 and 5, additional economic analyses were used to evaluate the model sensitivity and to identify the assumptions and input variables that most significantly influence overall profitability. The model assumptions and overall approach are identical to those described in Task 3.

Given the significance of HPC grade in dictating economic outcomes, a single-factor sensitivity analysis was applied using the base case economic assumptions with grade (i.e., REE production) being the single variable factor. **Figure 56** shows the results of this analysis and indicates that the base process design has a cutoff grade of approximately 0.70% REE. The "as-modeled" condition (0.6% REE) was slightly lower than this threshold; however, testing throughout the project showed that this grade was routinely exceeded with HPC in the 1% to 2% range.

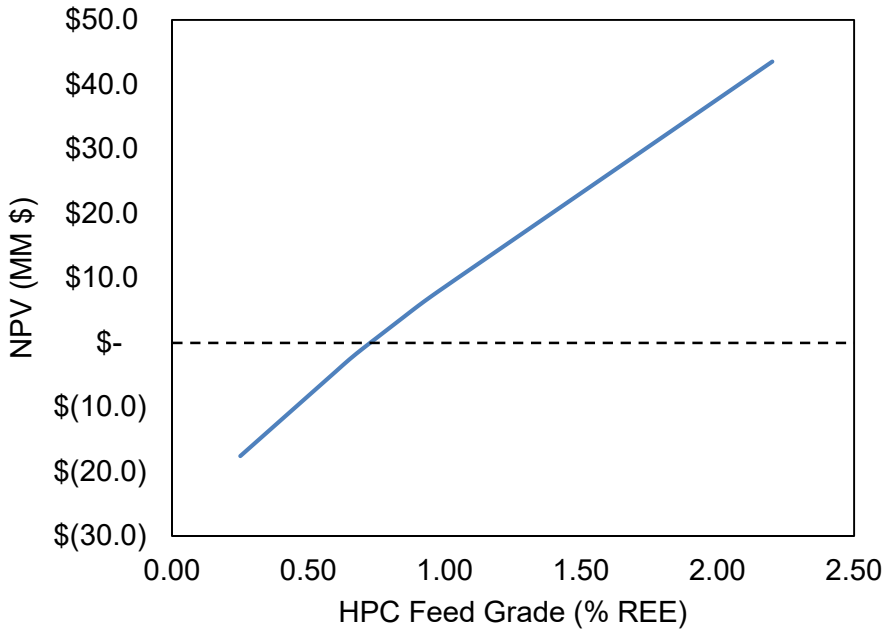

Figure 56. HPC Grade vs. NPV Sensitivity Analysis.

In addition to the grade sensitivity analysis, a separate cost-volume-profit analysis was conducted to determine the influence of plant scale on profitability for the increased grade, high pH leaching, and zeolite production scenarios. For this analysis, the REE production rate was incrementally adjusted, and the capital costs, operating costs, and revenues were recalculated at each production rate. Specifically, revenues were scaled in direct proportion to production rate, while costs were scaled according to the appropriate scaling model. Capital costs, for example, were scaled according to the power law relationship with an exponent of 0.6. Operating costs were split into a fixed portion (labor), which remained constant, and a variable portion (raw materials), which scaled linearly. Since energy and capital spares were factored from the capital cost, these were also scaled according to the power law relationship.

Results from this analysis are shown in **Figure 57** through **Figure 59** for the various scenarios. Each plot shows the capital cost relationship, the (pre-tax) operating cost and revenue, and the net present value (NPV) as a function of REE production rate. These curves show that each scenario has a breakeven

production rate where economy of scale provides sufficient revenue to cost. At a slightly higher production rate, the revenues are sufficient to offset operating cost, taxes, and capital cost to produce a positive NPV. **Figure 60** through **Figure 62** expound on this finding, showing the REE production rate needed to produce positive economic outcomes (breakeven NPV and gross margin) as a function of HPC feed grade. This result is shown for the baseline, increased pH leaching, and zeolite production scenarios.

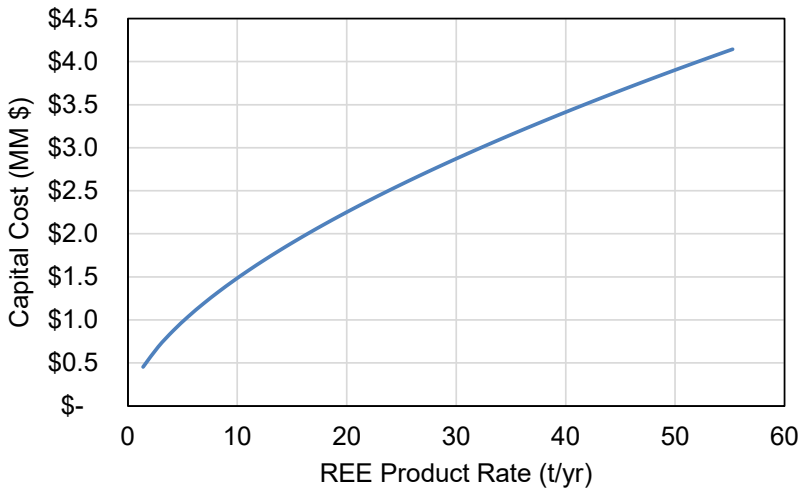

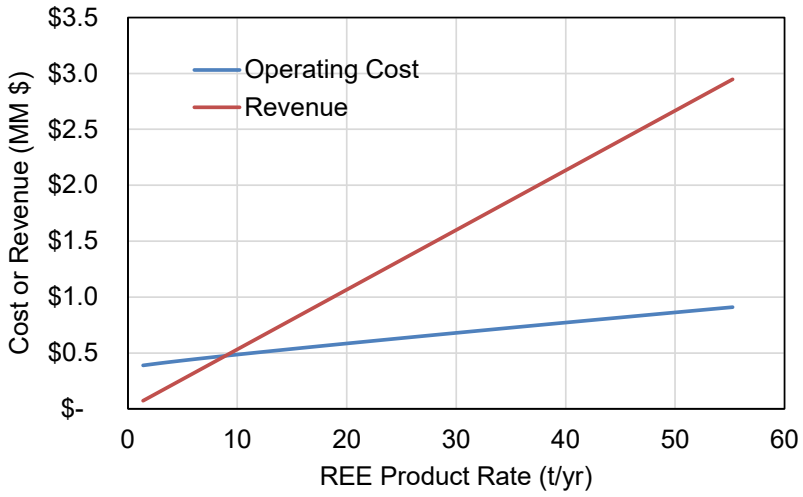

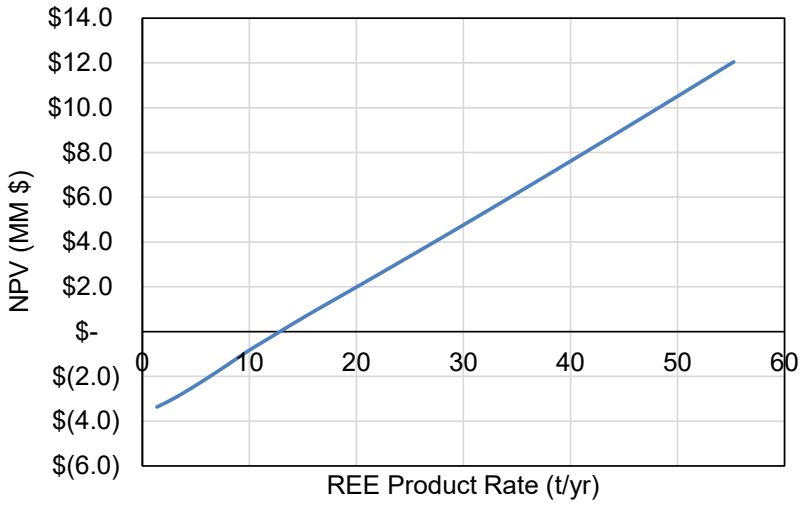

Figure 57. Cost-Volume-Profit analysis for increased pH Scenario. REE feed grade = 0.6% REE.

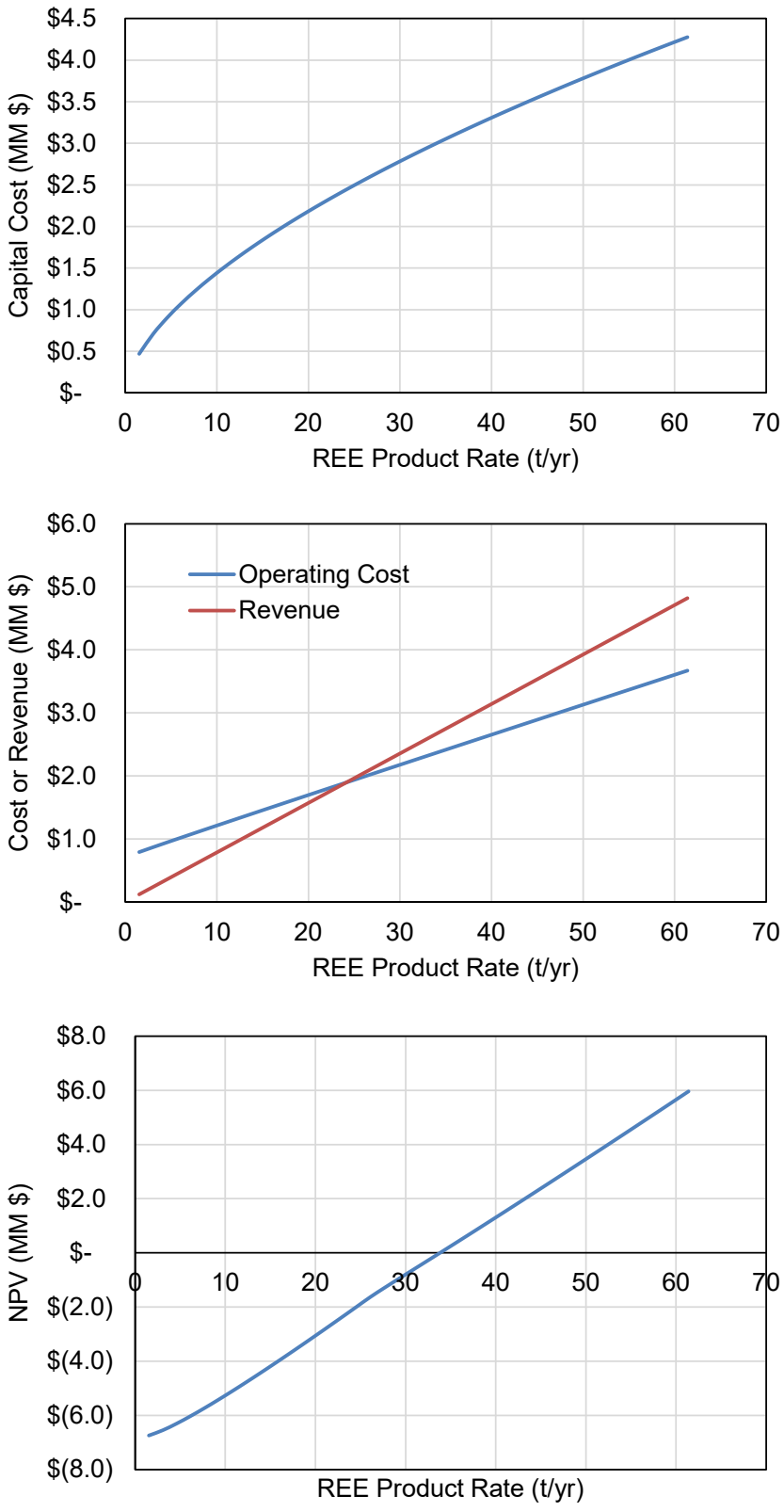

Figure 58. Cost-Volume-Profit Analysis for Zeolite Production Scenario. REE feed grade = 0.6% REE.

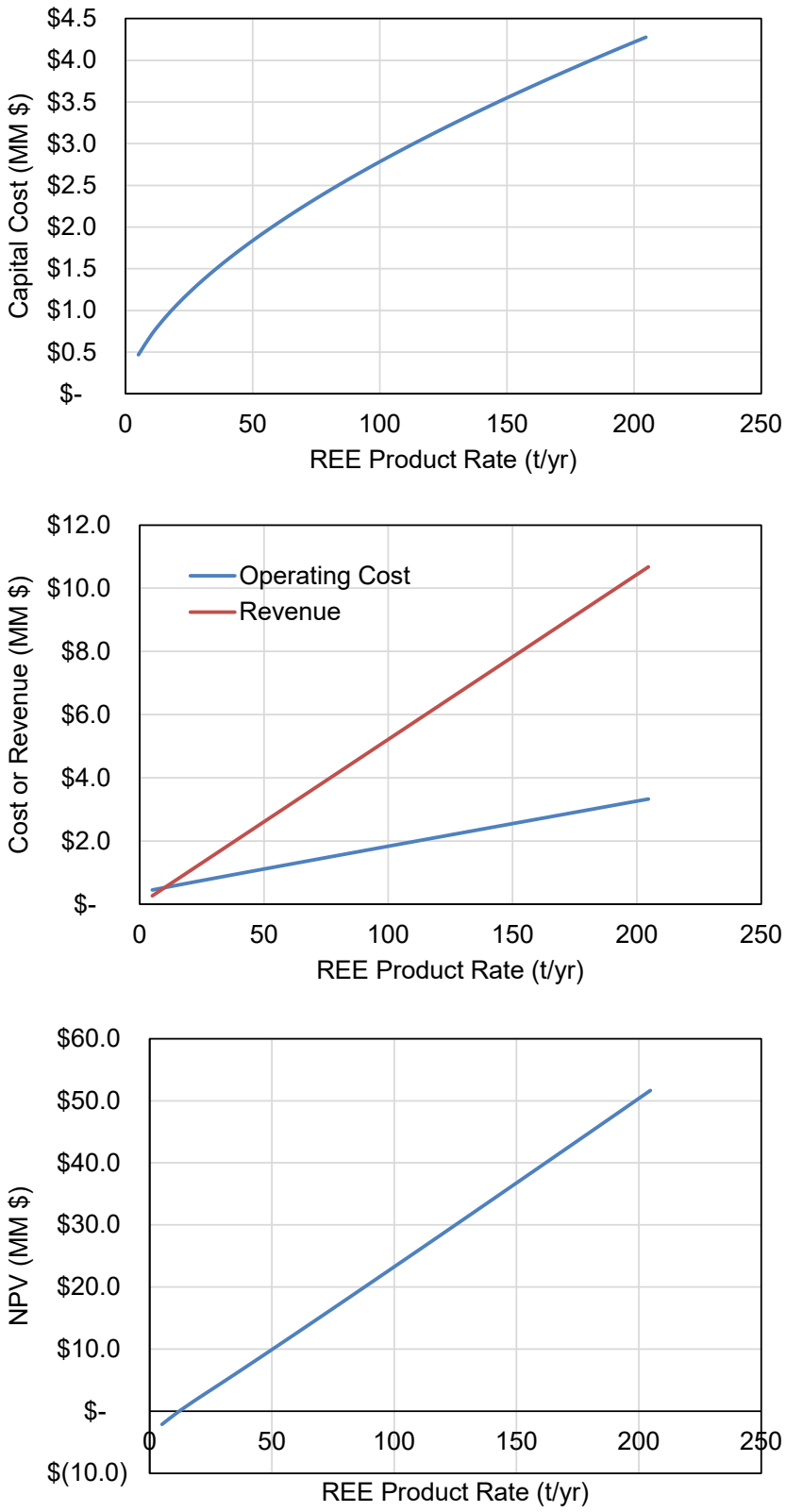

Figure 59. Cost-Volume-Profit Analysis for 2% Grade Scenario.

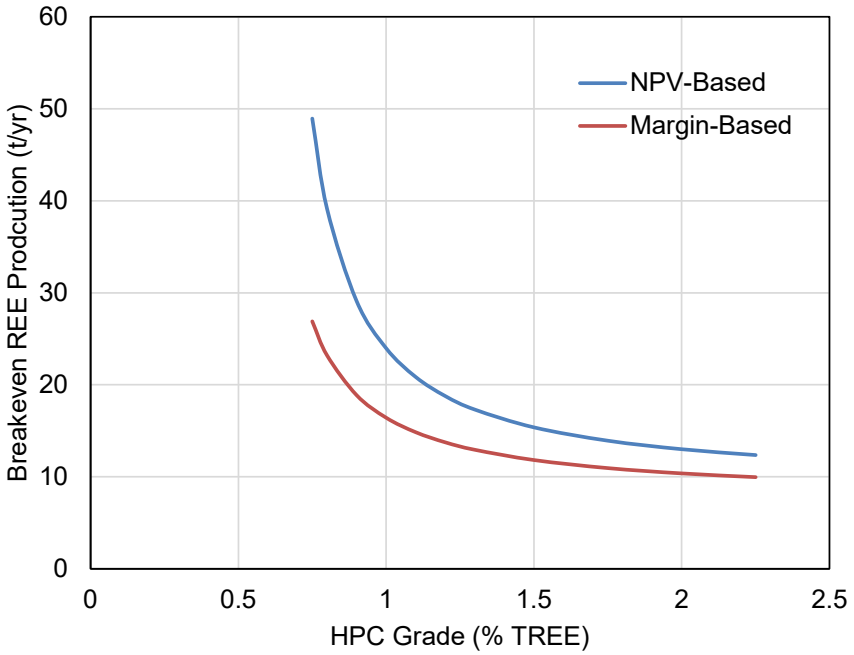

Figure 60. Breakeven REE Production as a function of HPC grade (Base case).

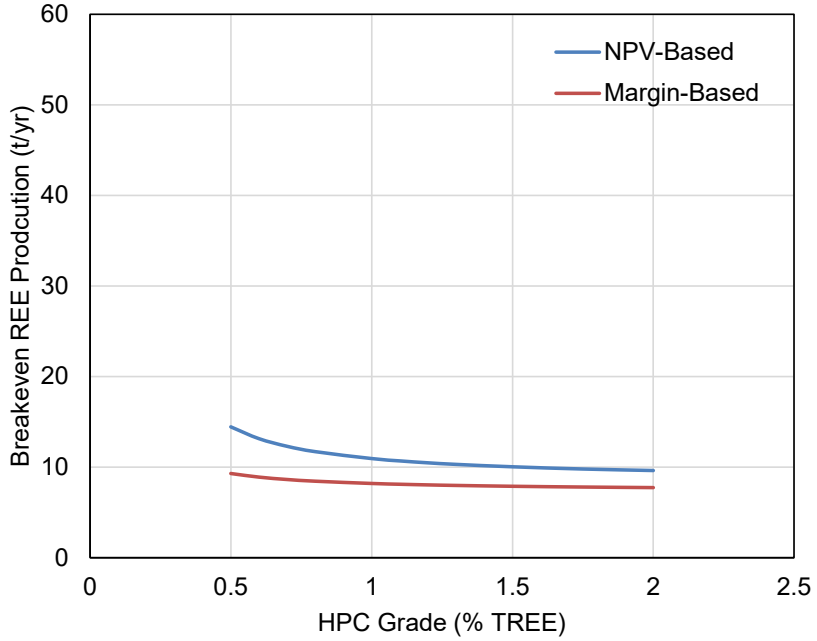

Figure 61. Breakeven REE Production as a function of HPC grade (Increased pH Leaching case).

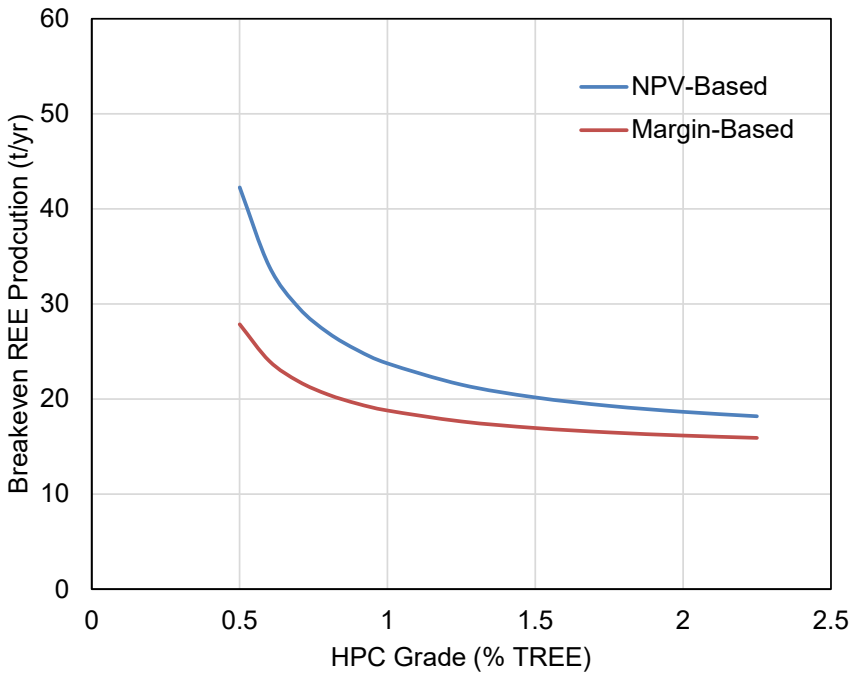

Figure 62. Breakeven REE Production as a function of HPC grade (Zeolite Production Case).

Task 19.0 – Environmental Systems Analysis

Approach

The environmental systems analysis will be conducted concurrently with the other project activities and will focus on two specific objectives: materials handling considerations and environmental compliance. The materials handling design will address the dewatering, filtration, and the short- and long-term material storage requirements for the upstream concentration process. Specific research tasks to be addressed for the material handling system design include:

1. Establish collaboration with the industry partner that manufactures the woven geotextile geotube bags proposed for the first and second splits. The partner will provide assistance with the following field scale elements: engineering strength and permittivity design, geotube proportion sizing (length and diameter ratios), geotubes stacking configurations and techniques to ensure safe and environmentally benign dewatering operations.
2. The Recipient will interface with the WVDEP to determine process treatment requirements for the geotubes water filtrate, primary liquid containment, liquid transport design and layout, and geotechnical material characterization consisting of material testing for physical, strength and permeability properties.
3. A series of numerical modeling activities will be performed for mathematical characterization of drainage in the system and the potential improvements. The outcome of the modeling is to compare and contrast with the laboratory testing and field results.
4. Increasing process efficiency will be studied to identify and reduce barriers to future technology entry into the REE/CM commercialization. One specific area for efficiency improvement is sediment dewatering of the feedstock from splits 2 and 3, and the iron-rich sediment from split 1.

In addition, the tasks to be performed for Environmental Compliance are listed as follows:

1. The Recipient will obtain samples from dewatered materials to evaluate dewatering and filtering efficiencies and material characterization for long-term disposition.
2. Preparation of project management plans and development of submission requirements for the National Environmental Policy Act (NEPA).
3. Environmental compliance oversight and reporting support to the WVDEP will be performed in order to quantify dewatered material (solid and liquid) characteristics from each split process for NPDES documentation.

Results and Discussion

Industry Collaboration

The project team collaborated with Solmax (previously TenCate) to develop and evaluate geosynthetic products for the storage and dewatering of hydraulic pre-concentrate (HPC). Solmax is a world-leading developer, manufacturer, and provider of geosynthetic materials. They contributed to the project in the form of consultation, technical support through their proprietary design tools and field-testing apparatuses, and materials fabrication. Throughout the project, Solmax provided recommendations on materials and fabricated new geobag and geotube prototypes based on filtration and dewatering tests conducted by the project team. Detailed information on Solmax materials used throughout the project is provided in previous quarterly reports. In general, the collaborative process with Solmax followed these steps:

1. Solmax recommended initial products and provided fabrics to WVU for laboratory-scale filtration testing.
2. WVU shared results with Solmax to choose an appropriate fabric for prototype designs.
3. Prototypes were designed by WVU and Solmax. Prototypes were subsequently manufactured by Solmax and provided to WVU for bench scale filtration testing.
4. Based on laboratory results, WVU collaborated with Solmax to design geobags and geotubes at various scales for onsite testing of short-term and long-term storage of HPC.
5. Solmax manufactured protype geobags and geotubes and provided them to WVU.
6. During ongoing testing, WVU collaborated with Solmax to modify the prototype designs and/or fabrication to align with the testing plan and improve product performance.

Material Classification

HPC was generated in the laboratory for characterization using the two-stage pH treatment on raw water from A-34. The HPC was classified based on particle size and strength properties.

Particle Size

A scanning electron microscope (SEM) analysis for grain-size distribution and surface characteristics was conducted on samples collected from the second split. Samples with and without polymer addition (flocculated and non-flocculated) were imaged at both 200 µm and 0.2 µm (**Figure 63**). Images indicated that most particles fall under the clay range (<2 µm) and would require flocculation for effective filtration.

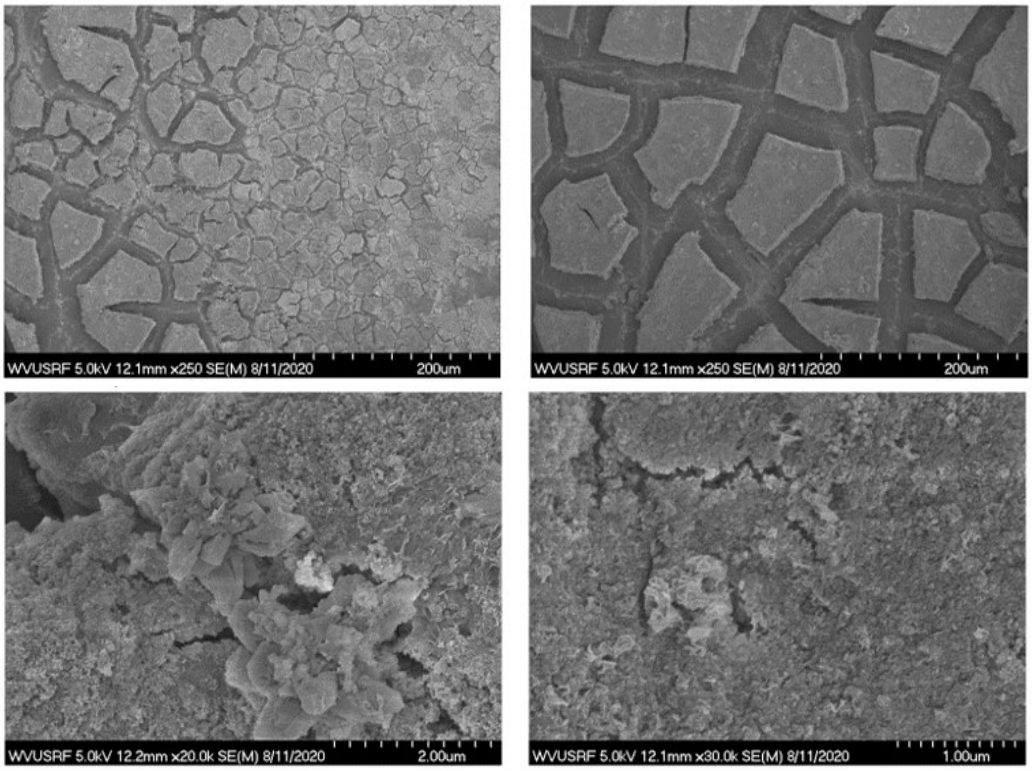

Figure 63. SEM microscope image comparing the flocculated (left) and non-flocculated (right) samples at macro-scale (200 µm, top) and clay-size range (2 µm, bottom).

Strength Properties

Geotechnical testing of HPC focused on the strength and consolidation properties by direct shear and consolidation. These tests were conducted to obtain the parameters necessary for designing the long-term storage of the materials in a safe and environmentally compliant way. Testing was completed on filter cake generated in the filter tube tests (process described in the "Fabric Evaluation" section). The following parameters were evaluated: internal angle of friction, consolidation coefficient, swelling coefficient, compression index, and friction angle.

Direct shear testing was conducted to obtain the internal angle of friction of the HPC. Shear stress and horizontal displacement were tested at varying axial stress for HPC dosed with polymer (refer to "Polymer Evaluation" section for polymer selection process) at concentrations of 2, 4, and 6 parts-per-million (ppm). The results obtained in the direct shear test were not valuable; the high moisture content of the HPC resulted in large strain under low stress conditions. The plot of stress versus strain did not follow the Mohr-Coulomb failure criterion, so no friction angle could be determined.

Consolidation tests were performed on HPC flocculated using polymer concentrations of 2, 4, and 6 ppm to evaluate the effect of polymer dose on consolidation with respect to settlement and void ratio (moisture content) reduction. Average consolidation parameters are provided in

Table 27. Average consolidation coefficient was a typical low value for clay soils. Average compression index was comparable to peat or very soft clay.

Table 27. Average consolidation parameters for A-34 pH 8.5 HPC.

Parameter	Average Value
Initial moisture content, ω (%)	94
Final total solids, TS (%)	19
Initial height of specimen (in)	1.00
Final height of specimen (in)	0.35
Compression Index, C_v	20.06
Swell Index	0
Consolidation coefficient, C_w	2.21×10^{-2}

Consolidation plots (void ratio versus pressure) for each test are provided in **Figure 64**. The material did not develop swelling, so no unloading was performed for the 4 and 6 ppm tests. A reduction in void ratio of approximately 60 percent was noticed in all samples.

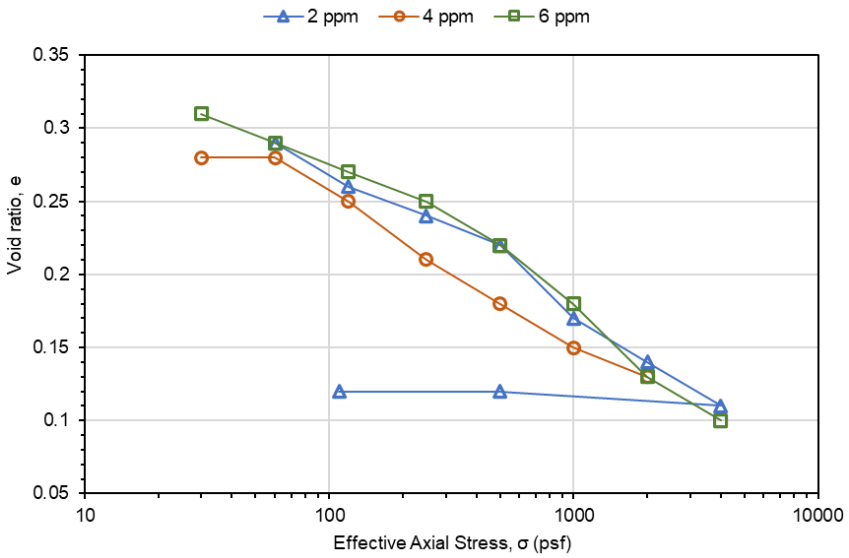

Figure 64. Consolidation plots for A-34 HPC at varied polymer dose.

The consolidation results were used to evaluate if stacking geotubes was a practical way to promote dewatering and achieve a desired percent total solids (TS) by consolidation. The percent TS generated by increasing overburden stress at varied polymer dose is presented in **Figure 65**. Each geotube layer (5 ft height) would produce a static total stress of 312 pounds per square foot (psf). A total of 12 bags stacked vertically (60 ft height, static total stress of 3,744 psf) would be required to reach a maximum TS of approximately 20%. Geotube stacking was assessed as an impractical way to achieve desired dewatering, as stacking higher than 10 feet vertically is neither safe nor feasible. It was determined that passive dewatering of the geotubes would be the preferred option for increasing total solids.

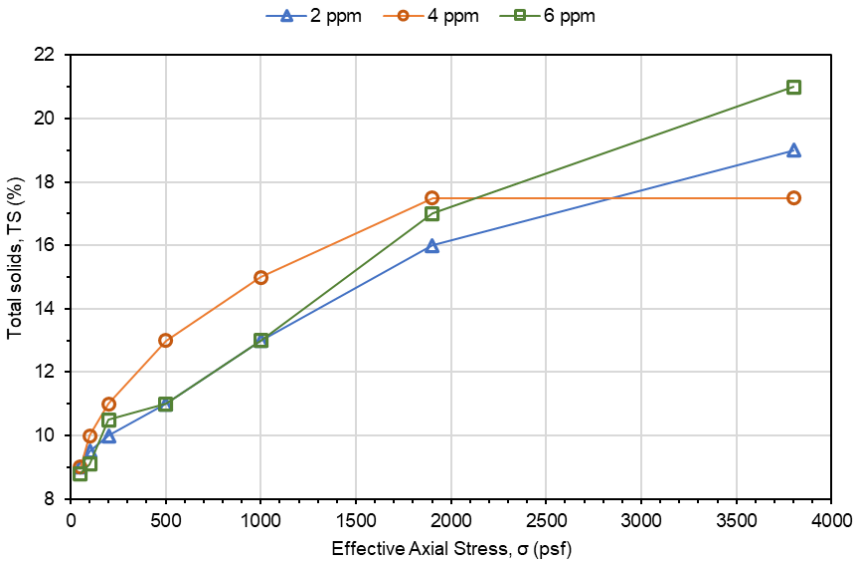

Figure 65. Total solids response to consolidation of A-34 pH 8.5 HPC at varied polymer dose.

Laboratory Scale (Filter Tube Tests)

Fabric performance was first evaluated in the laboratory scale filter tube tests using geosynthetic samples provided by Solmax. The test setup in shown in **Figure 66.** The test setup consisted of a clear PVC pipe with a graduated tape measure and a geotextile filter placed at the bottom of the pipe. HPC was placed within the pipe and allowed to filter through the geotextile. A graduated cylinder was placed underneath the apparatus to capture and measure the discharge. The following parameters were monitored: mass of solids in influent HPC, mass of solids retained on fabric, mass of solids entrained within fabric, mass of solids in filtrate, filter cake (accumulated solids) thickness, and head (water level). Solid masses were used to calculate filtration efficiency (percent passing, percent retained). Filter cake thickness and head were used to calculate hydraulic conductivity.

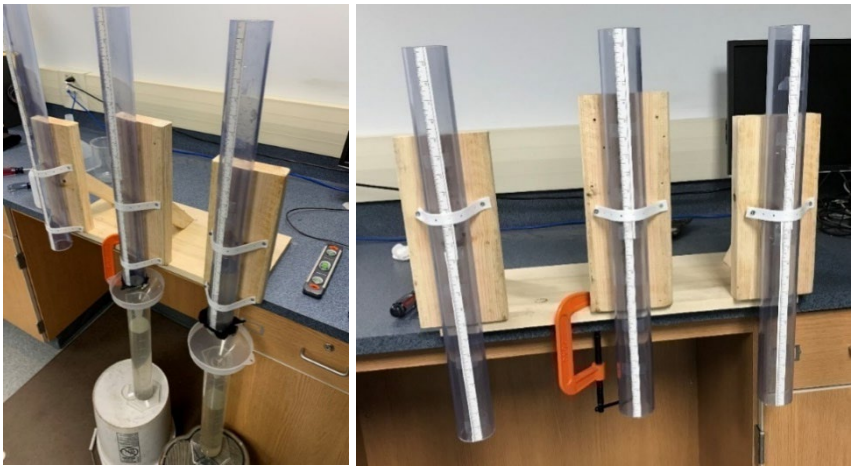

Figure 66. Filter tube test laboratory testing apparatus.

The filtration apparatus was tested and calibrated with a surrogate material (kaolinite clay) prior to testing of HPC. Kaolinite was tested for geotechnical properties and referenced to literature for validation of the predictive testing. The average specific gravity was 2.76. From grain size distribution, the kaolinite was 37% fines and approximately 25% clay. Atterberg limits were determined as liquid limit (LL) = 102%, plastic limit (PL) = 54%, and plasticity index (PI) = 48.

Tests were performed with two (2) concentrations of kaolinite slurry and two (2) geosynthetics. Solmax GT500 was used as a representative woven fabric. A GSE fabric was used as a representative nonwoven fabric. This was not a Solmax product but was readily available at the time of testing and used for comparison purposes. The AOS (0.212 mm) was similar to Solmax nonwoven products. Surrogate material test conditions and results are provided in **Table 28.** Results indicated the testing apparatuses were functioning properly and that nonwoven fabric performed slightly better with respect to filtration.

Table 28. Filter tube test conditions and results for surrogate kaolinite clay.

Test No.	Material	Material Mass (g)	Volume of DI Added (mL)	Fabric	Percent Retained (%)	Percent Passing (%)
1	Kaolinite	10	1000	GSE Nonwoven	92.4	7.4
2	Kaolinite	50	1000	GSE Nonwoven	97.3	2.6
3	Kaolinite	10	1000	GT500 Woven	65.4	34.6
4	Kaolinite	50	1000	GT500 Woven	97.7	2.4

After successful completion of the surrogate testing, filter tube tests were conducted using HPC. Filtration efficiency and hydraulic conductivity data were collected to evaluate the performance of the different fabrics with three variations of the HPC material (raw, flocculated, and sheared). “Raw” HPC was never treated with a flocculant. “Flocculated” HPC was flocculated with polymer and not disturbed so that the floc was intact throughout the test. “Sheared” HPC was flocculated but was disturbed after flocculation, causing flocculated particles to break apart and shear. A total of thirteen (13) tests were performed using the three (3) HPC material variants and two (2) geotextile fabrics

Results from raw, flocculated, and sheared HPC filter tube tests are presented in **Table 29**, **Table 30,** and **Table 31,** respectively. Results indicated that the flocculated samples and nonwoven geotextile had the best performance in terms of both solids retention and dewatering. The minimum filtration efficiency for nonwoven fabric was 80%, regardless of flocculation condition; 99-100% filtration efficiency was reached for all flocculated samples. Initial hydraulic conductivity ranged from 10^{-3} to 10^{-4} cm/s and was highest (best) for flocculated samples. Hydraulic conductivity typically reduced by one factor of 10 in subsequent passes of water; this effect was most pronounced for sheared samples.

Table 29. Filter tube test results for raw HPC.

Fabric	Percent Retained (%)	Percent Passing (%)	Filtration Efficiency (%)	Percent Lost (%)	Mass Lost ($g/cm^{2)}$	Moisture content, ω (%)	Initial Hydr. Cond., k_i (cm/s)	Recirculated Hydr. Cond., k_{recirc} (cm/s)	DI Passed Hydr. Cond., k_{DI} (cm/s)
1100N	85.5	12.2	87.8	2.3	2.02E-02	95.6	1.84E-04	-	1.39E-04
1100N	77.6	19.9	80.1	2.5	2.37E-02	94.8	1.85E-04	-	1.74E-04
1100N	96.4	0.0	100.0	3.6	3.50E-02	95.6	-	1.71E-04	9.50E-05
1100N	95.5	0.0	100.0	4.5	3.80E-02	93.9	-	3.46E-05	1.85E-06
1100N	89.9	3.8	96.2	6.3	2.61E-02	94.0	-	-	1.15E-04
1100N	96.4	0.0	100.0	3.6	1.53E-02	95.5	-	1.70E-04	9.34E-05

Table 30. Filter test results for flocculated HPC.

Fabric	Percent Retained (%)	Percent Passing (%)	Filtration Efficiency (%)	Percent Lost (%)	Mass Lost (g/cm^2)	Moisture content, ω (%)	Initial Hydr. Cond., k_i (cm/s)	Recirculated Hydr. Cond., k_{recirc} (cm/s)	DI Passed Hydr. Cond., k_{DI} (cm/s)
1100N	99.1	0.0	100.0	0.9	4.44E-03	93.5	5.02E-04	-	3.42E-04
1100N	97.1	0.8	99.2	2.1	1.18E-02	96.4	5.62E-04	-	1.14E-03
1100N	99.1	0.0	100.0	0.9	8.39E-03	94.8	5.66E-04	-	9.13E-04

Table 31. Filter tube test results for sheared HPC.

Fabric	Percent Retained (%)	Percent Passing (%)	Filtration Efficiency (%)	Percent Lost (%)	Mass Lost (g/cm^2)	Moisture content, ω (%)	Initial Hydr. Cond., k_i (cm/s)	Recirculated Hydr. Cond., k_{recirc} (cm/s)	DI Passed Hydr. Cond., k_{DI} (cm/s)
GT500	64.4	35.4	66.6	0.2	-	95.7	-	-	-
GT500	69.1	30.9	69.1	-	-	94.3	-	-	-
1100N	85.1	11.9	88.1	3.0	1.18E-02	96.8	1.41E-03	-	3.36E-04
1100N	98.0	0.0	100.0	2.0	6.91E-03	96.7	1.00E-03	2.47E-04	2.71E-04

Additional filter tube tests were completed to evaluate successive flocculation. The polymer dose at the first split (5 ppm) was constant and was determined in individual SRF tests. The optimum floc dose at the second split (4 ppm) was determined in successive flocculation SRF tests. The polymer dose at the second pH split was then increased by factors of 2, 3, 4, and 5. The results are summarized in **Table 32.**

Table 32. Filter tube test results for A-34 HPC with successive flocculant dosing.

Polymer dose at 8.5 pH split (ppm)	Percent Retained (%)	Percent Passing (%)	Filtration Efficiency (%)	Percent Lost (%)	Mass Lost (g/cm^2)	Slurry Total Solids, TS (%)	Filter Cake Total Solids, TS (%)	DI Passed Hydr. Cond., k_{DI} (cm/s)
4	83.6	15.1	85.0	1.4	4.74E-02	0.1	3.5	1.31E-02
8	64.0	33.3	66.7	2.7	6.02E-02	0.6	6.8	1.51E-02
12	95.0	3.9	96.1	1.2	1.68E-02	0.7	3.5	1.94E-02
16	98.7	0.5	99.5	0.7	5.92E-03	0.6	3.4	6.34E-03
20	96.4	2.7	97.3	0.9	1.18E-02	0.6	3.9	4.43E-03

The filtration efficiency at the optimum polymer dose from SRF testing (4 ppm) was 85%. In the initial filter tube tests and using the same geotextile (without successive dosing), a filtration efficiency close to 100% was achieved with a 4-ppm dosage. There was also a decrease in hydraulic conductivity by one order of magnitude with the polymer dose increase. The carryover of the 5-ppm dose from the first pH split appeared to impair the second pH split flocculation and consequently the overall geotextile filtration efficiency and dewatering. Previous results with lower polymer doses indicated better flocculation, higher filtration efficiencies, and no significant decrease in hydraulic conductivity. Based on these results, subsequent tests focused on flocculation at the second pH split only.

Bench Scale (Mini Bag Tests)

Upon completion of the filter tube tests, evaluation of the filtration performance of the nonwoven fabric was completed at a small bench scale. The bench scale tests (referred to as “mini bag tests”) used five-gallon-bucket-sized bags to evaluate fabric performance. These tests simulated the procedure of the filter tube tests at a larger but still controlled scale. Nonwoven fabric has low tensile strength compared

to a woven fabric, so it was used in composite with an outer layer of a woven fabric with a larger AOS and higher tensile strength (FW404). FW404 has similar hydraulic performance to but lower strength than GT500 (the conventual Solmax fabric used for geotubes). An additional drainage layer (Solmax Geotextile Filter Fabric) was used between the fabric and the bucket to allow free drainage while containing the filtrate. A slurry was poured into the bag and allowed to filter through the bag and into the bucket. **Figure 67** depicts the execution of the test.

Figure 67. Mini bag test execution (from left to right): retained HPC during filling; retained filter cake after filling and drainage; filtrate during bag filling.

Multiple flocculation scenarios were tested, including individual split and successive dosing. Retention was high for all tests, confirming the performance of 1100N found in previous tests. Results indicated that dosing at the first pH split alone was insufficient. Polymer addition at the second pH split was necessary and was insufficient at a low dose.

Onsite Parametric Tests

Observations and results from laboratory- and bench-scale tests were used to inform parametric and performance tests of fabrics at the pilot plant. Onsite tests evaluated fabric filtration and dewatering performance with HPC produced at the plant and at a near-operational scale. Onsite testing consisted of parametric tests to evaluate the effect of plant operational parameters on fabric performance. These included polymer dose, polymer application point, HPC inflow rate, and HPC source.

Onsite parametric tests utilized 10-gallon geobags. Bags were tested within the plant's short-term HPC storage area as hanging bags in steel containment units. The containment units are described in detail in the "Short-Term HPC Storage" section.

Parametric tests were completed for eleven (11) bags provided by Solmax. Each bag was filled (or "charged") three (3) times. During bag filling, samples were collected to determine influent TS. Samples to determine filtrate TS were collected during and after bag filling. After each charge, the liquid level in the bag was recorded over time as the bag drained. After the test, the bag was stored for further periodic collection of the retained solids for TS data. Pictures of this procedure are provided in **Figure 68**.

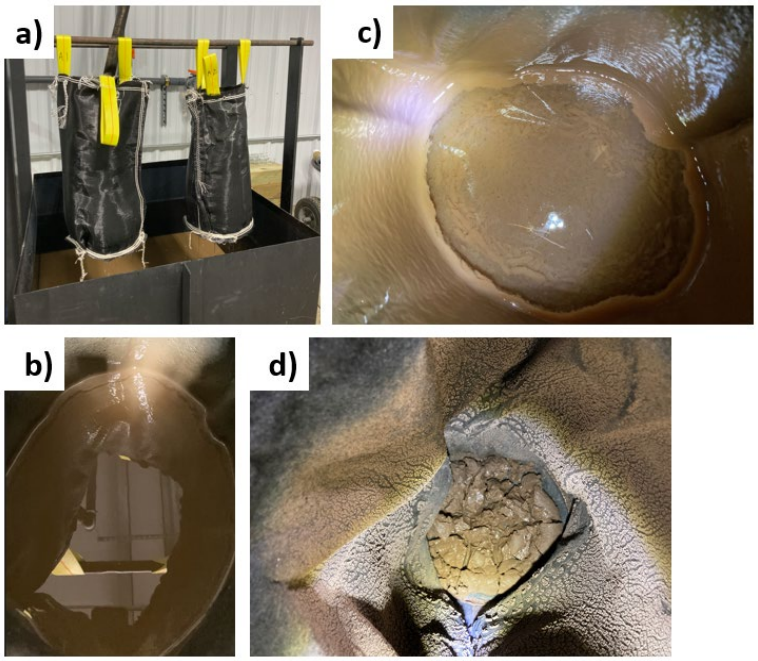

Figure 68. 10-gallon Geobag parametric tests setup: a) hanging bags in containment unit; b) bag during charging; c) bag during dewatering; d) retained HPC.

Plant parameters were varied among tests to determine which conditions resulted in the best geobag performance. The following parameters were tested: HPC source (directly from Clarifier 2 [CL2] or also routed through the cone tanks [CT]), primary polymer dose (within CL2), and/or secondary polymer dose (i.e., pre-spraying the bag with polymer). **Table 33** presents a summary of the parametric test scenarios.

Table 33. 10-gallon Geobag parametric test conditions.

Bag ID	Description	HPC Source	Pump rate (gpm)	Primary polymer dose (ppm)	Secondary polymer dose (ppm)
A1	From clarifier, higher floc dose, low flow	CL2	5	3	0
A2	From clarifier, higher floc dose, low flow	CL2	5	3	0
A3	From clarifier, baseline floc dose, low flow	CL2	5	1	0
A4	From clarifier, baseline floc dose, low flow	CL2	5	1	0
A5	Routed through cone tanks, baseline floc dose, high flow	CT	40	1	0
A6	Routed through cone tanks, baseline floc dose, high flow	CT	40	1	0
A7	From clarifier, baseline floc dose, high flow	CL2	40	1	0
A8	From clarifier, baseline floc dose, low flow, floc pre-spray	CL2	5	1	3
A9	From clarifier, baseline floc dose, low flow, floc pre-spray	CL2	5	1	3
A10	Routed through cone tanks, higher floc dose, high flow	CT	40	3	0
A11	Routed through cone tanks, higher floc dose, high flow	CT	40	3	0

Data on both solids retention and dewatering were gathered for each test. Retention was evaluated based on the percent total solids (TS) of the influent and filtrate. Dewatering was evaluated based on hydraulic conductivity and drainage time (i.e., at what rate and for how long effluent discharged from the bag during the draining phase). Dewatering was also evaluated based on the solids content over time of the HPC retained in the bag (i.e., at what rate retained HPC dried).

Retention results are provided in **Figure 69** and summarized as follows:

- While the polymer dose in Clarifier 2 was modified throughout the tests, early changes in dose (i.e., A1 and A2 versus A3 and A4) were not realized as actual changes in polymer dose due to clogging issues in the polymer lines. The results for bags A1 through A3 were therefore considered to be compromised due to the clogging. Results from bag A4 were eliminated due to an error in bag construction. Actual change in Clarifier 2 polymer dose was achieved in subsequent phases of testing.
- Incoming TS only substantially increased if additional dewatering occurred via settlement in the cone tanks (tests A5, A6, A10, A11).
- Higher incoming TS was also seen in the first Charge of bag A7 (high flow test of HPC directly from Clarifier 2). This was attributed to the high sludge level in the clarifier at the time of the test. Additional tests of TS content at different inflow rates, ranging from 5 to 50 gpm, indicated no change in incoming TS. Sludge level was included as a documented parameter in future testing.
- Initial effluent TS during the bag filling phase of Charge 1 was variable and followed the same relationship as incoming TS (i.e., higher incoming TS resulted in higher initial effluent TS). The exceptions to this were bags A10 and A11, which exhibited immediate high filtration efficiency. This was attributed to the incoming TS (>2%) being the highest seen in any tests. High flow tests only exhibited good filtration if the incoming TS was high.
- The impact of higher TS in the effluent depends on how long the bags takes to fill; longer bag filling resulted in extended durations of higher solids discharge. Fill time for Charge 1 was variable. Fill times decreased as incoming TS increased. The time needed to fill a bag was consistent and short in Charges 2 and 3.
- Test parameters did not appear to impact retention performance beyond Charge 1 (first bag fill). Initial and final effluent TS in subsequent bag filling (Charges 2 and 3) were consistent for almost all tests. The exception was bag A7, where the high flow rate either resulted in limited seeding of the bag (i.e., less filling of pores with HPC) or in material being pushed out of the pores in response to repeated filling.
- The lowest effluent TS within the first charge (0.2%) was achieved with bags that were also pre-sprayed with polymer prior to filling. In these tests, the polymer acted as a “bag seeding” without the addition of HPC. The “pre-spray” was representative of a secondary polymer application point, which was further investigated in subsequent phases.
- Higher flows (e.g., 40 gpm) were necessary to effectively pump HPC when solids content was high (>1%).

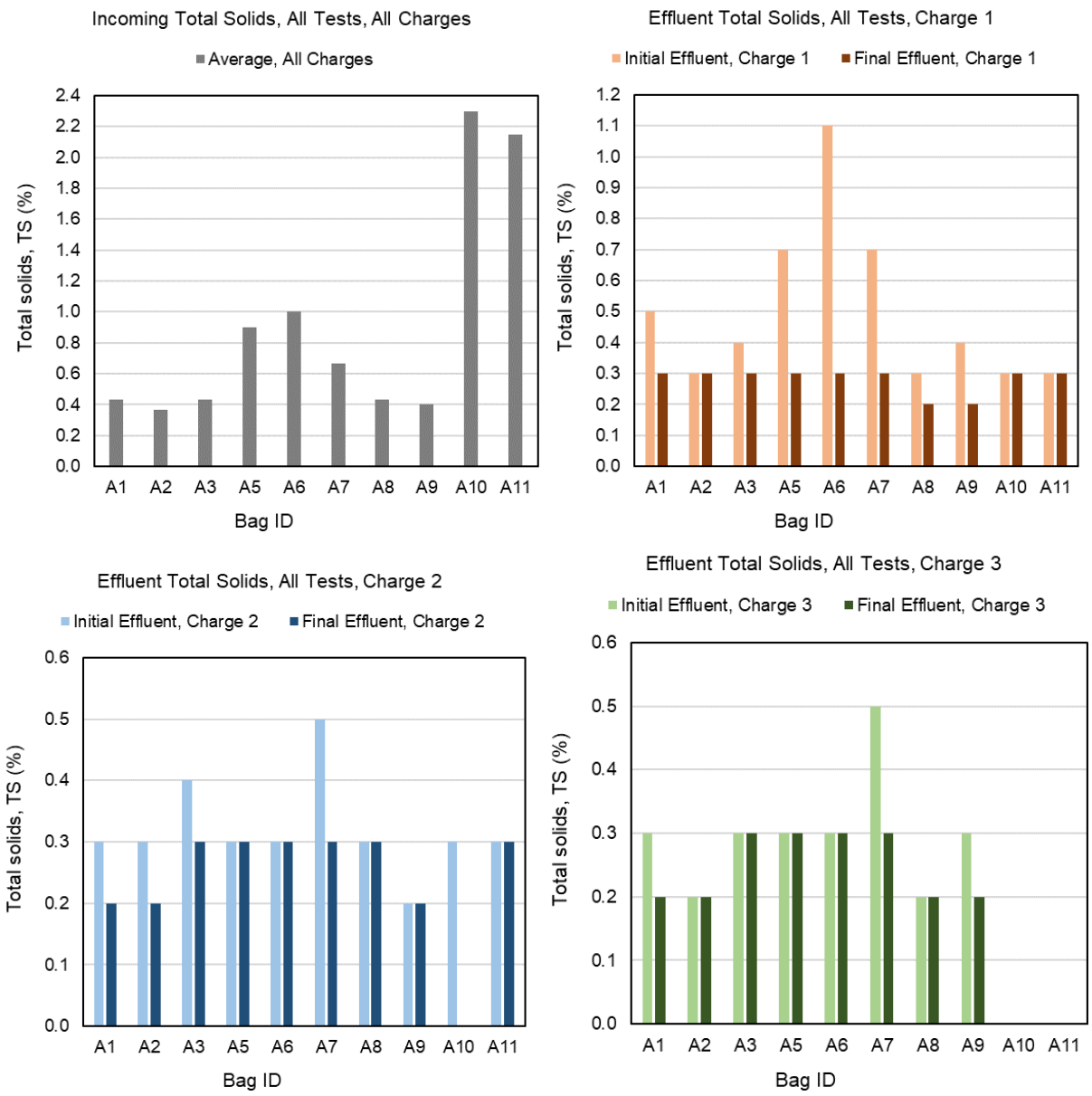

Figure 69. Retention results from onsite geobag parametric tests.

Dewatering results for the drainage phase are provided in **Figure 70** and summarized as follows:

- Hydraulic conductivity and drainage time were variable among tests. The variability was most pronounced in Charge 1 (first bag filling).
- Hydraulic conductivity and drainage time decreased and increased, respectively, as the number of charges increased. Dewatering performance decreased as bags were filled multiple times.
- The worst dewatering performance occurred in tests where the incoming TS was highest (bags A5, A6, A10, A11). These tests were also conducted with HPC that was routed through the cone tanks. Because the cone tank settlement step included another pump in addition to the clarifier pump, it is hypothesized that the floc produced in the clarifier was sheared prior to getting into the bags. Intact floc is critical to achieving the desired dewatering performance.
- The best dewatering performance occurred in tests where the bags were pre-sprayed with polymer (bags A8, A9). In these tests, the polymer pre-spray appeared to improve retention without relying

on HPC particles to seed the bag. Therefore, the bag pores remained unclogged for a longer period and promoted efficient dewatering. This was further evidence that a secondary polymer application point may be more effective and was investigated further in subsequent phases.

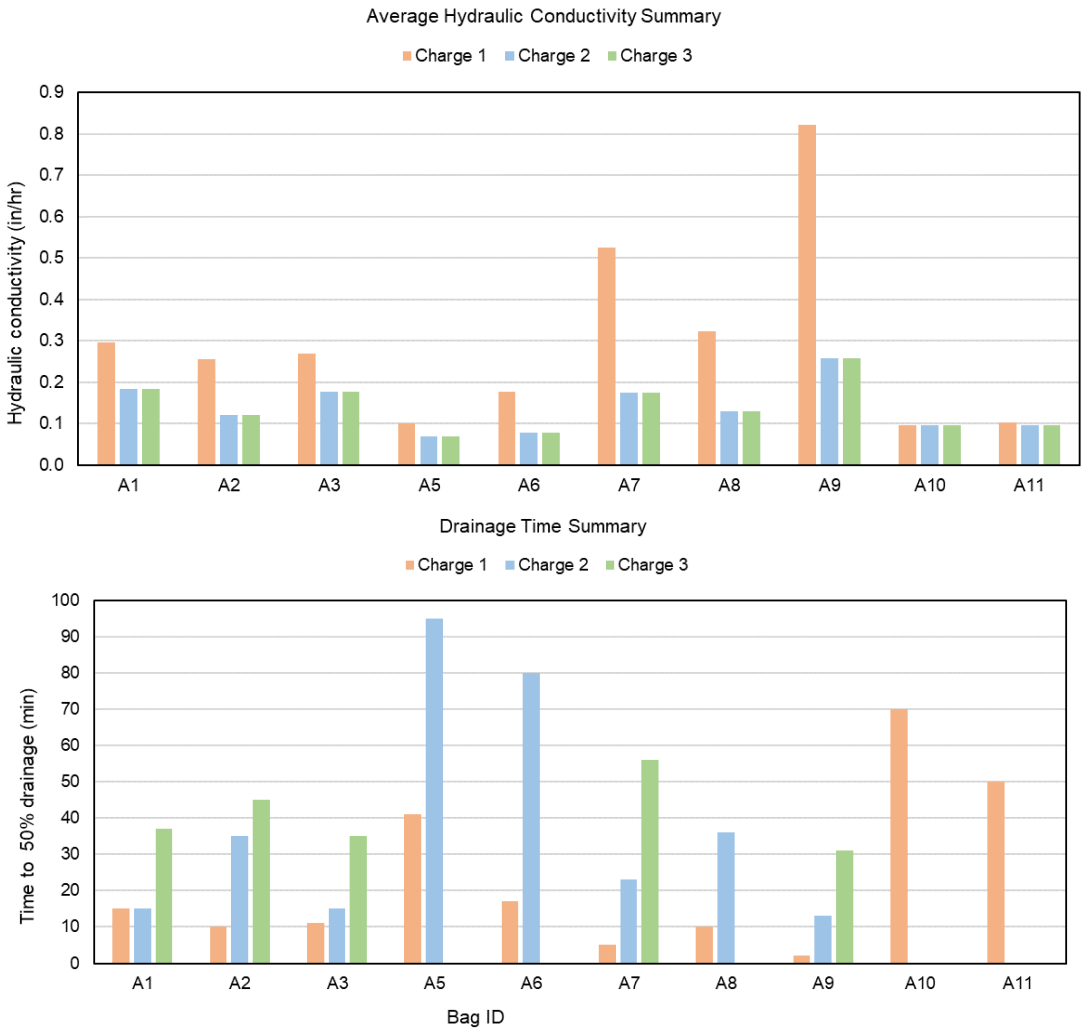

Figure 70. Drainage phase dewatering results from onsite geobag parametric tests: hydraulic conductivity (top) and drainage time (bottom).

Dewatering results for the drying phase are provided in **Figure 71** and summarized as follows:

- Drying rates of retained HPC followed a similar pattern for all tests. Initial drying rate (immediately after the test was concluded) was high, as the HPC changed from the incoming low solids slurry to the retained semi-solid sludge. Drying rate then decreased over time until it reached its minimum and then began to increase. This minimum is hypothesized to correspond to the point at which dewatering ceased to be controlled by bag drainage and began to be controlled by internal evaporation. It also is hypothesized to correspond to a critical point at which more surface area of dried HPC is exposed for accelerated drying. The drying rate was further investigated in subsequent phases with larger quantities of HPC. The actual drying rates seen at this scale are not likely to be indicative of those at full operational scale.

- TS of retained HPC followed a trend that corresponded to drying rates. The TS curve followed a general exponential increase, where the shallower initial section of the curve corresponded to dewatering via drainage, and the sharper later section of the curve corresponded to dewatering via evaporation.
- The lowest drying rates were in bags with HPC that was routed through the cone tanks (A5, A6, A10, A11). This was indicative of potentially sheared floc as a result of additional pumping and was consistent with the poor dewatering performance observed during the bag drainage phase.

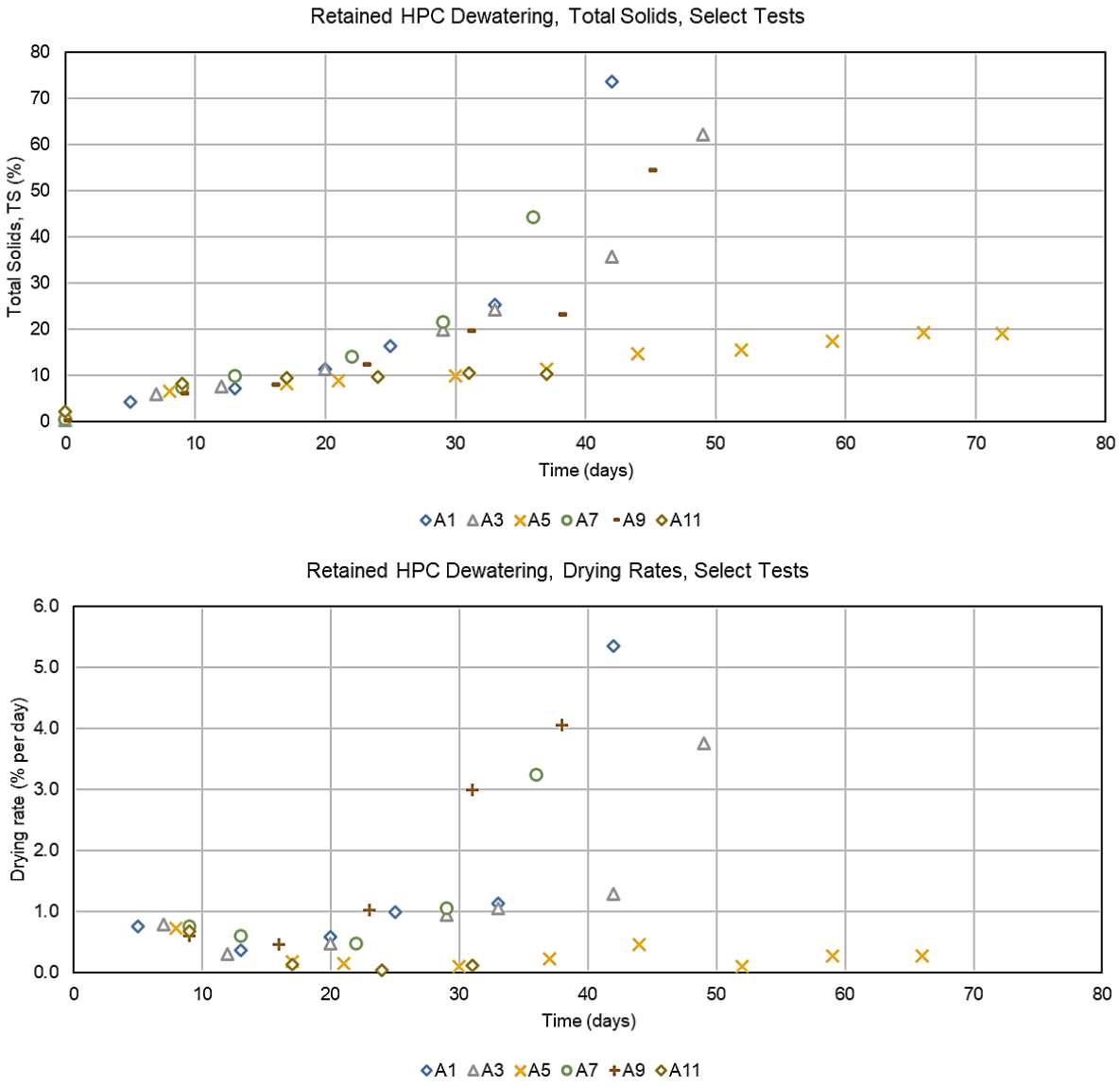

Figure 71. Drying phase dewatering results for onsite geobag parametric tests: total solids (top) and drying rates (bottom).

The following recommendations were developed for subsequent testing based on the results of the onsite parametric tests:

- While higher solids are necessary to promote retention, particularly in the initial bag filling, care must be taken to ensure that the quality of the floc in the material is not sacrificed. The beneficial high solids content provided by additional settlement in the cone tanks corresponds to hindered dewatering performance. Larger scale tests should confirm this.
- While higher incoming solids result in higher initial effluent solids, the solids are only discharged for a short time. Higher solids tests have better overall retention, so controls should be put in place to manage initial solids discharge if needed (e.g., recirculating to plant or to storage).
- Larger-scale tests should investigate a secondary flocculation method. This would consist of adding polymer at the HPC pump itself as opposed to or in addition to adding polymer within the clarifier. It is hypothesized that different polymer doses will be effective for the clarifier, which has a goal of settlement, versus for HPC storage, which has a goal of dewatering. The objective of this polymer addition would be to increase TS of incoming HPC while maintaining floc structure to avoid initial solids discharge, while also exhibiting the retention and dewatering benefit seen in the "pre-spray" parametric tests.

Onsite Performance Tests

Performance tests were conducted with larger bags to evaluate similar conditions to the onsite parametric tests at an increased scale. Performance tests also allowed for capture of larger quantities of HPC for future analytical testing. A performance test was conducted with a 55-gallon geobag provided by Solmax and constructed with the same materials as the 10-gallon geobags.

One (1) 55-gallon geobag was filled with HPC produced under the same conditions as parametric tests A10 and A11 (3 ppm polymer dose in CL2, routed through cone tanks). The bag performed well in filtration (2% incoming TS; 0.3% effluent TS), consistent with the smaller-scale tests. The drying rate of retained HPC was consistently less than 0.1% per day, which was slightly lower than the smaller scale bags. This decrease in dewatering rate is hypothesized to be a result of the larger volume of retained material and exacerbated by the testing conditions discussed in the parametric tests (i.e., additional pumping from cone tanks sheared floc and hindered dewatering).

A performance test was also conducted with a 400-gallon geobag. These bags were constructed as a 45-in-long by 45-in-wide by 45-in-high cube to fit within the constructed short-term containment units. Bags were constructed in the same manner as the 10- and 55-gallon bags. The bag represents the full operational scale for short-term storage and was designed in collaboration with Solmax.

An initial test was conducted on one protype bag (C1) provided by Solmax. The test was used to evaluate general bag performance and to determine any necessary changes to the test procedure and/or bag design and fabrication. HPC was pumped to the bag after being flocculated only in CL2 at a dose of 1 ppm and settled in the cone tanks. Photos from throughout the test are provided in **Figure 72.**

Figure 72. 400-gallon geobag performance test C1: a) hanging bag; b) bag following Charge 1; c) HPC dewatering after three charges and one week of drainage; d) HPC after 57 days of indoor drying; e) HPC after two additional months of outdoor drying.

The bag was filled (or "charged") three (3) times over 13 days. The solids content of the influent HPC was approximately 1%. Charge 1 placed 250 gallons of cone-tank-settled HPC into the bag. Effluent TS in response to the initial bag filling was measured as 0.6%. Pass-through decreased after bag filling was complete and as the bag began to drain. Charges 2 and 3 placed an additional 250 and 200 gallons, respectively, of HPC into the bag. In each of these fills some pass-through occurred but at a lower magnitude than Charge 1.

After filling, the bag was allowed to drain and dry for approximately ten months without any new contact with HPC. The first phase of bag drying occurred in a controlled environment at room temperature. After about one week of drying, it was observed that the material in the bag was drying more on the perimeter than on the inside. This was a result of filter cake buildup along the bag exterior, which clogged and then prevented uniform dewatering in the bag. A solution for this dewatering profile was evaluated with additional 400-gallon bags (refer to "Short-Term HPC Storage" section). After 57 days of drying, the bag was removed from the stand. Material from the bag had an average TS of 6.8%. The drying rate over this dewatering period was approximately 0.1% per day, consistent with other parametric and performance tests.

The bag was then moved outside of the facility and monitored for approximately eight months to evaluate the effects of outdoor exposure (e.g., evaporation, freeze/thaw). Within four months, the percent TS had increased to 18.5% and the material particle size was uniform. By the end of the test, TS had reached approximately 30% while drying at 0.1-0.2% per day.

Full-Scale Plant HPC Storage Operation

Upon successful completion of all onsite parametric and performance tests, necessary plant modifications were made, and full-scale operational tests were completed at the plant to evaluate short-term and long-term storage of HPC.

Plant Modifications

Performance and parametric tests indicated a need for polymer application in place of or in addition to flocculation within the clarifier. To further evaluate alternative polymer application points, a polymer line was installed from the existing polymer skid to the suction side of CL2's HPC pump (**Figure 73**). This allowed full-scale testing of HPC storage in various scenarios: flocculation only within the clarifier before being pumped to storage, in line at the pump itself while being pumped to storage, or a combination of both.

Figure 73. Polymer line (red) to CL2 HPC pump.

Short-Term HPC Storage

Geobag performance was evaluated at the full scale of short-term (indoor) storage. Short-term storage was used when HPC was not being processed in the pilot recovery plant. Based on the findings of the bag C1 test (particularly the dewatering performance) and upon consultation with Solmax, the design of the 400-gallon geobag was revised to include capillary channel fibers (CCFs). The purpose of the CCFs was to promote unsaturated drainage and uniform dewatering throughout the bag profile. CCFs have been used successfully in various sludge dewatering applications but had yet to be evaluated with sludge of this type (HPC). Short-term geobags were stored in steel containment units that captured filtrate for pumping back to the clarifier, which created a closed-loop system with no offsite discharge (**Figure 74**).

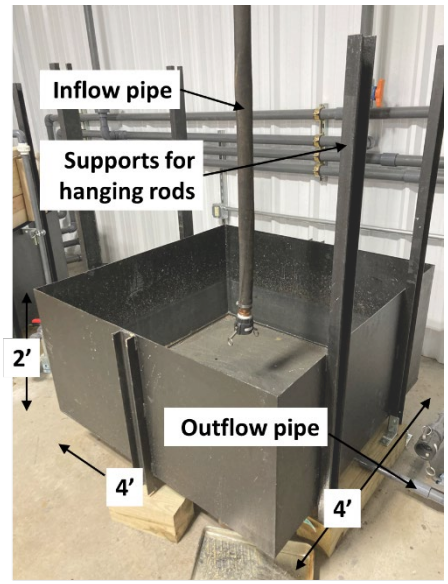

Figure 74. Short-term HPC storage containment unit.

Five (5) tests (bags D1 through D5) were conducted with 400-gallon geobags which included CCFs. In each test, the bag was filled with approximately 250 gallons of HPC. Short-term storage tests are summarized in **Table 34**. Photos from a typical test are provided in **Figure 75**.

Table 34. Short-term HPC storage tests summary.

Bag ID	Description	HPC source	Pump rate (gpm)	Primary polymer dose (ppm)	Secondary polymer dose (ppm)
D1	From clarifier, dosed in clarifier, higher floc dose	CL2	50	3	0
D2	Routed through cone tanks, dosed in clarifier, higher floc dose	CT	50	3	0
D3	From clarifier, dose in clarifier, baseline floc dose	CL2	50	1	0
D4	From clarifier, dosed at pump, higher floc dose	CL2	50	0	3
D5	From clarifier, dosed at pump, highest floc dose	CL2	50	0	6

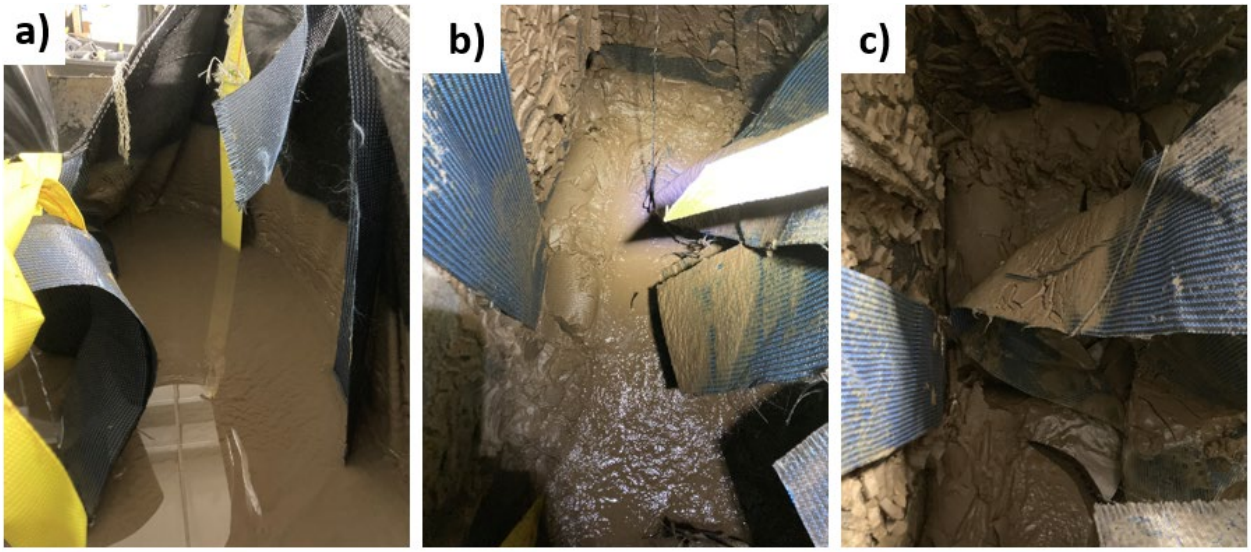

Figure 75. Photos from typical short-term storage test. Retained HPC in bag D1: a) after being filled; b) after 1 week of drying; b) after 3 weeks of drying.

Influent and filtrate TS samples were collected to evaluate filtration performance. Filtration performance was consistent with smaller-scale parametric and performance tests. Influent TS was variable and ranged from 0.4% to 1.4%. Influent TS was higher and more consistent for the tests that flocculated the HPC at the pump (D4 and D5). Effluent (filtrate) TS ranged from 0.2% to 0.3%. For all tests, filtrate was clear almost immediately, but retention performance was best for tests D4 and D5. In these tests, no visible pass-through occurred whatsoever. Comparisons of influent and effluent samples for each type of test (flocculated in clarifier [e.g., D1]; flocculated at pump [e.g., D4)] are provided in **Figure 76.**

Figure 76. Typical influent and effluent samples from short-term storage tests: test D1, flocculated in clarifier (left); test D4, flocculated at pump (right).

Dewatering performance was evaluated during the drainage phase (drainage time, hydraulic conductivity) and drying phase (retained HPC moisture profile and drying rate). Dewatering results are provided in **Figure 77**. Dewatering rate during the drainage phase (i.e., hydraulic conductivity) was highest for tests that flocculated the HPC at the pump. The lowest hydraulic conductivity occurred for HPC routed through the cone tanks (test D2), likely due to floc shearing and consistent with previous

tests. The initial drying rate for retained HPC was approximately 0.3% per day. No difference in initial drying rate was apparent among tests. Consistent with previous findings, preferential drying was evident during the initial drying phase; the perimeter of the bag dried faster, while the center of the bag remained wet (approximate difference in TS of 3%). The moisture profile, however, became more consistent (less than 1% difference in TS) within two to three weeks, indicating that the CCFs were effective. After the initial dewatering during the drainage phase, dewatering rate was at or below 0.1% per day during the drying phase. This drying rate was consistent across all tests.

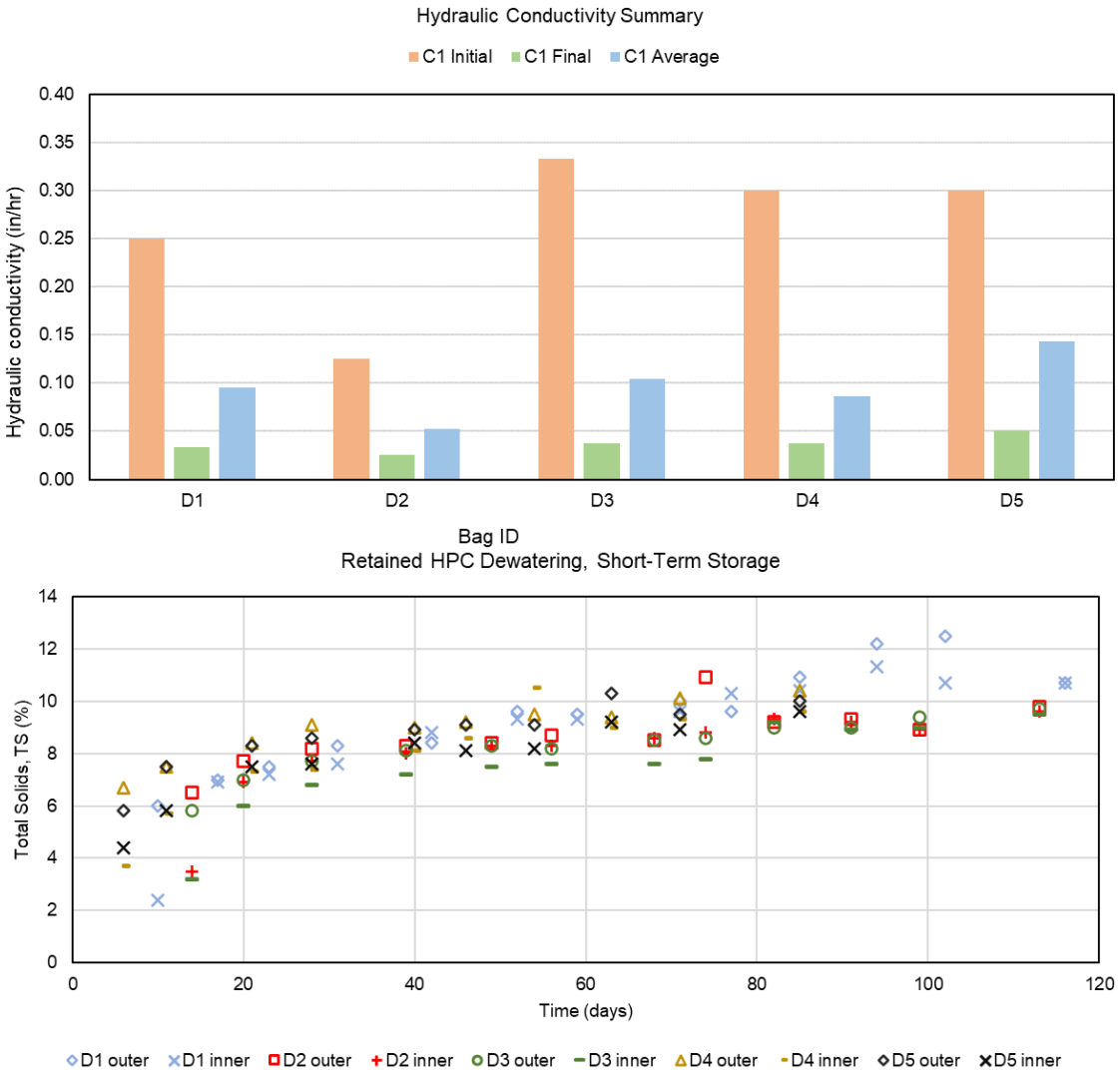

Figure 77. Short-term HPC storage dewatering results: hydraulic conductivity (top), total solids (bottom).

Short-term HPC storage tests confirmed that the composite geobag design was effective at capturing HPC at full scale. Results indicated that adding polymer at the pump would be more efficient than only within the clarifier, especially with respect to filtration and immediate dewatering during the drainage phase. This also used less polymer to flocculate the HPC than when added within the clarifier at the same dose. In the drying phase of dewatering, however, the impact of the polymer application point was less evident, and tests were consistent in their drying rate.

Long-Term HPC Storage

Long-term storage of HPC was evaluated using geotubes. Like short-term storage, this process was used when HPC was not being processed by the pilot recovery plant. Long-term storage increased the scale at which HPC could be captured and dewatered. Demonstration of effective long-term storage was also necessary to evaluate the capture and dewatering of HPC for potential transport to a future central REE/CM refinery.

An estimator tool was developed to determine the volume of HPC that would be produced at the facility and the corresponding size and number of geotubes needed for storage. The estimator incorporated geotechnical data determined through previous testing (e.g., specific gravity), operational data (e.g., incoming HPC total solids), and desired production data (e.g., target dewatering rate, pumping schedule) to estimate the total dewatered weight of HPC on an annual basis (approximately 350 tons/year). This production rate would require nine (9) geotubes per year if the bags are 40-ft-cirumference by 43-ft-long. The estimator tool is depicted in **Figure 78**.

Project Name:	A34
Location:	Mt. Storm
Contact:	Nate
Date:	10/12/2023
Type of Material:	HPC

Input	
Output	

Input			Output		Units
Specific Gravity	2.74		Wet Volume per Day	12,000.0	Gallons
% Solids During Pumping	1.0%		Wet Volume per Day	59.4	CY
Target dewatered % Solids	40.0%		Wet Volume per Year	3,348,000.0	Gallons
			Wet Volume per Year	16,576.4	CY
Production			Total Bone Dry Tons per Day	0.5	Tons
Pumping Rate (GPM)	50		Total Bone Dry Tons per Year	140.5	Tons
Hours per Day	4		Est. Dewater Volume per Day	1.1	CY
Days per Year	279		Est. Dewater Volume per Year	311.2	CY
% Efficiency	75%		Est. Dewater Weight per Day	1.3	Tons
			Est. Dewater Weight per Year	351.3	Tons
Material Type:			Density of Dewatered Slurry		Relative Density

Water?
Percent of Maximum Filled Capacity
75%

Bag Length (ft)	43
Bag Circumference (ft)	40
Pumping Height (ft)	3
Filled Volume (CY)	37.61
Bags per day	0.03
Bags per year	8.27
Total Volume per year (CY)	311.17

Figure 78. Geotube estimator tool workspace with inputs, outputs, and project data.

The long-term storage area (geotube pad) was developed adjacent to and above the plant building. The conceptual design was proposed for a maximum area of 200 ft x 60 ft to accommodate the estimated nine (9) geotubes required. Due to construction constraints, the pad area was reduced to accommodate six (6) geotubes. The pad was excavated approximately three feet to provide a contained area for the geotubes. The pad was sloped from left to right to promote drainage of geotube filtrate. A sump was installed in the corner of the pad to collect filtrate and drain to the polishing pond downstream of the treatment plant. A geosynthetic liner was installed to protect groundwater from filtrate. Geotextile Filter Fabric (GFF) a structured woven fabric provided by Solmax, was also installed above the liner to provide a drainage layer between the geotubes and the liner. A manifold was constructed to transfer HPC inflow to multiple hoses that attached to geotubes. A schematic and photo of the geotube pad are provided as **Figure 79.**

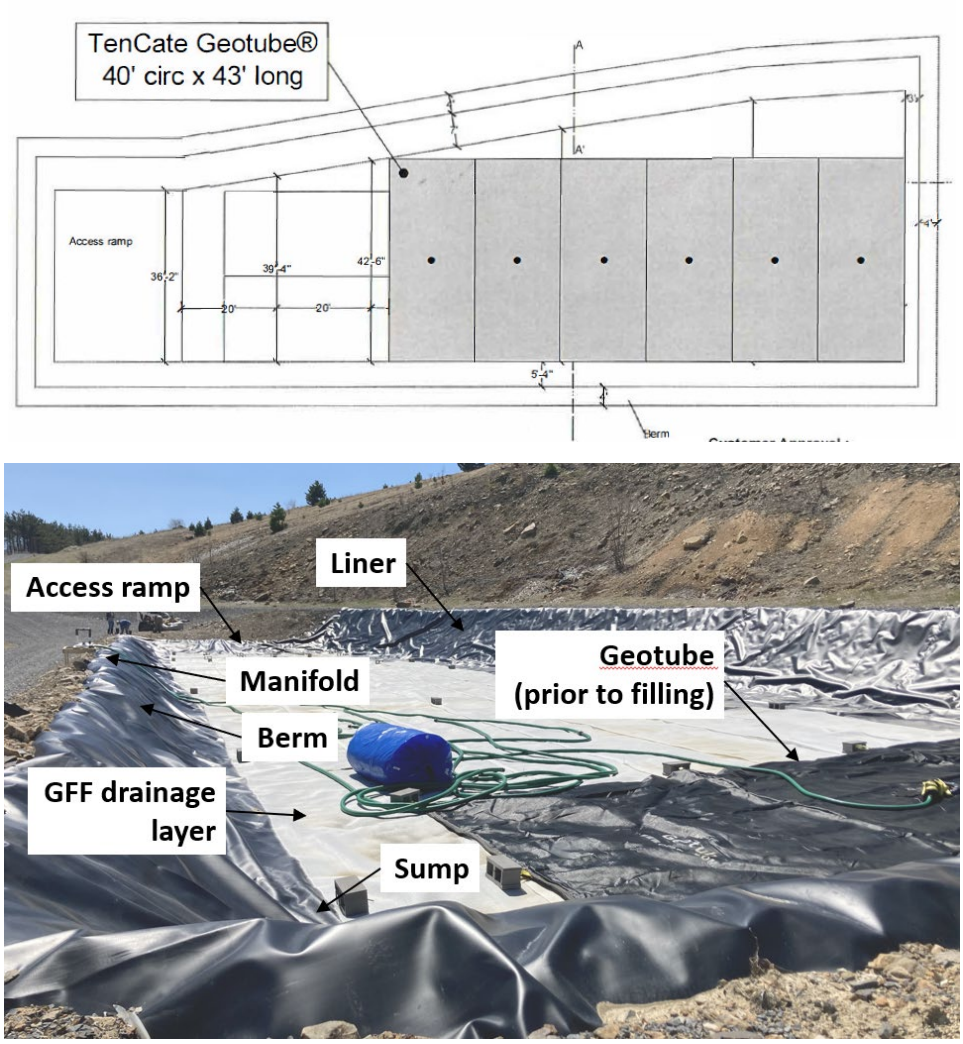

Figure 79. Geotube pad area: schematic developed by Solmax (top), labeled photo after construction (bottom).

In consultation with Solmax, the appropriate geotube size was determined to be 48 ft-long by 20 ft-wide (40-ft-circumference). The geotubes were constructed by Solmax using the same material as used for the 10-, 55-, and 400-gallon geotube bags.

Operational parameters were established based on the results of the onsite parametric and performance tests. The polymer dose in CL2 was maintained at 2 ppm. While not necessary for retention in the geotube, this baseline dose of polymer within the clarifier was deemed necessary to promote solid particle settlement and avoid compliance issues with the supernatant discharge. Secondary polymer dosing at the HPC pump was 3 ppm, consistent with the dose found effective in previous tests. Pump rate ranged from 40-50 gpm and was variable based on solids content to avoid excessive pressure on the pump. The sludge level in CL2 was generally 30 inches or greater before a pumping cycle began. In general, HPC was only pumped when the sludge level was below zero inches for equal to or less than the time that it was above zero inches. For example, most pumping cycles were conducted for 25-30 minutes, with the first 12-15 minutes at sludge levels from approximately 30 inches to zero inches and the second 12-15 minutes at sludge levels below zero.

HPC was pumped to the geotube forty-three (43) times in July, August, and September 2023. Approximately one-third of the fills were conducted in-person at the plant, while the remaining two-thirds were conducted remotely from the WVWRI office. The site was visited one to two times per week to conduct in-person fills and to confirm that remote operations were not producing any negative consequences.

For in-person fills, influent HPC samples were collected to determine incoming TS. Incoming TS was used to evaluate the clarifier response to pumping (e.g., how TS changed over time, how long pumping could occur before HPC TS was substantially below average, how long was required for the clarifier to recover [increase sludge level] for subsequent pumping, and to estimate HPC production). Based on the pumping times described above (i.e., equal duration of pumping with sludge level above and below zero inches, approximately 30 minutes), TS samples were collected approximately every five (5) minutes. Total solids data from in-person fills are presented in **Figure 80**. Data were variable from test to test but followed the same trends. Influent TS ranged from 0.4 to 2.6% and decreased as clarifier sludge level decreased. TS was highest in the first 5-10 minutes and approached 1.0% as the sludge level approached zero inches after 10-15 minutes. Once sludge level was below zero inches, TS decreased to and maintained a consistent level of approximately 0.5%. A typical variation in TS with respect to time and sludge level is presented as **Figure 81.** Average TS was approximately 1.0% for all testing periods and was consistent across tests.

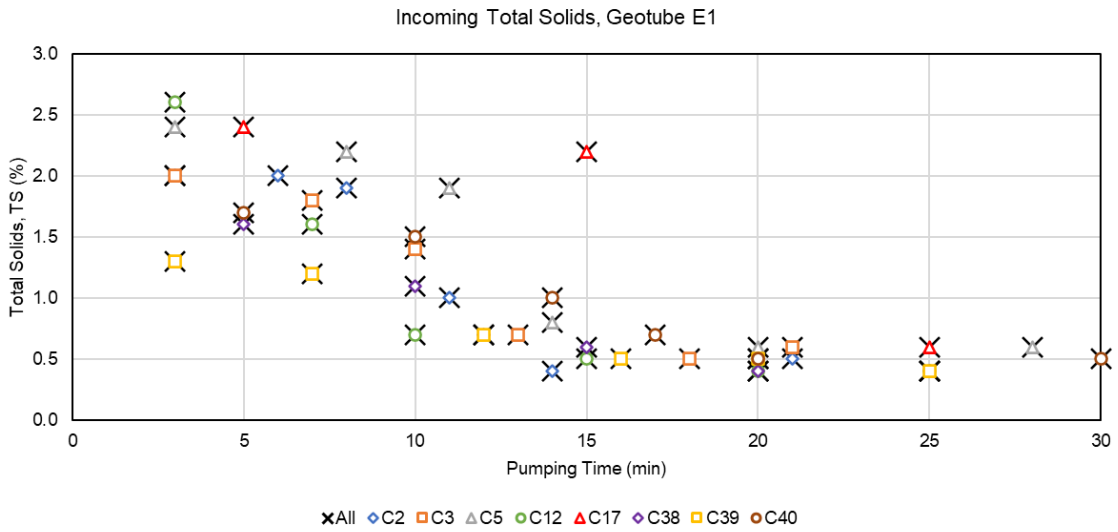

Figure 80. Total solids (TS) over time when pumping from Clarifier 2 to geotube E1.

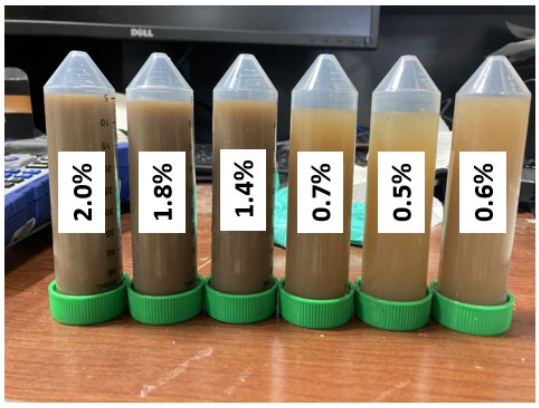

Figure 81. Typical variation in total solids when pumping form Clarifier 2 to geotube E1.

Filtration performance of the geotube was excellent, consistent with previous fabric performance tests at the prescribed polymer dosing. Filtrate was clear throughout the operation; filtrate TS was measured as 0.2%. Over the performance period, over 50,000 gallons of HPC was pumped to the geotube. Using the geotube estimator described earlier with an incoming TS of 1% and a target dewatered TS of 40%, this corresponded to approximately 5.3 tons of dewatered material. Photos of the geotube during and at the end of the performance period are provided as **Figure 82**. The operation confirmed that the geotube, combined with the operational parameters determined via onsite testing, was an effective method for storing HPC on a large scale. Because pumping of HPC into the geotube continued until the end of the project, no data on dewatering within the geotube were collected, but dewatering rates are expected to be consistent with the short-term tests.

Figure 82. Photos of geotube E1 (clockwise from top left): clear filtrate during pumping, front view at end of performance period, full view at end of performance period.

Environmental Compliance Material Testing

To evaluate any potential environmental impact associated with HPC generation and storage, a representative AMD sludge was characterized, and toxicity characteristic leaching procedure (TCLP) testing was conducted on HPC and residuals.

Representative AMD Sludge Characterization

Testing was conducted to characterize sludge from an active AMD treatment plant. This testing was beyond what was required for design of the HPC dewatering process described in previous sections (e.g., SRF, strength), but was conducted to fully characterize a representative AMD sludge. AMD sludge characterization was conducted prior to the A-34 plant being operational, so the AMD sludge was sourced from an active treatment plant operated by WVDEP. Samples were collected from the WVDEP Omega Plant, located south of Morgantown, WV. The raw AMD was sourced from an underground mine, treated by precipitation at a pH around 3.2, and then clarified by raising the pH to 6.7 using lime. The sludge produced during the clarification process was flocculated with polymers at a dose of 20 ppm to create filterable solids and then dewatered using geotubes. The sample sludge tested in the laboratory was collected from a filled geotube during the dewatering phase (not actively receiving sludge). Tests included moisture content, particle-size analysis, specific gravity, Atterberg limits, and soil classification. All tests were conducted according to the appropriate American Society for Testing and Materials (ASTM) standards. Tests results are summarized in **Table 35.**

Table 35. Omega AMD sludge geotechnical properties.

Property	Value
Moisture content, ω (%)	1645
Total solids by weight, TS (%)	5.75
Specific gravity, G_s	2.48
Liquid Limit, LL (%)	1297
Plastic Limit, PI (%)	223
Plasticity Index (%)	1074
Soil Classification	Fine-grained sand

TS was higher than that seen with A-34 HPC, likely due to the sample being collected after some dewatering in the geotube had occurred. Specific gravity was slightly lower than that measured with AMD sludges in previous projects. Atterberg limits (liquid limit [LL], plastic limit [PL], plasticity index [PI]) indicated that the material is meta-stable. Overall, the charge of the flocculated particles in relation to their surface area is extremely high, and the behavior of the sludge is similar to expansive clay.

Each dried soil portion underwent two repetitive dry sieve analyses. **Figure 83** depicts the four trials and their individual and average distributions. Due to the high percentage passing the number 200 sieve (fines fraction), a hydrometer test was conducted to determine the distribution of the finest particles.

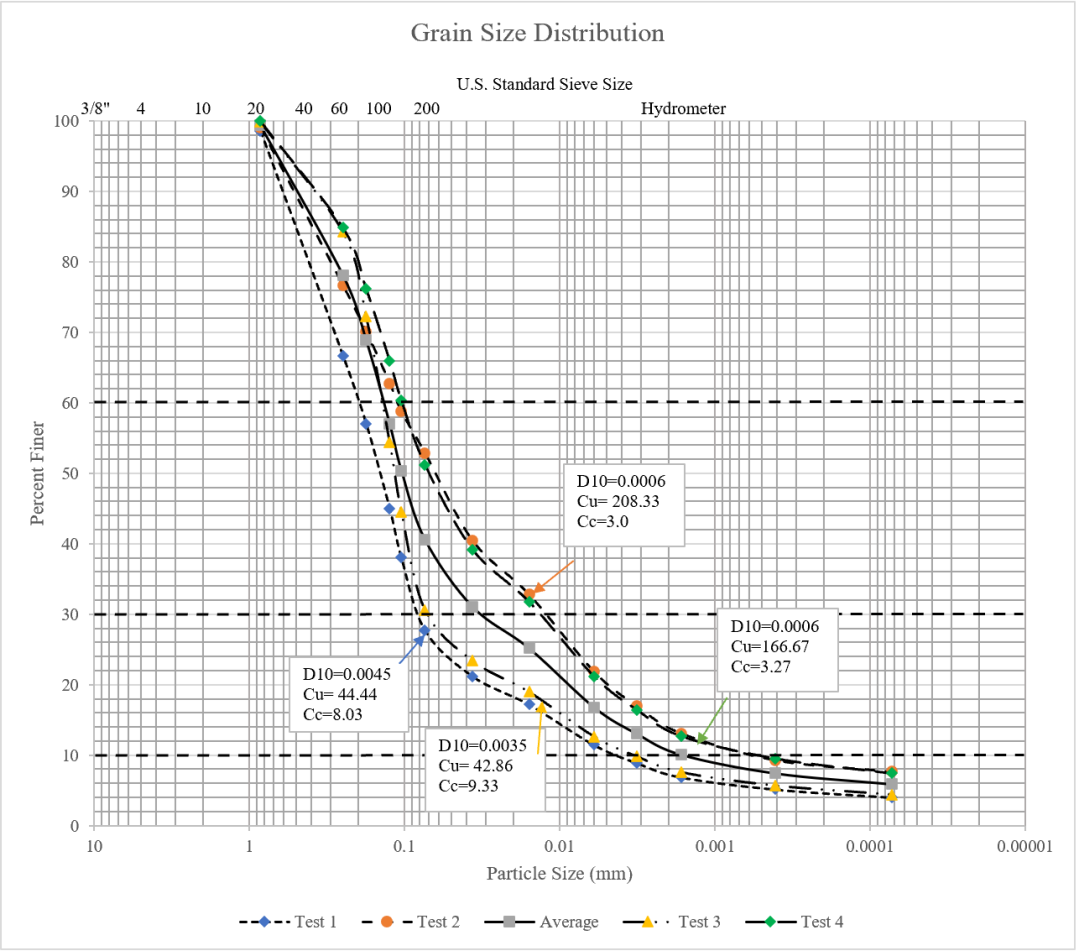

Figure 83. Grain-size distribution curve for Omega AMD sludge from dry sieve analysis.

Due to the high fines content of the sludge, wet sieve analyses were also conducted. Wet sieving allowed for a more efficient and complete separation of larger particles when working with materials that were considerably finer than a No. 200 sieve. The wet sieve was conducted in two trials (**Figure 84**). In the first trial, the weight retained on the No. 20 sieve created an inaccurate representation of retained percentages due to lack of mixing and particulate disturbance. To create a more representative distribution, the No. 20 sieve data was not included when creating the graphical representation of the grain size analysis. To avoid this situation in the second trial, more homogenous mixing was undertaken when preparing the saturated sludge for wet sieve analysis.

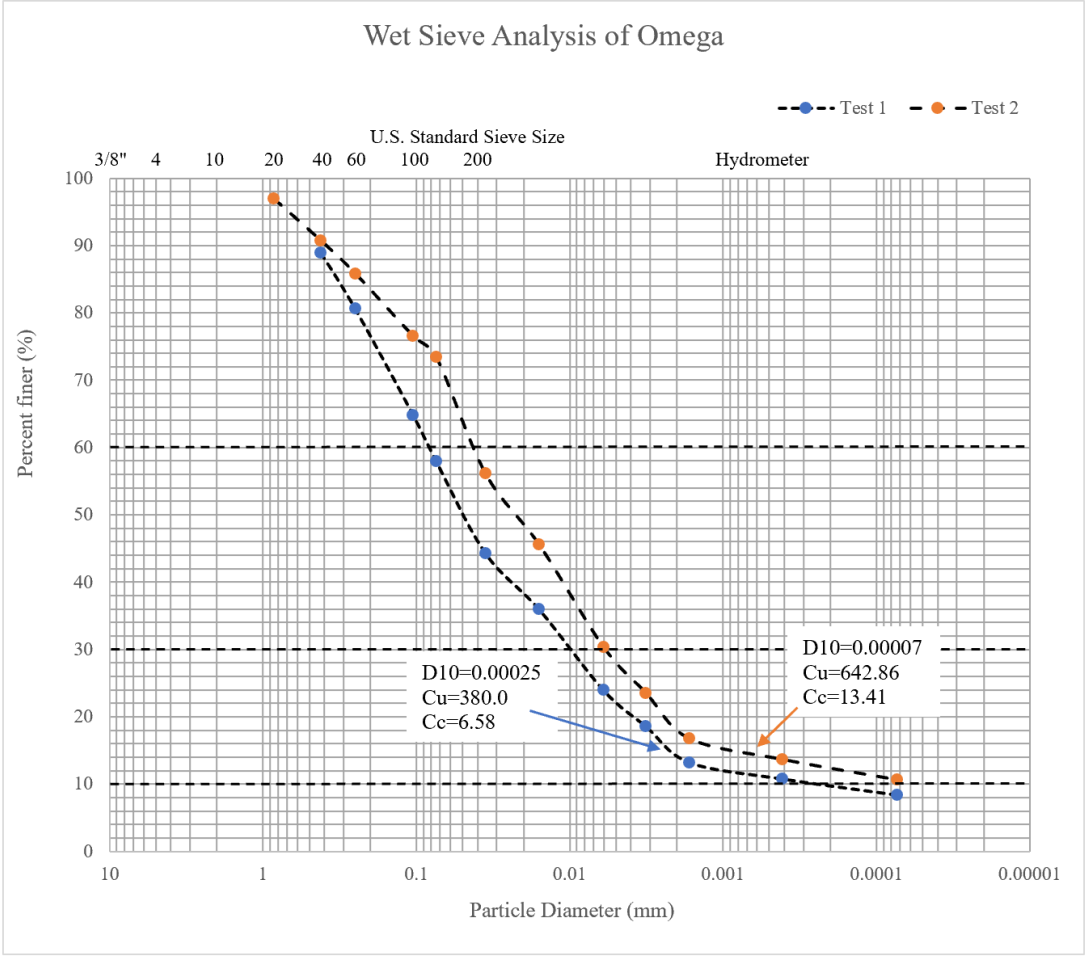

Figure 84. Grain-size distribution curve for Omega AMD sludge from wet sieve analysis.

The dried AMD sludge was classified as a fine-grained sand. When dried, the specimen had a very hard consistency and moderate cementation. The color varied from coarse grains of brown to super fine grains of rusty orange. The dry samples lacked any noticeable odor and were not tested for reaction to hydrochloric acid. No environmental compliance issues related to the sludge were evident from geotechnical characterization.

Toxicity Characteristic Leaching Procedure Testing

To investigate potential handling and disposal issues associated with intermediates and residuals resulting from the processes at A-34, a toxicity characteristic leaching procedure (TCLP) test was performed on the solid HPC generated from AMD treatment and on the residuals generated from acid leaching. In addition, the final discharge water after staged precipitation was analyzed for a similar set of metals using Inductively Coupled Plasma Mass Spectrometry (ICP-MS), EPA method 200.7 for metals, and EPA 245.1 for mercury. Specific methods utilized in the TCLP test included preparation method EPA 3010A, TCLP metals method EPA 6010D, and leach method EPA 1311. For mercury, relevant methods included preparation method EPA 7470A and leach method 1311. All tests were performed by a third party (Pace Analytical Labs). Results are shown for solids and liquids in **Table 36** and **Table 37**, respectively. Both results show negligible concentrations of metals of concern, indicating that the wastes from the process are nonhazardous.

Table 36. TCLP solids results for HPC and leaching residual.

Element	Pace Detection Limit (mg/L)	HPC (mg/L)	Leaching Residual (µg/L)
Arsenic	0.5	ND	ND
Barium	2.5	ND	ND
Cadmium	0.05	0.11	ND
Chromium	0.12	ND	ND
Lead	0.25	ND	ND
Selenium	0.1	ND	ND
Silver	0.12	ND	ND
Mercury	0.001	ND	ND

ND: not detectable

Table 37. TCLP metals aqueous results for discharge water.

Element	Pace Detection Limit (mg/L)	pH 8.5 Water Total Solids (µg/L)	pH 8.5 Water Dissolved Solids (µg/L)
Arsenic	20	ND	ND
Barium	5	11.6	13.6
Cadmium	2	3.2	3.5
Chromium	5	ND	ND
Lead	10	ND	ND
Selenium	20	ND	ND
Silver	5	ND	ND
Mercury	0.2	ND	ND

ND: not detectable

Conclusions

The following primary conclusions have been provided from analysis and interpretation of all tests conducted for this task:

- HPC was a very low solids material that required flocculation both to settle within the clarifier and to be retained using geosynthetics. This flocculation was effectively achieved using cationic emulsion polymers at low doses. The appropriate polymer dose and location at which the polymer was applied were important factors in filtration and dewatering of HPC.
- Secondary polymer application (at the HPC pump) was effective in increasing incoming total solids and promoting effective filtration immediately. No significant changes, however, were apparent with respect to the long-term dewatering rate via drying.
- Composite geobags composed of a combination of nonwoven fabric for filtration and woven fabric for strength were effective in retaining and storing HPC. The effectiveness of these fabrics was demonstrated at a full operational scale, both in short-term and long-term storage applications.

- Production and storage of HPC did not result in any issues with environmental compliance, neither with the HPC solids retained within geobags and geotubes, nor with the filtrate that discharged from the dewatering process.

References

1. Larochelle, T., & Kasaini, H. (2016). Predictive modeling of rare earth element separation by solvent extraction using METSIM. Proceedings of the IMPC.

Products

Journal Papers

1. Koermer, Scott, and Aaron Noble. "Estimation of process steady state with autoregressive models and Bayesian inference." Minerals Engineering 191 (2023): 107965.

Conferences

1. Ziemkiewicz, Paul, Aaron Noble, John Quaranta, Lian-Shin Lin, Harry Finklea, Jim Constant, and Tommee Larochelle (2020). “Development and Testing of an Integrated AMD and Rare Earth/Critical Mineral Plant.” DOE-NETL’s 2020 Integrated Project Review Meeting – Rare Earth Elements. Online Conference. September 15-16, 2020
2. Ziemkiewicz, Paul, Jim Constant, Harry Finklea, Lance Lin, David Hoffman, John Quaranta, Aaron Noble, and Tommee Larochelle. (2021). “Development and Testing of an Integrated AMD Treatment and Rare Earth/Critical Mineral Plant.” DOE-NETL’s 2021 Project Review Meeting: Rare Earth Elements – Critical Minerals. Online Conference. May 25, 202
3. Noble, Aaron, Tommee Larochelle, Jim Constant, Paul Ziemkiewicz. (2022). “Design and Testing of an Integrated Pilot-Scale AMD Treatment and Rare Earth Recovery Process.” 2022 SME Annual Meeting and Exhibit. Salt Lake City, UT. February 27 – March 2, 2022.
4. Koermer, Scott and Aaron Noble. (2022). “Bayesian Mass Balancing of Hydrometallurgical Processes.” 2022 SME Annual Meeting and Exhibit. Salt Lake City, UT. February 27 – March 2, 2022.
5. Koermer, Scott and Aaron Noble. (2022). “Gaussian Process Modeling of Hydrometallurgical Separations with Uncertain Dynamics.” 2022 SME Annual Meeting and Exhibit. Salt Lake City, UT. February 27 – March 2, 2022.
6. Noble, Aaron and Paul Ziemkiewicz. (2022). “A Process for Integrating Acid Mine Drainage Treatment with REE/CM Recovery.” The 46th International Technical Conference on Clean Energy. Clearwater, FL, August 2022.
7. Noble, Aaron, Paul Ziemkiewicz, and Tommee Larochelle, "Integrated Treatment of Acid Mine Drainage and Rare Earth Element Production." SME's 8th Current Trends in Mine Finance Conference. New York City, NY. May 10, 2023.

Theses/Dissertations

1. Koermer, Scott. (2022). Mining Engineering, Virginia Tech. Dissertation Title: Bayesian Methods for Mineral Processing Operations.

Participants and Other Collaborating Organizations

Table 38. Listing of Key Project Personnel.

Personnel	Role	Business Association	Primary Contact E-Mail
Paul Ziemkiewicz	PI	West Virginia University	pziemkie@mail.wvu.edu
Aaron Noble	Co-PI	Virginia Tech	aaron.noble@vt.edu
John Quaranta	Co-PI	West Virginia University	JDQuaranta@mail.wvu.edu
Lance Lin	Co-PI	West Virginia University	lance.lin@mail.wvu.edu

Changes/Problems

During the week of latter weeks of March 2020, laboratories at both West Virginia University and Virginia Tech were moved to "essential personnel only" status due the COVID-19 outbreak. This status change did not drastically impact project activities, as the initial efforts focused on process design and construction. Regarding the COVID-19 setbacks, while the pandemic caused delays to experimental tasks in spring of 2020, as of early June, laboratories at both universities were reopened and operated at normal capacity. All work was conducted under an approved COVID-19 mitigation plan that included provisions for face coverings and physical distancing as required.

The COVID-19 outbreak caused numerous operational challenges associated with laboratory access, travel, procurement delays, and supply chain disturbances. The research team closely monitored the situation and developed contingency plans for various scenarios, and the pandemic did not result in significant delays to project work.

Due to the new DOE directive regarding foreign nationals, WVU was notified via a letter from NETL dated April 16, 2020, that Co-PI Dr. QingQing Huang was not approved to work on this project.

Regarding ALSX system procurement, WVU was proactive in acquiring needed chemicals, tanks, pumps, valves, flowmeters, and other required parts. Prolific supply chain delays occurred throughout the country during the project performance period, but those delays were largely mitigated.

While the installation of the building began in the early 2021, it could not be completed in a timely manner due to a shortage in the needed insulation to finish the interior of the building. WVDEP originally stated that the building would be complete in March of 2023, but the delay in getting needed insulation delayed completion to June of 2023. The project team was not permitted to begin work on the REE recovery plant until the building was completed.

Lockdowns caused by COVID 19 resulted in construction delays and severe supply chain/labor access problems. For example, on the upstream side of our facility, WVDEP's construction of the AMD treatment plant was delayed by over a year. During that time, the WVU team took the opportunity to significantly modify its upstream Operation 1, moving from plate and frame presses for concentrate dewatering to a fully hydraulic and continuous preconcentrate (HPC) production process). In addition, an alternative solvent extraction process was developed that reduced operating cost and complexity while increasing throughput volume. The new process and the incorporation of HPC feedstock required a reconfiguration of the solvent extraction process power and automation controls for operation. New specifications were sent out for bid in April 2022. In the meantime, industrial partner Rockwell Automation's plants were offline, and it was necessary to source electrical and control components on the open market. Bids were not returned until late August and proved far in excess of budgeted amounts. In order to minimize time to full operations and to remain within budget, the project team proposed a modification of the project Statement of Project Objectives (SOPO) that eliminated the need

to fully automate the rare earth recovery portion of the pilot facility. This modification also allowed for a revision of the original design that was both cost effective and could efficiently meet major project goals.

Budgetary Information

The SF-425 Federal Financial Report will be submitted by WVU's Sponsored Research Accounting (SRA) Office. All financial reports and official numbers are submitted through this office and will cover federal costs and recipient cost share incurred. Our Cost Plan/Status table can be found below in **Table 39**. Amounts contained within reflect internal adjustments currently making their way through WVU's financial systems.

Table 39. Cost Plan/Status Table.

Baseline Reporting Quarter	Budget Period 1										Budget Period 2												Budget Period 2/3		Budget Period 3					
	Q1		Q2		Q3		Q4		Q5		Q6		Q7		Q8		Q9		Q10		Q11		Q12		Q13		Q14		Q15	
	01/1/20 - 03/31/20		04/1/20 - 06/30/20		07/1/20 - 09/30/20		10/1/20 - 12/31/20		1/1/21 - 3/31/21		4/1/21 - 6/30/21		7/1/21 - 9/30/21		10/1/21 - 12/31/21		1/1/22 - 3/31/22		4/1/22 - 6/30/22		7/1/22 - 9/30/22		10/1/22 - 12/31/22		1/1/23 - 3/31/23		4/1/23 - 6/30/23		7/1/23 - 9/30/23	
	Q1	Cumulative Total	Q2	Cumulative Total	Q3	Cumulative Total	Q4	Cumulative Total	Q5	Cumulative Total	Q6	Cumulative Total	Q7	Cumulative Total	Q8	Cumulative Total	Q9	Cumulative Total	Q10	Cumulative Total	Q11	Cumulative Total	Q12	Cumulative Total	Q13	Cumulative Total	Q14	Cumulative Total	Q15	Cumulative Total
Baseline Cost Plan																														
Federal Share	$229,856	$229,856	$229,856	$459,712	$229,856	$689,567	$229,856	$919,423	$229,856	$1,149,279	$569,713	$1,718,992	$569,713	$2,288,706	$569,713	$2,858,419	$569,713	$3,428,133	$569,713	$3,997,846	$500,847	$4,498,693	$500,847	$4,999,541	$0	$4,999,541	$0	$4,999,541	$0	$4,999,541
Non-Federal Share	$71,078	$71,078	$165,849	$236,927	$165,849	$402,776	$165,849	$568,625	$329,656	$898,281	$329,656	$1,227,938	$329,656	$1,557,594	$329,656	$1,887,250	$0	$1,887,250	$0	$1,887,250	$0	$1,887,250	$0	$1,887,250	$0	$1,887,250	$0	$1,887,250	$0	$1,887,250
Total Planned	$300,934	$300,934	$395,705	$696,639	$395,705	$1,092,343	$395,705	$1,488,048	$559,512	$2,047,560	$899,370	$2,946,930	$899,370	$3,846,300	$899,370	$4,745,669	$569,713	$5,315,383	$569,713	$5,885,096	$500,847	$6,385,943	$500,847	$6,886,791	$0	$6,886,791	$0	$6,886,791	$0	$6,886,791
Actual Incurred Cost																														
Federal Share	$172,109	$172,109	$320,418	$492,527	$364,237	$856,764	$199,427	$1,056,191	$697,136	$1,753,328	$128,085	$1,881,413	$243,066	$2,124,479	$314,309	$2,367,545	$349,113	$2,716,658	$589,657	$3,306,315	$450,469	$3,756,783	$377,956	$4,134,739	$366,724	$4,501,463	$100,019	$4,601,482	$398,059	$4,999,541
Non-Federal Share	$14,250	$14,250	$11,200	$25,450	$15,560	$41,010	$22,414	$63,424	$73,122	$136,546	$37,550	$174,096	$1,142,100	$1,316,196	$203,850	$1,520,046	$144,850	$1,664,896	$171,794	$1,836,690	$195,750	$2,032,440	$0	$2,032,440	$0	$2,032,440	$0	$2,032,440	$0	$2,032,440
Total Incurred Costs	$186,359	$186,359	$331,618	$517,977	$379,797	$897,774	$221,841	$1,119,615	$770,258	$1,889,874	$165,635	$2,055,509	$1,385,166	$3,440,675	$518,159	$3,887,591	$493,963	$4,381,554	$761,451	$5,143,005	$646,219	$5,789,224	$377,956	$6,167,180	$366,724	$6,533,904	$100,019	$6,633,922	$398,059	$7,031,981
Variance																														
Federal Share	$57,746	$57,746	-$90,562	-$32,816	-$134,381	-$167,197	$30,429	-$136,768	-$467,281	-$604,049	$441,628	-$162,421	$326,648	$164,227	$255,405	$490,874	$220,600	$711,475	-$19,944	$691,531	$50,379	$741,910	$122,891	$864,801	-$366,724	$498,077	-$100,019	$398,059	-$398,059	$0
Non-Federal Share	$56,828	$56,828	$154,649	$211,477	$150,289	$361,766	$143,435	$505,201	$256,534	$761,735	$292,106	$1,053,841	-$812,444	$241,398	$125,806	-$571,046	-$144,850	-$715,896	-$171,794	-$887,690	-$195,750	-$1,083,440	$0	-$1,083,440	$0	-$1,083,440	$0	-$1,083,440	$0	-$1,083,440
Total Variance	$114,575	$114,575	$64,087	$178,661	$15,908	$194,569	$173,864	$368,433	-$210,746	$157,687	$733,734	$891,421	-$485,796	$405,625	$381,211	-$80,172	$75,750	-$4,421	-$191,738	-$196,159	-$145,371	-$341,530	$122,891	-$218,639	-$366,724	-$585,363	-$100,019	-$685,381	-$398,059	-$1,083,440

Baseline Reporting Quarter	Budget Period 2/3		Budget Period 3					
	Q12		Q13		Q14		Q15	
	10/1/22 - 12/31/22		1/1/23 - 3/31/23		4/1/23 - 6/30/23		7/1/23 - 9/30/23	
	Q12	Cumulative Total	Q13	Cumulative Total	Q14	Cumulative Total	Q15	Cumulative Total
Baseline Cost Plan								
Federal Share	$500,847	$4,999,541	$0	$4,999,541	$0	$4,999,541	$0	$4,999,541
Non-Federal Share	$0	$1,887,250	$0	$1,887,250	$0	$1,887,250	$0	$1,887,250
Total Planned	$500,847	$6,886,791	$0	$6,886,791	$0	$6,886,791	$0	$6,886,791
Actual Incurred Cost								
Federal Share	$377,956	$4,134,739	$366,724	$4,501,463	$100,019	$4,601,482	$398,059	$4,999,541
Non-Federal Share	$0	$2,032,440	$0	$2,032,440	$0	$2,032,440	$0	$2,032,440
Total Incurred Costs	$377,956	$6,167,180	$366,724	$6,533,904	$100,019	$6,633,922	$398,059	$7,031,981
Variance								
Federal Share	$122,891	$864,801	-$366,724	$498,077	-$100,019	$398,059	-$398,059	$0
Non-Federal Share	$0	$145,190	$0	$145,190	$0	$145,190	$0	$145,190
Total Variance	$122,891	$1,009,992	-$366,724	$643,268	-$100,019	$543,249	-$398,059	$145,190

Milestone Status Report

Our Milestone Status Report is contained in **Table 40** below.

Table 40. Milestone Status Report.

Milestone Title/Description	Verification Method	Planned Completion Date	Actual Completion Date	Percent Completed To date	Comments
Finalize Techno-Economic Assessment	Have collected sufficient data (results, costs, benefits, risks, uncertainties, and timeframes) to effectively evaluate economic performance of the REE/CM recovery system.	6/30/2022	9/7/23	100%	Request to extend project end-date to 9/30/23 was approved. Still collecting pertinent data.
Feasibility Study Complete	Feasibility report submitted to DOE for review and approval.	10/1/21	9/1/21	100%	Submitted to DOE 9/1/21.
Complete Pilot Scale Unit Construction	Pilot-scale unit construction completed.	3/31/20	1/15/20	100%	Was delivered to WRI January 2020—currently functional.
Go/No Go Decision Made	Project meets proposed technical and economic success criteria as listed in Section G below.	10/1/21	2/8/22	100%	DOE authorized project to proceed forward.
Complete ALSX System Design	ALSX system sent out for bid.	3/31/20	10/29/19	100%	Was approved for construction 10/19/19.
Complete ALSX Construction	ALSX shakedown testing can begin.	3/31/21	3/10/23	100%	Unit is stored at NRCCE building, will add modulating valves.
Finish ALSX Shakedown Testing	Begin continuous processing of upstream concentrate in ALSX plant.	2/1/22	7/1/23	100%	Request to extend project end-date to 9/30/23 was approved. Have begun shakedown testing.